The Fabrication of Artificial Facial Muscles

A review of the parameters required for their creation and experimental validation of the concepts

Submitted in partial fulfillment of the requirements for an MSc Degree in Smart Design.

Fergal Brian Coulter

N0357851

Nottingham Trent University
School of Architecture, Design and Built Environment

July 2011

Abstract

This thesis examines various methods and materials required for the design and fabrication of active artificial facial muscles. The primary use for these would be the reanimation of paralysed or atrophied muscles in sufferers of non-recoverable unilateral facial paralysis. The premise upon which these muscles would function is that of sensing the movement of natural muscles on the healthy side of the face, and replicating it via implanted solid-state polymer actuators on the paralysed side. This would lead to the creation of a symmetrical expression across the whole of the face.

The research carried out for this report investigates four main areas – facial anatomy and expression with emphasis on muscles used in the creation of a smile, muscle motion sensing methods, polymer actuators and materials and computer vision and facial recognition. The latter being primarily for reasons of automated calibration and reconfiguration of the artificial muscle, but also forming the basis of an occupational therapy program to aid the recovery of any sufferer of facial paralysis – be it temporary such as resulting from Bells Palsy or permanent perhaps as a result of a stroke.

An experimental prototype was built and is detailed. This animatronic device is based on Shape Memory Alloy actuators and uses either a flex-sensor or computer vision smile detection system to measure and control the amount and area of movement. This proof of concept device was not designed specifically to be suitable for implantation, but instead was created to investigate some of the challenges associated with non-linear solid-state motors, along with reading and recreating facial expressions.

Table of Contents

1. Introduction

Facial Paralysis without chance of spontaneous recovery can occur in a patient following a stroke, tumour or trauma from accident or various congenital issues such as Moebius syndrome and muscular dystrophy. The most common result is one half of the face is left with little or no movement. The underlying issue stems from damage or maldevelopment of the facial (VII cranial) nerve, though on occasions such as damage from accident, the issue can also stem from the non-function of the muscles themselves.

Where there is a level of function remaining in facial nerves, modern surgical procedures can sometimes be used to approximate reanimation of the face. Transplantation of functioning muscle from elsewhere on the body can be combined with static procedures such as eyelid weights and cosmetic enhancement. This solution tends to fall short of the required subtleness, elegance and naturalness of facial movement. It is also a hugely complicated and invasive procedure which takes many hours to complete, and many months for partial recovery.

It is proposed that the development of artificial muscles will eventually enable affected individuals to achieve effortless, coordinated facial movement. To achieve this a number of areas must be addressed. Surface appearance such as changes in feature shapes, and appearance of wrinkles and bags should be achievable instantly and with minimal power consumption. Along side this, creating sufficient forces to achieve the motion of the skin and paralysed muscle, the timing of that movement, and the independence or interdependence of various muscles must be understood and factored in to the actuator design.

This thesis investigates the best potential methods for the fabrication of a*rtificial* facial muscles. These muscles would be intended primarily for use as *in-vivo* replacements of existing paralysed muscles in patients of non-recoverable facial paralysis.

This project is a continuation of earlier work by Breedon and Vloeberghs [1] which investigated the use of Shape Memory Alloys (SMAs) as dynamic facial prosthetics for sufferers of facial paralysis. A 'proof of concept' device has been constructed using SMA based 'Miga-motors' attached to a silicone musculature which attempts to recreate some of the general actuations associated with smiling. The rationale was to create and test algorithms that can infer facial expressions, to be recreated in an animatronic head via a minimum number of sensors.

While SMAs show a lot of promise regarding their actuation strain and force, this investigation shows that they have relatively high power consumption, slow response time, hysteresis, and are susceptible to changes in ambient temperature. This suggests that much further work is needed to find and explore other suitable candidates for use within an *in vivo* device.

2. Background Research

The main problems associated with non-recoverable facial paralysis can be split into three basic groups : physical, aesthetic and communicative.

Physical symptoms can include drooping of the corner of the mouth, which leaves the sufferer unable to prevent drooling. The inability to blink can mean the cornea can become dry, potentially leading to blindness if left untreated. These problems can be solved using passive surgical methods, such as pulling the corner of the mouth up to a level using a gold wire, or weighting the eyelid down with a small gold weight inserted beneath the skin. While these passive solutions lead to an improvement, it is arguable that a more active solution would be preferable. An extreme active solution involves the transplantation of muscle tissue from the groin (gracilis muscle) into the cheek, though this is limited by implant extrusion, donor site morbidity, and surgical candidacy. [3].

Procedures are also practiced where a sufferer can undergo facial nerve grafting, cross-face jump grafts (splitting the signal of the functioning facial nerve to both sides of the face), or anastomosis (reconnecting a previously branched nerve) with other cranial nerves, for example the hypoglossal-facial nerve, which affords the patient an ability to move the face voluntarily by tongue thrusting [4]. These have varying levels of success, depending on candidate's age (preferably young), level of atrophy of the paralysed muscle (more than two years will make it unlikely to function again) and also on what nerves are still functional – this is particularly an issue following stroke induced paralysis.

The aesthetics issues associated with facial paralysis can leave a sufferer feeling self-conscious arising from what could be considered a disfigurement. Asymmetry of the face could also lead to social complexities such as Brown and Moore's [5] assertion that asymmetry in smiling is shown to relate to negative social judgments and lower ratings of trust worthiness in observers, though this could fall more in the category of communication.

Communication is an area that is hugely affected by facial paralysis. Non-verbal communication via facial expression plays a vital role in conversation. Emphasis for punctuation and questions are placed via movement of the '*medial*' and '*lateral frontalis*' (forhead) or '*corrugator*' (eyebrow) muscles. Whilst listening to someone else speak, movement of the zygomatic major (cheek) or contraction of the orbicularis oris (eye) can imply understanding and attention. When verbal communication is impossible such as in a noisy environment, 'emblems' become important. An emblem is "*a symbolic action that has a precise definition known to all members of a culture of subculture*" such as a wink or the pursing of the lips. [6]. Perhaps the most universal emblem is the smile, which can infer numerous emotions such as joy, embarrassment, uncertainty, sympathy, contempt or compliance. [6][7]. As Ekman points out there can be eighteen classifications of smile, but only one accompanies spontaneous positive emotions.

It is clear that the major consequences of facial paralysis justify a comprehensive investigation of the feasibility of replacing damaged muscles by artificial prostheses. The design and construction of artificial facial muscles requires multifaceted considerations. Great emphasis must be placed on surface appearance, shapes or wrinkles and bags, along with timing, forces and independence or interdependence.

To convincingly recreate a level of symmetry in the face, sensors must know when a particular actuation is taking place. There are a number of utilisable methods available, ranging from the sensing of electrical impulses generated by the healthy muscles (EMG), sensing their displacement via flex and stretch sensors, or perhaps reading the expression at brainwave level via EEG sensing. While the latter may seem far-fetched, commercial EEG devices are becoming common and relatively cheap, thus bringing this technique into the realm of plausibility. The fewer sensors required to read the nerve impulses, the more desirable it is. The reasoning for this can be seen as each implanted device in a patients face increases the risk of damaging the muscle nerves that are still healthy, along side an increase in the devices overall power consumption.

As with any normal surgical muscle procedure, following its implantation an artificial muscle requires some form of 'physiotherapy' in order to move correctly according to the individuals physiognomy. This process involves machine learning and computer vision. The symmetry of actuations or facial expressions must be assessed, and the artificial muscle adjusted accordingly as asymmetries are detected. Consequently a correlation of sensor readings to motion would be built up, thus refining and customising the device to the individual wearer.

The areas of the face that move synchronously during an emotive expression require investigation (see Fig 1). Of particular interest is the "Facial Action Coding System" (FACS) [2], where the muscle groups are classified according to their timing and natural tendency to act together during a particular facial expression. While FACS concentrates on the activity of the underlying facial muscles from a perspective of surface feature displacement, anatomical studies of the maxillofacial region are also required. Alongside published data on facial movements, specific data is needed on displacement, timing and the force required to move various regions of the face.

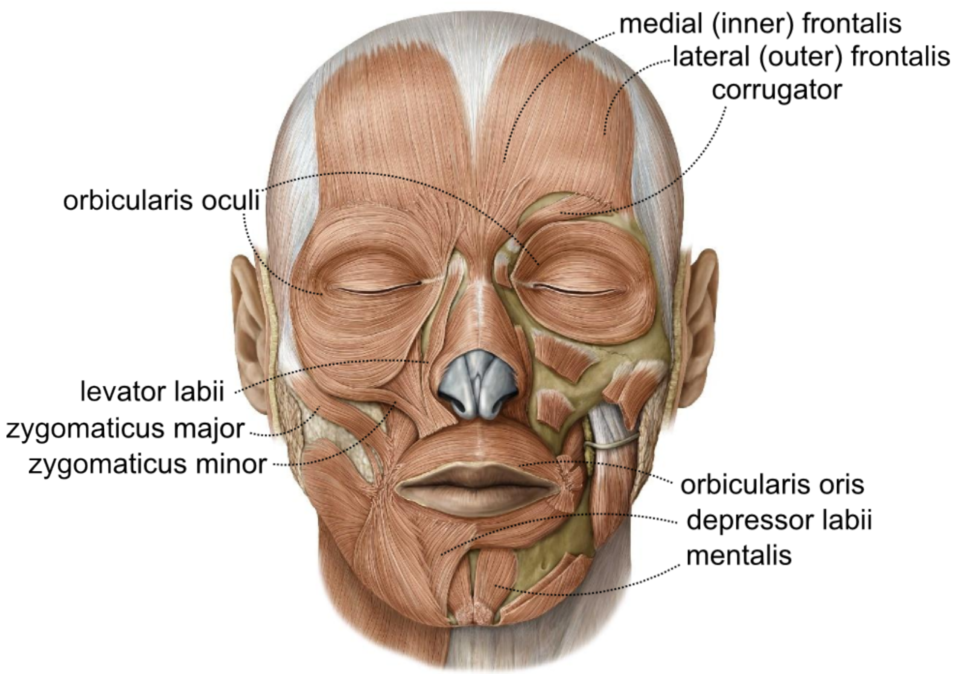

Figure 1: The major muscles that influence facial expression

(image modified from Patrick J. Lynch Creative Commons cc-by-nc)

By researching the Facial Action Coding System, various algorithms are created to infer what actuation areas should be active in the artificial muscles. The more efficient these deduction algorithms are, the fewer sensors are needed to realise a wide range of expressions. With this in mind, preliminary research and development of computer vision algorithms are conducted. A generically made implant would have to be re-programmable via learning algorithms if it were to function convincingly across numerous different face shapes and types.

With regard to materials suitable for the device, an investigation is conducted into Electro Active Polymers, with particular emphasis on the Ionic polymer metal composite (IPMC) group. These silent actuators feature rapid and large displacements, impressive force to weight ratio, ease of shaping and low power consumption. In terms of bio-compatibility, they are soft and flexible, inert (as they are generally coated in a noble metal such as gold, platinum or palladium) and work in a moist environment. Much has been published about IPMCs with reference to their suitability as artificial muscles. Yet impressive as their force and displacement are; in their current state of development these are not sufficient for replacement or aids to the powerful limb and trunk muscles in humans. On the other hand their quick and subtle movement points to them as suitable candidate for the complex facial muscles.

2.1 Facial Actions and the Anatomy of a Smile

Musculature of the maxillofacial region:

All muscles that affect the smile originate in the bony structure of the head, and insert into the Orbicularis Oris; terminating in the overlying skin and vermilion (lip border) at various depths. [8]. The direction and the varying strengths of each muscle are the main reasons for variation between peoples smiles, though hereditary variations in lip width and length, tooth structure, bony anatomical variations such as overdeveloped mandible or maxillae also influence the shape greatly. A study of one thousand people [9] found that 67% of people smiled with the zygomatic major muscle dominating. 35% had a smile caused by contraction of a strong levator anguli oris (caninus) muscle, exposing the canine teeth first, and just 2% were the “full denture smile” where all maxillary and mandibular teeth became exposed at the same time, due to all the muscles attached to the vermilion contracting at once.

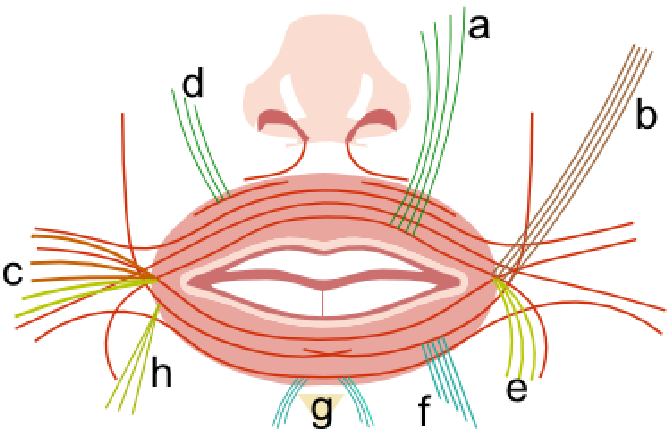

Figure 2: Attachment points for muscles around the orbicularis oris. a) levator labii superioris, b) zygomaticus major, c) buccinator d) the caninus, e) triangularis, f) quadratis labii inferioris, g) mentalis, h) the risorius [9]

The muscles around the lips are anatomically grouped as follows :

- The upper elevators (a) and (d) shown in green
- The corner elevators (b) and part of (c) shown in orange
- The depressors of the corner (e), (h) and part of (c) in yellow
- The depressors of the lower lip (f) and (g) in blue
- The orbicularis oris itself has anterior fibers which purse the lips, shown in red.

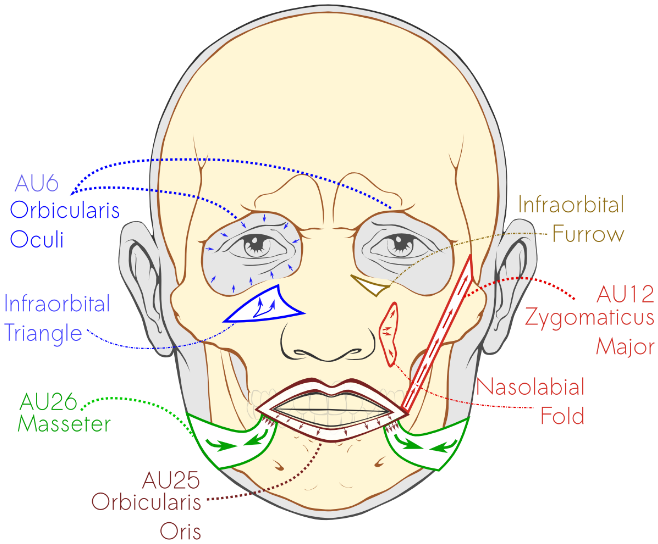

Fig 3: Diagram of Action Units attributed to the creation of an involuntary "Duchenne Smile", alongside; some of the more common furrows that appear during actuation.

Wrinkle lines are formed on the face when muscle contractions throw the skin into folds, at a right angle to the contracting force - known as “Langers Lines”. The most pronounced fold that appears when a smile becomes pronounced is the naso-labial fold at the bottom corner of the nose (see Fig 3). In animation and facial reconstruction surgery, the particular fold is considered a key in recreating a realistic smile, so much so that Rubin declared it “the keystone of the smiling mechanism” [9]. In that paper he explained the mechanics and motion of the muscles, in particular how the muscle attaches to the dermis below the fold.

When a smile begins to appear, the upper elevators raise the lip to the level of the nasolabial fold. As the teeth get exposed, the lip meets resistance at the fold. At this stage the corner lip elevators continue to contract creating the smiling mouth shape. The cheeks then become more prominent as the fat above the fold becomes compressed.

Facial Action Coding:

The Facial Action Coding System (FACS) [2] was devised in the late 1970's in order to systematically categorise various facial expressions and momentary changes of appearance (micro-expressions). The various movements are divided in “Action Units” or AUs, of which there are forty six specificity related to underlying facial muscle contraction and their effects on the skin and subcutaneous fascia. There are a further fourteen based on head movement.

It is unusual for a single AU to happen alone, without others triggering in tandem. Should this happen, it can very easily be inferred that the expression is being forced. An example of this is the insincere and voluntary smile involving contraction of Zygomatic major alone (AU12) (*see Fig 3)* verses the sincere and involuntary "Duchenne Smile", which (at a minimum) includes both the zygomatic major contraction and also a closure of the orbicularis oculi (eye) muscle (AU12 + AU6).

The following action units have been examined in relation to creating a realistic smile :

- AU6 - Cheek Raiser – Lower orbicularis oculi contracts
- AU12 - Lip Corner Puller – zygomaticus major contracts
- AU25 - Lips Part - Relaxation of orbicularis oris or depressor labii inferioris
- AU26 - Jaw Drop – Relaxation of masseter

AU 6

1. Skin is drawn towards the eye from cheek and temple as the outer orbicularis oris constricts.
2. The infraorbital triangle becomes raised, lifting the cheek upwards.
3. Bunching of skin around the eye towards the socket. This narrows the eye aperture and can bag or wrinkles the skin below the eye.
4. "Crow's feet" lines or wrinkles may appear, extending radially from the outer corners of the eye.

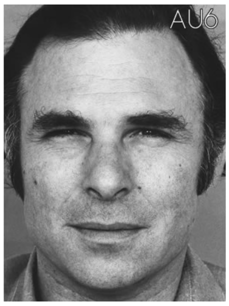

Figure 4 AU6 [2]

AU 12

The zygomatic major emerges above the ear, near the cheek bones and attaches at the corner of the lips. Its action will :

1. Pull the corners of the lips backward and upward. This creates the oblique shape of the mouth.
2. Deepen the nasolabial furrow. When contracting AU12, the furrow will be pulled laterally and upward. The skin adjacent to the nasolabial furrow is raised up and pulled laterally.

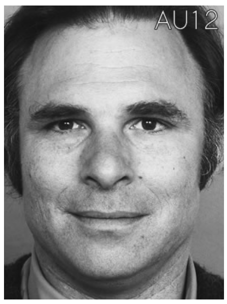

Figure 5 AU12 [2]

A stronger AU12 actuation will :

a. Push the infraorbital triangle upwards.

b. Increase deepening of the infraorbital furrow

c. Bag the skin below the lower eyelid.

When a strong action of 12 is seen, often it is difficult to be certain whether the changes seen are due to AU12 alone or to the combination of 6 plus 12 . A strong 12 hides many of the effects of 6.

AU 25

The lips part, which may expose the inner mucosal area of the lips. The teeth and gums may become exposed.

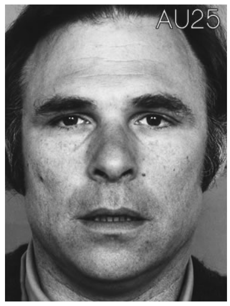

Figure 6 AU25 [2]

AU 26

1. The mandible is lowered by relaxation - separation of the teeth can be inferred.
2. If the lips part, space between the teeth may be seen.

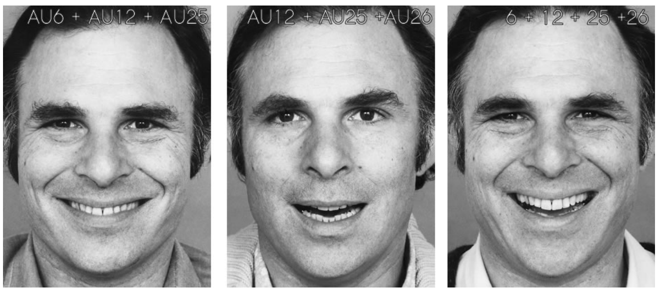

Figure 7: Combination of multiple AUs [2]

Timing of synchronous motions in a smile :

Frank and Ekman [7] propose that there are five different markers that differentiate types of smile :

- **Duchenne Marker** - Movement of the Orbicularis Oculi in conjunction with Zygomatic major
- **Symmetry Marker** – The symmetrical action of the two Zygomatic Major muscles. Spontaneous movements tend to be much less symmetrical.
- **Smoothness Marker** - Smooth and regular Zygomatic contraction. The motion will be longer in onset and smoother for spontaneous movements.
- **Duration Marker -** Consistency of duration of Zygomatic contraction. A posed smile will generally have shorter and less consistent duration, whereas the spontaneous smile will often be ½ to 4 seconds dependent on the person.
- **Synchrony Marker** - Zygomatic and Orbicularis Oculi reaching peak contraction (apex) at the same time.

There are differing neural pathways mediated when spontaneous or voluntary facial actions appear. “The voluntary facial movements originate in the brains cortical motor strip and arrive at the face via the pyramidal motor system”. Involuntary movements, for example those which are elicited “from emotional response arise mainly in the subcortical nuclei and arrive at the face via the extrapyramidal motor system.” [7] This could have implications for sensing motion via EEG, which will be discussed further in section 2.4.

Cohn and Schmidt [10] examine the timing of posed and spontaneous smiles from a different perspective – employing computer analysis of taped video to achieve automatic expression recognition and interpretation. Their findings backed up Ekmans suggestion of the five markers, discovering a linear relation between duration and amplitude for the onset phase of spontaneous smiles, whereas no same relationship existed for posed smiles. Using automatic feature tracking linked to the inside corners of the eyes via a Lucas-Kanade algorithm (section 2.3) allowed for accurate measurement in the case of small head movements. As their sample set comprised of 81 individuals, their data is much more comprehensive than that which has been collected for this report, so is reported side by side.

	Spontaneous		Deliberate	
	Mean	SD	Mean	SD
Duration (secs)	0.52	0.32	0.54	0.15
Amplitude (change in radius)	0.05	0.07	0.14	0.04
Ratio of duration to amplitude	17.96	13.49	4.02	1.39

Table 1: Cohn and Schmidts descriptive statistics [10]

Head movement is further analysed, discussing the correlation of movement of head direction to differing emotions associated with smiling. Examples given are 'surprise' having -an upward pitch, and embarrassment pitching down.

Schmidt *et al* [11] follow up their study with a second more indepth investigation into timing, this time using 87 subjects and with FACS coding done along side automated facial image analysis (AIFA). In this study, more definite timing and movement characteristics were presented using sub pixel acuracy in the Lucas-Kanade optical flow algorithm. They found that timing differences between deliberate and spontaneous smiles occur in both onset and offset phases, particularly evident is the difference in amplitude during onset. In fact they saw no major difference between amplitudes of the offset phase between voluntary and involuntary smiles.

What was perhaps the most interesting finding of this paper was the inclusion of Orbicularis Oculi contraction (AU6) in posed smiles – 60.1% of subjects showing movement of AU6 when either deliberately or spontaneously smiling, with a further 29.6% showing no AU6 during involuntary expression, but doing so during a voluntary motion. The remaining 9.4% was split evenly between those showing no eye movement at all, and those that showed the expected 'Duchenne response' of eye-movement only during spontaneous smiling.

In summation, spontaneous smiles are slow in onset, and can have multiple AU12 apexes during the course of the expression. These peaks in mouth corner are often held in short steps during the offset phase. For the most part, an involuntary motion will be accompanied by or followed by at least one other AU during the first second of expression. [12]

Data analysis of recorded facial movements and forces.

The analysis done for this particular study (table 2) found head movement to be a limiting and confounding factor when collecting useful data. Even though the sequenced still shots (see Appendix F for a sample) were normalised (rotated and moved) to line up the inner eyes as best as possible, the out of plane movement – predominantly a twist of head to left and pitch upward and backward was found to occur frequently when spontaneous smiles were involved. This was particularly the case when the subject got close to breaking into laughter. Of those sequences that remained (8), the right and left lip corner were represented as a mean displacement of the corner points.

$$d = \sqrt{x^2 + y^2}$$

Formula 1 – Mean displacement of mouth during smile

The values of d were then be standardised by the division of the initial value of lip corner width. Having broken the video sequences into 66ms frames which could be analysed in step form, a 10mm grid was overlayed. To calibrate the grid with the face being analysed, guide dots were drawn on each face before filming. This also helped to keep track of individual points as they moved throughout the duration of expression.

	Mean	SD
Duration (secs)	1.3	0.9
Displacement (mm)	0.707	0.65

Table 2: Measured Values

As well as manually tracking, an attempt was made to record and track some smile sequences via automated supervised corner tracking systems. (Voodoo Camera Tracker [80], and EyesWeb [81]). The a feature of both programs was an ability to export CSV files containing all the motion tracking information. While this was primarily designed for mapping video sequences onto 3D meshes in 3DS Max or Bryce3D, but in this case it was imported into a MySQL database for analysis. The main problem found with this was the sheer number of tracking points (see Fig 8). Efforts had been made to introduce “points of interest” (PoI) on the face with a coloured marker before filming, but even still the tracker program chose a large number of corner PoI in the eyes and hair. Before running the program, these features were removed, as shown in Fig 8.

There are many commercially available motion capture programs that would meet this task more effectively.

Figure 8: Tracking points from Voodoo Tracker. Green points do not move from one frame to the next, whereas red signifies movement. Each frame represents 66ms (15FPS)

2.3 Computer Vision and Facial Recognition

To manufacture artificial muscle at a realistic cost, they must be designed as generic devices with facility to re-adjust actuation parameters to suit the implantees physiognomy and natural expressions. This could be seen as a form of 'training' or physiotherapy for the muscle. Theoretically, a computer connected camera could view the facial motion of the person, detect the asymmetries between the natural and artificial muscle actuation, then adjusting the artificial one accordingly.

An investigation has been made into computer vision (CV) algorithms most suitable for this task. Within computer vision there are a number of open source frameworks available each with their own version of motion tracking algorithms and facial classifications. The most popular, and one on which most of the others are based is the Intel OpenCV library. This is a C/C++ library who's focus is real time application. There are more than 500 functions that span many areas of computer vision including medical imaging, factory product inspection, user interface, robotics etc. OpenCV contains a full general purpose Machine Learning Library (MLL) whos focus is on statistical pattern recognition and clustering. [13]. Along side OpenCV, the jMyron library for Processing based on OpenFrameworks, and Machine Perception Toolbox (MPT) libraries were both used to make an interactive interface for the prototype device detailed in Section 3

Face Detection

There are a number of ways for a CV system to find and track the movement of a face. Depending on the algorithm used, flesh tones, contours and complex templates involving neural networks, or filters can all be used. A problem common to all these methods is that they are computationally expensive, which make it hard to maintain high frame rates. Instead it is more common to use Haar-like classifiers (based on Viola-Jones object detection) [14].

Following location of a face, specific regions of interest (RoI) can be found centered on the facial features such as eyes and mouth.

Haar Classifiers

A Haar-like classifier is created by setting an algorithm to examine a large database of differing faces for specific features. Each classifier uses a number of rectangular areas (Haar features – see Fig 4) to make decisions about the region based on weather it matches certain requested features of a predefined image or not. The algorithm is a 'weak learner', with a probability of success only just above random guessing. This means a large initial dataset of faces must be input - preferably tens of thousands are required to describe an object with sufficient accuracy. [15]. Common facial data repositories include the Cohn-Kanade DFAT [22], CMU-PIE [23], MMI [24], UT Dallas [25]. Following the creation of many Haar-like features, results are organised and assembled into an XML file called a cascade. This cascade forms the basis of a strong learner algorithm.

The key to the Haar classifier's speed over traditional methods of feature detection is its use of an integral image algorithm (called by cvIntegral() function in Open CV) which considers and then sums the pixel intensity of adjacent rectangular regions (see Fig 9) at a specific location in a detection window. The result is a calculation of differences between the regions which can be used to categorize subsections of the image.

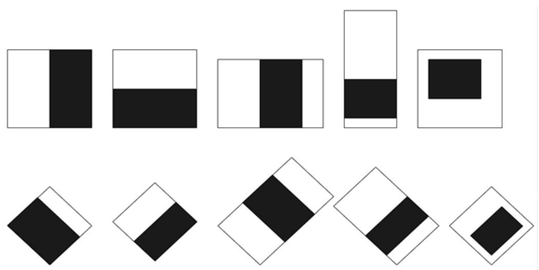

Figure 9: Types of rectangular regions used in Haar Features - white representing addition, black representing subtraction

The Haar decomposition of an image with n^2 pixels involves n^2 wavelet coefficients. Each of these coefficients correspond to a distinct 'Haar wavelet'. The first wavelet extracted is the mean pixel intensity value of the whole image (Fig 9). Following that, the rest of the wavelets are computed as the difference in mean intensity values of horizontally, vertically, or diagonally adjacent squares [16].

Following integral imaging, statistical boosting – “Adaboost” - is used to create binary classifications (face or no-face) according to characteristics of high detection and weak rejection. This data is kept in the XML rejection cascade, which is correlated to picture or video in real time. [13].

The rectangle features used in Haar-Cascades could be considered primitive in comparison to alternatives such as steerable filters [17]. Steerable or oriented filters are excellent for the detailed analysis of boundaries, motion and edge and texture analysis. Rectangle features are sensitive to the presence of edges and bars but in general their detection and analysis is quite coarse. The trade off is the speed benefits of Haar which keep it a popular choice.

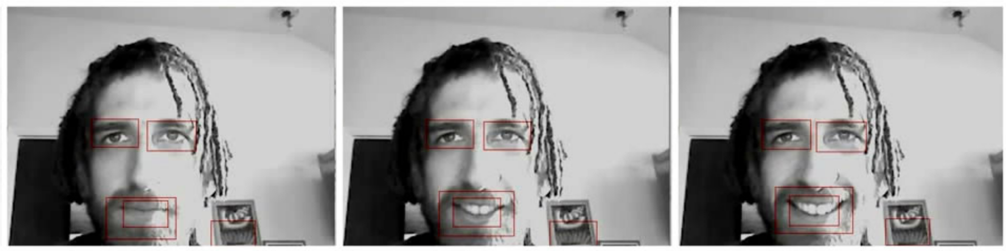

Figure 10: Haar Detection with mouth and eyes as the region of interest (RoI).

Note : A false positive is found in the background picture - perhaps owing to its mouth like shape and colour.

Whitehill and Omlin [18] demonstrated that Haar classification could be used for FACS AU detection with the same accuracy (over 90%), and a computation speed two orders of magnitude faster than similar tests run using steerable Gabor filters. A weakness described by [19] is when the background of the captured image has a similar color or characteristics with mouth region. When this happens, the classifier recommends many candidates for the ROI, many of which are poor. This is normally compensated for by refining the region of interest according to the proximity of other features such as eyes.

Laplace & Canny Edge detection

Finding the edges or boundaries of various facial features is an important step in feature detection and feature extraction. The method employed in the prototype working model (Section 3) is Canny Edge detection, which in itself is a derivative of the Laplace operator. It works by identifying points in an image where the image brightness changes sharply or has discontinuities.

The Laplace operator is a second order differential operator that calculates the divergence of the gradient of a function in n-dimensional Euclidean space, with divergence ($\Delta\cdot$) of a gradient (Δf).

$$\Delta f = \frac{(\partial^2 f)}{(\partial x^2)} + \frac{(\partial^2 f)}{(\partial y^2)}$$

Formula 2 : Leplace Operator

While not specifically an edge detector (being better suited to blob detection), it does exhibit similar characteristics to the more advanced detector algorithms. When the first derivative of the function is large, it shows the function to be changing rapidly. This is a sign that it is approaching an edge like discontinuity. The product shrinks rapidly when it moves past that discontinuity. This single derivative will be at a local maximum somewhere with that range, which is called the 'Sobel derivative'. Looking to the 0s of the second derivative will yield the locations of the local maxima – i.e. edges in the original image will be 0s of the Laplacian. [13] Less important edges will be detected too, though they can be filtered out by ignoring anything with values higher than the first (Sobel) derivative.

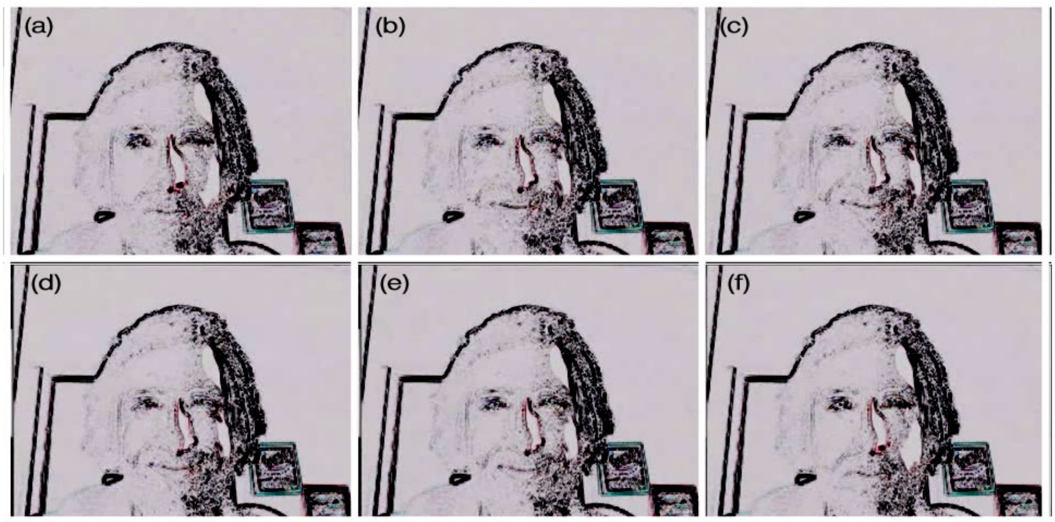

Figure 11: Canny Edge detection

Canny edge detection is a more complicated Laplace operation as it computes the first derivative of both the x and y planes, and combines them into four directional derivatives (0°, 45°, 90° and 135°). The Local Maxima are chosen as candidates to be drawn as an edge. Before doing so it must apply a Gaussian (blur) filter to remove small groups of noisy pixels.

Following formation of a candidate set for edges, Canny will apply a hysteresis threshold to convert the edges into contours. (see Fig 12). With an upper and lower threshold, contours can be formed by accepting values above the upper, rejecting those below the lower, and selectively accepting those in between- only when it connects to a pixel that is above the upper. The ratio of upper to lower threshold is configurable, with a high ratio resulting in a reduced number of edges detected.

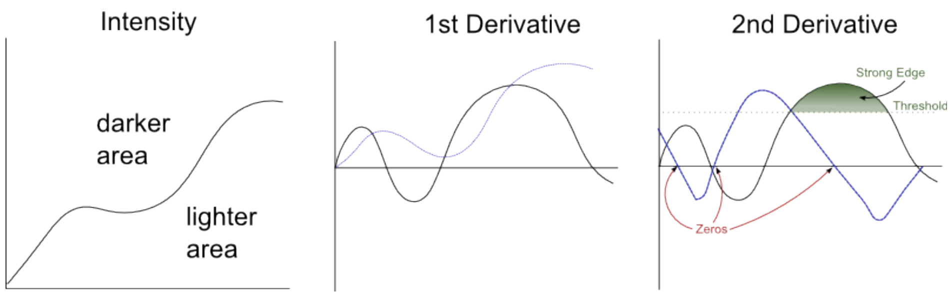

Figure 12: Laplace transformation - the 0s in the second derivative correspond to edges and the upper threshod values correspond to a strong edge. [13]

Blob and Corner detection

Having found the edges and extracted the features of the face, corner points must be found in order to track motion. The corner points chosen should be unique (or as near as possible) within the scene. Points that have significant change in them – eg strong edge derivatives – are normally chosen as starting points. These points are examined in two orthogonal directions and should the derivatives be strong in both directions then it can be assumed to be unique. The most common corner detection algorithms is the Harris [19] detector. OpenCV and MPT both have functions that automatically find strong features to track (such as the `cvGoodFeaturesToTrack();` function in OpenCV)

Tracking and Motion:

Optical Flow ***:***

To assess motion between two frames without prior knowledge of the content in the frames, an optical flow algorithm can be used. There are two types – dense and sparse. Dense tracking such as the *Horn-Schunck method* attempt to calculate a velocity for a tracked point from frame to frame. As every pixel in the image is considered from one frame to the next, dense tracking puts a large strain on computational resources.

To get around this problem, sparse optical flow techniques can be employed. In a sparse algorithm, a subset of points with unique features or high contrast such as a corner point are chosen before tracking commences. This limited number of points greatly decreases computation load, while retaining a robust tracking of objects.

Figure 13: Dense tracking, where lines on dots represent direction and velocity.

Note : CPU overhead means frame-rate reduction at output - see (b) where velocity is shown before the movement itself is rendered in (c), and again from (d) to (e)

The Lucas Kanade Algorithm :

Perhaps the most popular sparse technique is the Lucas-Kanade (LK) [20], or later the Lucas-Kanade-Tomasi (LKT) feature tracking algorithm [21]. The LK can be considered sparse as it relies on local information derived from a small area around pre-specified regions of interest – in this case, the eyes and nose. This greatly reduces the number of computations required to track movement.

A downside of this method is the danger that a large motion would put a track point outside the '*local window*', thus becoming impossible for the algorithm to find [13]. This is overcome by the use of image pyramiding, which starts at low detail and iteratively increases the detail (upsampling) as the tracking commences.

LK implementations have three basic assumptions :

- *Consistency in brightness and colour*. A pixel should not change appearance while being tracked from one frame to the next. Automatic adjustment brightness and contrast in some cameras can reduce tracking ability.
- *Temporal persistence*. Motion of a pint changes slowly in time.
- *Spatial coherence*. Neighboring points belong to the same surface, and have a similar motion to each other. [13]

These assumptions give a 'close enough' solution to tracking motion and velocity at low resolution, which improves as detail iteratively increases.

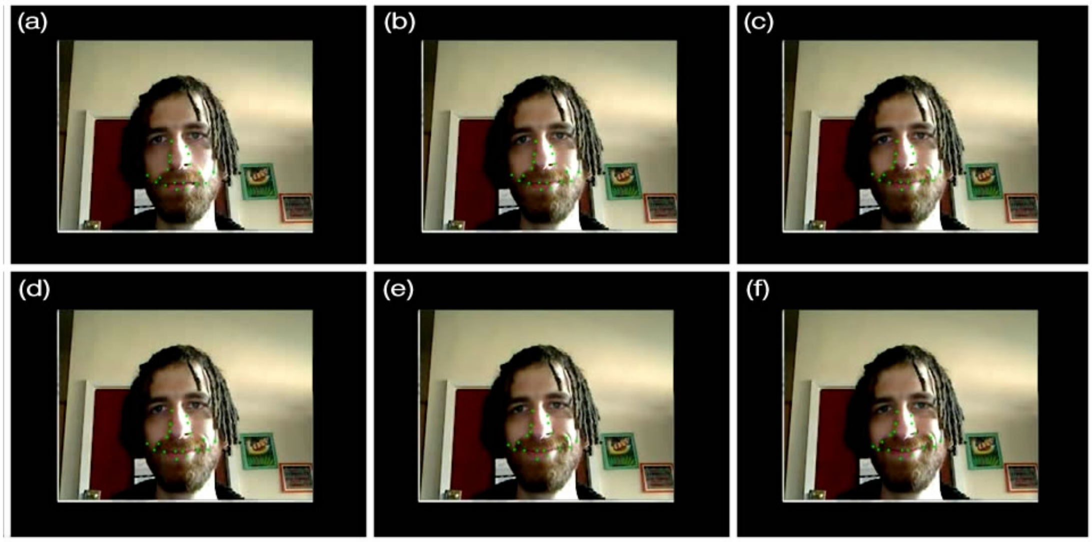

Figure 14: Lucas-Kanade tracking with a specified RoI around mouth and nose.

2.4 Sensors

There are a number of ways in which the movement of the contralateral healthy muscles could be sensed in order find how much the artificial muscle must be actuated. It is a necessity to be as non-invasive as possible while gathering the maximum information on the timing and distance required.

Breedon and Vloeberghs [1] suggested electromyography (EMG) as their chosen method, though it is equally permissible to envisage implanted flex sensors or surface electroencephalography (EEG) being a viable solution.

Electromyography

EMG is the technique used for recording electrical activity produced during muscle contraction. The potential generated can range anywhere between ~50µV and up to ~25mV, depending on the muscle [26]. Due to the (relatively) small displacements and force required to contract a facial muscle, the measured potential falls at the lower end of this scale.

There are a number of issues regarding accuracy of facial EMG (fEMG) including the muscle fiber length - where some muscle fibers do not run continuously from the origin to insertion point, but instead may only traverse a small distance. This can vary the characteristics of the muscle fiber action potential (MFAP), and thus making the recorded signal location specific, even across an individual muscle. [27]. Another issue is the partitioning of some muscles into different actuation 'zones', each with different uses or abilities for independent movement. This is particularly apparent in the orbicularis oris muscle. [28]. If EMG electrodes span across different zones, the recorded results can be skewed and difficult to interpret.

The distribution of sensory receptors is considered to be non-homogeneous across the muscle. This can lead to regions with a greater density of receptors providing regional information about localised changes in muscle length, force and displacement. Even with that in mind, as the recorded readings would only need to provide information on gross movement at any sensor site, fEMG should be more than accurate enough. When reading EMG signals, two differing measurement methods can be used – surface electrodes and indwelling electrodes.

Surface Electrodes.

At its simplest, an EMG signal can be detected by placing a simple metal electrode with a thin layer of electrolyte gel on to the surface of the skin, above the muscle to be measured. This method is susceptible to “Motion Artifact” - mechanical disturbance changing thickness of the electrolyte during motion. Modern sensors reduce this problem by removing skin contact of the plate and allowing formation of an “electrolyte bridge” [27] This floating electrode arrangement means changes in orientation of the electrode go unaffected, so long as a conductive path is maintained. There tends to be a high signal to noise ratio when using passive electrode techniques, and there is a necessity for a reference electrode at some non-active muscle site, normally the forehead or ear.

A better quality signal can be gathered when active electrodes are employed. These incorporate a pre-amplifier on the sensor casing. Metal contacts are directly placed on the skin, which increases the magnitude of the EMG signal by a factor ten [27]. There is a requirement for very clean skin as a natural electrolytes in the derma can conduct the signal. The complex interaction between the metal surface and electrolyte gel is eliminated. [29] This results in an EMG signal strength that is large in comparison to surrounding noise. The trade off for this improvement is one of size and the number of possible attachment positions, owing to the non-flexible nature of the metal electrodes.

An inherent problem with both types of surface sensing is the fact that the presence of the electrodes will create an unpleasant aesthetic for the wearer

Indwelling Electrodes.

A more appropriate method of sensing the muscle contractions would be via indwelling or implanted electrodes. These record the electrical activity using either a single needle or two wires implanted within the muscle. The electromyogram is then far less affected by the architectural characteristics of the muscle fibres. The signal strength is increased and cross-talk decreased as the muscle is probed further in towards its core – see Fig 15

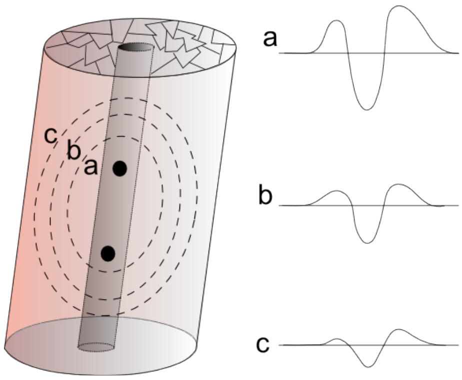

Figure 15: Indwelling EMG readings vary in strength according to the electrode depth

There are two electrode types used in IEMG – Needle and Fine-wire. The needle type is only suitable when the detection is to be temporary, whereas fine wire (insulated platinum, gold or silver of diameter ~50µm) can be inserted below the skin for a more permanent solution. Fine-wire probing electrode preparation is shown in Fig 16.

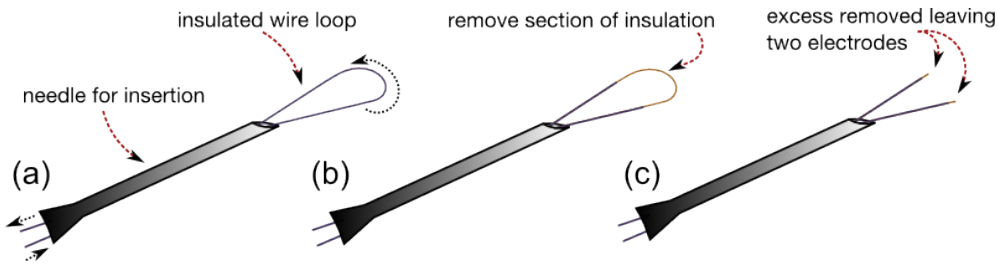

Figure 16: iEMG electrode preparation

It is important to situate the bared electrode tips deep in the muscle, in an effort to keep cross-talk to a minimum, and also prevent movement of electrodes, which could ultimately result in a short circuit. [27]

An interesting purpose built sensor, designed by the Alfred Mann Foundation (AMF) is shown in Fig 17. These small hermetically sealed capsules are passive, and can be inductively telemetered for information by an ex-vivo sensor / processor. It is claimed that this device mitigates the problems associated with multiple-component EMGs. [30].

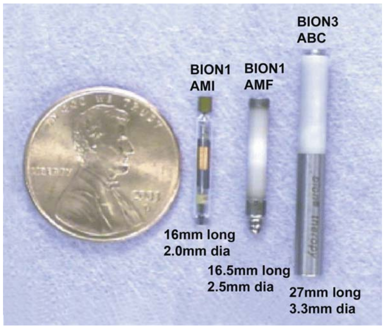

Fig 17: - Hermatically packaged Implantable EMG sensors (AMF)

The sensors have been designed for use in the control of prosthetic limbs, so their 16mm x 2mm (min) size is more advantageous than when dealing with the finer facial muscles, as they can sample a larger section of muscle.

They are high resolution, with two different sampling rates depending on the band they are selected to work on - Integrated EMG (band 1) is the format used in commercial myoelectric systems, and outputs 120 samples per second. Raw EMG capability (band 2) is designed in for future applications, and can support 444 samples per second. . The system is designed to communicate with up to 32 separate sensors, and these have been tested in monkeys and found to be functional over more than two years testing [30][31].

Electroencephalography (EEG)

EEG is the measurement of brain waves through the skull and scalp. These brain waves are in fact voltage fluctuations stemming from a micro-current created when there is an ionic flow within and between the brain's neurons. [32] The accepted method to record EEG signals is by placement of electrodes on the head as defined by the "International 10-20 System". This is based on a relationship between the location of an electrode and the underlying area of cerebral cortex. The 10 and 20 refer to a percentage that electrodes should be spaced apart in relation to the measured head. In this system, 19 electrodes are used, plus reference and ground (often the earlobe). Many more electrodes can be used – up to 256 in a high density array, as used in cognitive psychology, and psychophysiological research. The electric potential created by a single neuron firing is far too small to be detected, so an EEG reading will reflect the summation of thousands or millions of neurons acting synchronously within the same spatial orientation.

Normally when research is to be carried out using EEG, the subject is 'evoked' to provide specific responses via a directed stimulus. When this process is repeated numerous times (more than one hundred), a pattern emerges that shows areas of the brain that consistently become active according to the stimulus. These readings are termed “evoked potentials” (EP) when the stimulus is simple, and “event related potential” (ERP) when multiple or complex stimuli are introduced. Much has been studied and published with regard ERP in relation to the emotional reaction to a strangers facial expression [33], but less so the pre-motor potential (Bereitschaftspotential) involved in the creation of involuntary facial expressions.

Bereitschaftspotential (BP) is an electroencephalographic potential that exhibits negative polarity. It is predominantly seen during the milliseconds preceding a motion, and has mainly been studied in relation to voluntary, self-paced limb movements. Korb et al discuss weather there is a BP involved in posed smiles, and find that there is, albeit relatively late in onset, small in amplitude and with a symmetrical bilateral distribution (when compared to finger, hand or foot movements). [34].

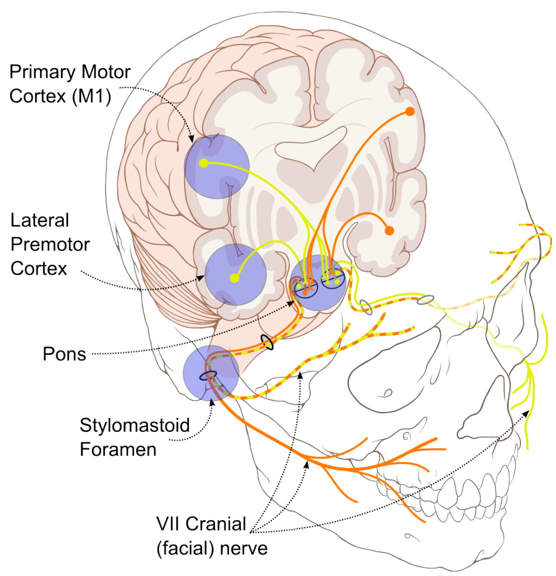

Figure 18: The basic neural locations and nerves involved in facial expression.

(image modified from Patrick J. Lynch Creative Commons cc-by-nc)

One complexity that challenges EEG as a sensor method is the uncertainty of origin regarding a motor command. Spontaneous and voluntarily expressions rely at least in part, on separate neural pathways from the Primary Motor-Cortex (M1) and Lateral Premotor Cortex (LPMC) either via the direct pyramidal (corticobulbar) tract for voluntarily, or the extrapyramidal pathways with spontaneous expression. Signals are sent to the muscles via the VII Cranial (facial) Nerve beginning in the ventrolateral region of the inferior pons (at the brainstem) and exits the skull via a hole near the ear called the Stylomastoid Foramen. [35] These areas are highlighted in Fig 18.

EEG sensing can be further complicated when a facial expression is emotionally triggered – ie spontaneous, but subsequently suppressed (for example diminished in amplitude or duration) by a desire to display certain expressions differently in a particular social context, or not to reveal it at all. [36].

These variables may mean EEG is overly complex as a sensing method, but commercial EEG sensors are beginning to appear – particularly the "Emotiv EPOC" device which has specific application programming interfaces (API) designed for reading and capturing specific facial expressions. This area will need to be investigated further, as discussed in Section 4.

Piezoelectric and Flex Sensors.

The final method investigated for sensing movement are various forms of complaint flex sensors. These could be piezoresistive conductive polymers such as a bi-layer composite, consisting of a compliant polymer films coupled with crystals of molecular conductors. These consist of ion-radical salts (IRSs), typically based on tetrathiafulvalene (TTF) derivatives "such as bis(ethylenedithio)tetrathiafulvalene (BEDT-TTF), which exhibits dramatic changes in conducting properties under isostatic pressure or uniaxial strain" [37]. These bio-compatible all-organic sensing devices have been prototyped by Laukhina *et al* into a device for monitoring a person's breathing rhythm. In the same paper they discuss the possibility of using these sensors for detection of tissue movements. They exhibit high sensitivity (sensing changes in pressure down to single mbar range) exhibiting a linear change in resistance.

Alternatively piezoelectric thin films such as polyvinylidene fluoride (PVDF) could be used. PVDF is not piezoelectric in its raw state, but becomes piezoelectric when heated within an electric field. PVDF can be purchased in sheet form ranging from 5 microns to 2 mm thick. The sheet must be coated with an electrical conductor on both sides in order to collect charge and permit connection to an electrode. In addition it can be moulded into any shape desired. [38]. A low thickness film makes for a very small cross-sectional area. Relatively small longitudinal forces therefore create very large stresses within the material. [39] Metalised PVDF can be purchased commercially from numerous manufacturers such as MEAS Spec.

2.5 Materials

When investigating materials most suitable for the creation of artificial muscle actuators, prerequisites such as low-power consumption, biocompatibility, affordability and controllability must be considered. Polymers have been developed that respond to numerous varying stimuli with a change that can be either temporary or permanent. The stimulation sources include heat, light, chemical (pH), pressure, magnetic and electric field. [40] Many of these sources are unfeasible for in-vivo stimulation, so only those materials which are electrically or heat activated are to be considered here.

Electro active polymers (EAPs), consisting of various classes of conjugated and ionic polymers, along with dielectric elastomers are collectively a relatively new class of material. They are are only recently at the stage of being well understood and documented in terms of their mechanical efficiency, physical constraints, stability and best fabrication practice. EAPs fall into two broad categories – 'dry' or electronic and 'wet' or ionic.

Dry / Electronic EAPs :

Within the dry category there are a number of sub classes such as piezoelectric, electrostrictive and dielectric elastomer. These polymers change shape or dimension due to the migration of electrons across an applied electric field. [41] The term 'dry' refers to the fact that the material can actuate in air, or without the presence of an electrolyte. They tend to exhibit large strain and actuation force, and can hold their position without back relaxation under an applied DC field, but generally require very high voltages to activate.

Piezoelectric EAPs such as the polymer Polyvinylidene-Fluoride (PVDF) and ceramic Lead Zirconate Titanate (PZT) undergo longitudinal expansion when exposed to an electric field, and conversely produces a polar voltage when mechanically strained. While their response time is fast, the strain is low (0.1-0.2%) and require large voltage (up to 100V for PZT) [42]

Electrostrictive Graft Polymers exhibit a non-reversible deformation when their crystal structure changes due to charge attraction. This results in a reduction of material thickness and an increase in orthogonal direction. [41]

Dielectric Elastomers such as silicone (NuSil® CF19-2186) and acrylic (3M® VHB 4910) actuators are perhaps the most interesting dry EAP in terms of artificial muscles, showing strains up to 380% for VHB (120% for NuSil) and able to exert large forces. In fact, as a comparison to natural skeletal muscle they perform as well or better in many of the main characteristics such as stress and strain, actuation pressure, density, elasticity and speed [43] (see table 3) They act as a capacitor which undergoes mechanical deformations proportional to the square of the electric field, unlike piezoelectric materials where this relation is linear. The actuation is longitudinal and caused by electrostatic pressure from Maxwells stresses from electrostatic fields that squeeze the elastomer film. The typical electrodes used are Carbon or Silver pastes, painted on to the base polymer, coated and cured in a vacuum oven. The polymer is occasionally doped with a large metal oxide particle such as TiO_2 [78] in an effort to increase the dielectric constant. It has been shown that spin coated conductive rubbers [77], sprayed graphite [78] and superelastic nano-tube sheets [79] all exhibit performance advantages when used as electrode.

The material can be made to hold its induced displacement while activated under a DC voltage. Unfortunately this action can only take place at when the applied voltage is greater than 10 V/μm^2 – hundreds of volts for a muscle with an area the size of the cheek, and several thousand volts for larger trunk and limb muscles. The material has a very low current consumption (in the μA range), but the use of high voltages has the ability to cause blood clots due to potential voltage breakdown and shorting through body tissue. [44][45] There is the possibility of isolating the elastomer inside a protective case, as per Tollefson and Senders proof of concept artificial “blinking” muscle [46]. This involved electrically isolating EPAM™ (Artificial Muscle Inc.), via encapsulating and connecting the resultant muscle to a pair of inert expanded Polytetraflouroetheylene (ePTFE) 'slings' – one above and one below the eye. Contraction of the EPAM caused the eyelid to close. While this experiment was conducted on cadavers, SRI, the parent company of Artificial Muscle Inc. claim they have been testing bio-compatiblility of EPAM in live gerbils. [unpublished]

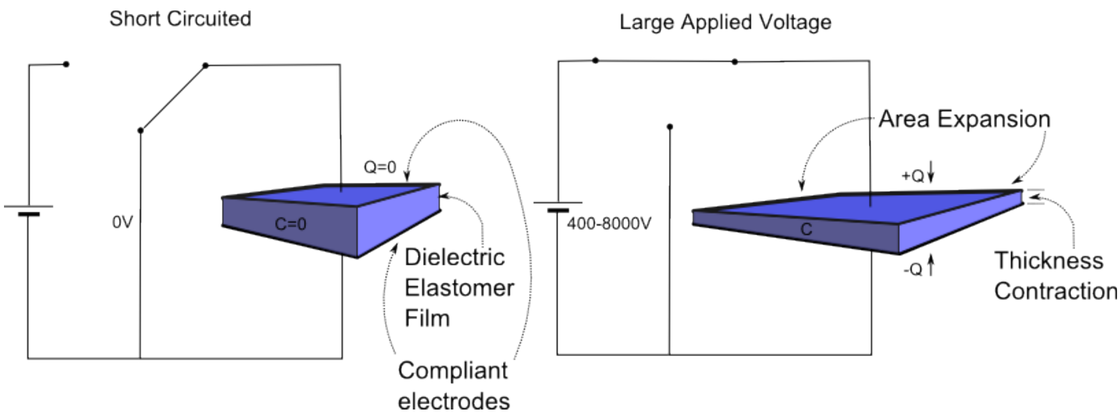

Figure 19: Dielectric EAP operating principle

Wet / Ionic EAPs :

A interesting option comes from the ionic class of EAPs. These are divided into four main classes : Ionic Polymer-Metal Composites (IPMC), Conjugated Polymers (CP), and Ionic Gels. These actuators change their shape due to the movement of diffused ions which are encapsulated in the membrane or gel. All three are soft and flexible, bio-compatible and have low power consumption (normally less than 1W). There are numerous ways to fabricate each type - with varying success. The ionics do suffer some drawbacks and face challenges if they can be considered viable – often they produce quite a low blocking force, can be difficult to maintain their static position, or are chemically sensitive, thus require sealing against contamination of the ionic content. This encapsulation can result in a reduced performance efficiency.

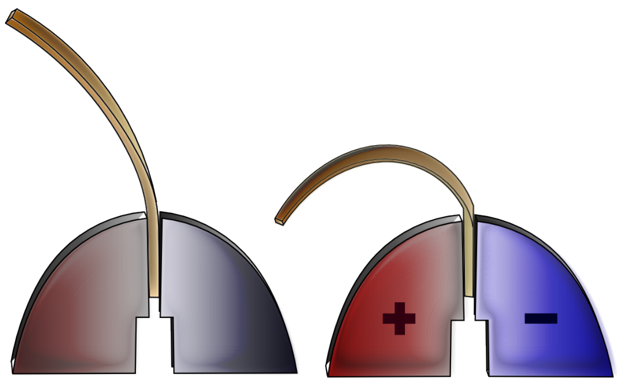

Figure 20: Motion from ionic actuators when subjected to an applied voltage

Ionic Gels such as Polyacrylic acid (PAAc) or Polyvinyl alcohol (PVA) work on the principle of an applied voltage causing movement of hydrogen ions in to or out of the gel. An interesting factor with regard these gels is their generative force and energy density comes close to matching that of biological muscle, while at a low driving voltage. Unfortunately this force comes at the expense of speed. To be of sufficient speed, only a very thin layer may be used, and coupled with that, no reliable electrode exists that can be used to stimulate the muscle gel. For this reason, they can not be seen as a viable solution at the moment.

Ionic Polymer-Metal Composites.

Ionic Polymer-Metal Comopsites were first discovered and fabricated by Oguro et al [8]. Their method of fabrication involved the plating of the ion exchange membrane DuPont Nafion™ 117 (Perfluorosulfonic Acid) with platinum. The measured actuation power of the materials was initially underwhelming, but research in the intervening years has produced methods that can now theoretically produce a blocking force of up to 20 times its own weight [47]. - A gold plated Nafion membrane of 0.8mm thickness was made to lift 10 grammes of weight when stimulated by 3 Volts of potential. [48] This power comes at the expense of speed and frequency response.

The characteristics of an IPMC is defined by an ion-exchange membrane (IEM) acting as a solid electrolyte to two porous electrodes. The ionomer is normally a perflourinated compound (all hydrogens replaced by fluorine on a carbon chain). Various membranes can be used in production, each one possessing differing functional groups attached to the backbone such as a sulfonate group in Nafion™ (DuPont) and Aciplex™ (Asahi Chemical), a carboxylate group in Flemion™ and Selemion™ (Asahi Glass) and an amino group in Neosepta (Tokuyama). Short side-chains provide ionic groups that interact with water and the passage of appropriate ions. [49].

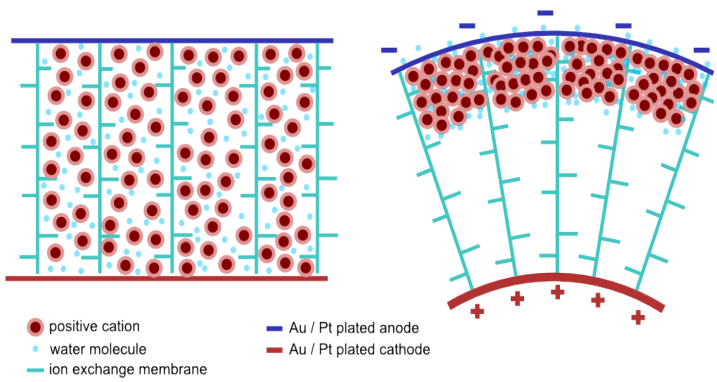

Figure 21: Working principle of IPMC

The most modern methods of fabrication involve a number of individual steps :

Membrane treatment : Choice of exchange membrane affects a number of factors. The use of a sulfonate based IEM such as Nafion will result in an IPMC that bends quickly to the anode, but then has a back relaxation towards its cathode when held under a constant DC potential. The carboxylate based IEMs on the other hand have a back-relaxation that travels in the same direction as the flexing itself. [50]. Sulfonated polystyrene (sPS) are reported to have virtually no back-relaxation when used as the membrane. Luqman *et al* [51] fabricated IPMCs based around sPS and compared the results to Nafion based materials which were fabricated under the same conditions. Their rationale was to find a solution to the short operation time, low generative blocking force and extreme expense, and their conclusions are extremely encouraging. The new backbone polymer means the IPMC has an increased water-uptake and retention (due to a considerably thicker electrode layer), thereby significantly increasing blocking force – for their figures : 2.76 vs. 1.51 gf of displacement, 44 vs. 23 mm)and response rate (10.3 vs. 2.9 mm at starting 3 s), while decreasing back relaxation (420 vs. 205 s).

Membrane thickness plays a significant role in response and blocking force of the actuator. There are two main methods to achieve a thicker membrane when using the more traditional membranes – Hot pressing, a number of strips of IEM together (180°C and 50 MPa) [54] or dissolve the IEM in a solvent and then cast it into the shape required.

Lee et al [52]. discuss the casting of liquid Nafion into a mold. They discovered that power density increased significantly, but at a cost of tip displacement. This casting method often leads to cracking in the membrane due to the rapid evaporation of a low boiling point solvent. He *et al* [53] suggest a solution to this problem by introducing an additive dimethylformamide (DMF) that makes the mixture act like an azeotrope. This more stable fabrication process produces satisfactory and constantly predicable results – the increase in thickness reduces current consumption, and displacement, but increases blocking force by up to 100% at 32mm thickness (dropping tip displacement proportionally by 50%.

Lee *at al* [54] also investigate the 'hot-pressing method' of Nafion films. Their method achieved impressive results - 8 grammes of tip force for an applied 4 Volts using 5 stacked Nafion layers (in a 30mm x 5mm strip). The disadvantage to this was the requirement of expensive platinum electrodes (electroless plating up to 5 times).

Fang *et al* [55] take a different but interesting approach to the fabrication, as their requirement is to use IPMC for disposable active catheter systems. With their novel casting method they claim to reduce the fabrication time to half (24 hours, as opposed to the average 48) while keeping the cost low and reliability high. Their method firstly involves mixing and baking Nickel Nano-Powder into the cast Nafion membrane, then electrolessly plating the result in a gold plating bath. This cast moulding of the ion exchange membrane is interesting as it frees up the need to create actuators based around cantilevered strips. Instead, possible arrangements could include helical and honeycomb patterns. (Shown in section 4, Fig 44 and 45)

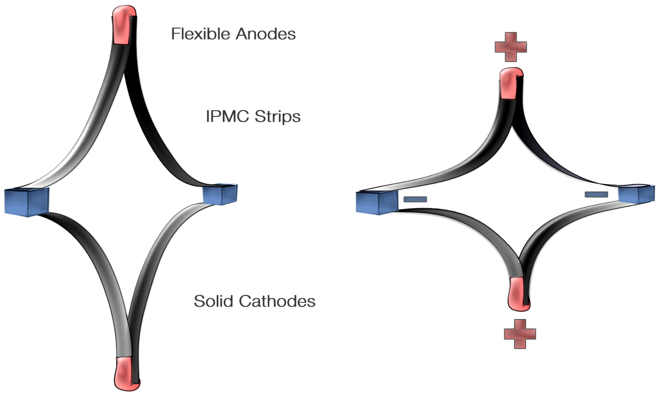

Figure 22: IPMC strips combined to form a "single cell" linear actuator.

Following casting or thickening of the membrane, it must be roughened. This can take the form of simply rubbing with emery paper and cleaning with an ultrasonic bath, or the more complicated plasma etching method. Kim *et al* [56] used a method of plasma surface treatment using oxygen (chemical etching) and argon (physical etching) to improve efficiency of IPMC – doing so increased the uniformity and thickness of the electroless plated electrode. The O_2 treatment proved more successful than Ar by reducing the resistance of the electrode by 20% and improving the displacement by 60% and the lifetime by 90%.

Recently, much of the focus on IPMC development has focused on refining and altering the electrical and water carrying properties of the ion exchange matrix. Nguyen *et al* [57], developed a method of doping / filling Nafion with layered silicate and montmorillonite (MMT) in order to form a nano-composite. This resulted in approximately three times the blocking force (gwf) and two times the displacement alongside a more rapid response than a standard procedure Nafion-based IPMC produces under the same conditions. Lee *et al* [58] take a different approach to achieve similar improvements by integrating the conductive polymer Polypyrrol with Alumina as their filler.

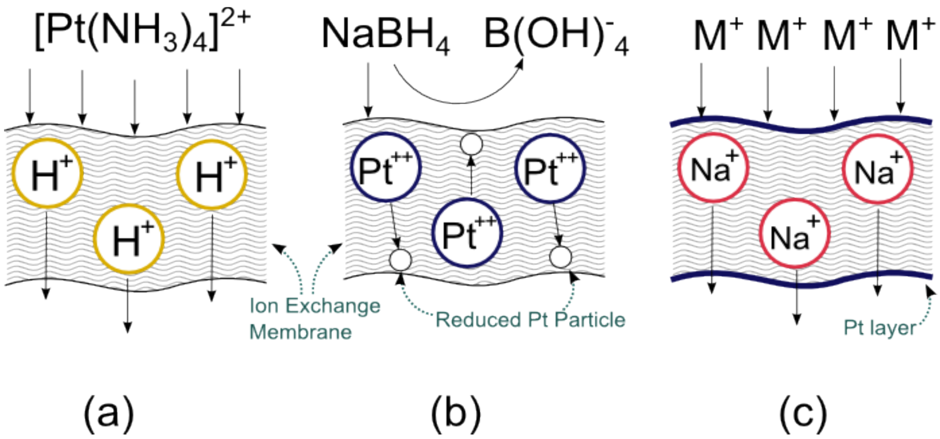

Figure 23: (a) Ion Exchange with noble metal salt, (b) Chemical reduction of metal at membrane surface (c) further ion exchange with desired cation. [48]

Initial compositing process – Ion Exchange / Absorption. The H^+ protons in the membrane are replaced with nobel metal ions. This requires the chemical reduction of an appropriate platinum or gold complex salt such as $Pt(NH_3)_4HCl$ or $[Au(phen)Cl_2]Cl$ [41]. The principle of the compositing process is to metallize the inner surface of the material by a chemical reduction means such as low concentration lithium or sodium borohydride ($LiBH_4$ or $NaBH_4$). Following the ion exchage, a proper reduction with $LiBH_4$ or $NaBH_4$ is introduced to platinize the materials via molecular plating. The reduction agent can be based around any alkali metal, but a higher atomic weight of cation will increase axial stiffness, density and decrease water uptake. Hydrophobic large organic molecules such as tetramethylammonium (TMA+) and tetrabuthylammonium (TBA+) can also be used, but these increase the stiffness further and the final IPMC is found to have a reduced generative force in comparison to the alkali based forms.

The reduction process is carried out a number of times – eight being optimal according to Shahinpoor and Kim [50], each time increasing the platinum concentration at the polymer boundary. This leads to a higher double-layer charge capacity. [50]. The metallic particles are not homogeneously formed across the membrane but concentrate predominantly near the interface boundaries. Shaninpoor and Kim show how the particulate layer is buried up to 20 microns below the IEM surface, and highly dispersed.

Surface Plating - Following the electroless plating of platinum, a further surface plating is often carried out. This is done to decrease the overall surface resistivity, thus increase the charge carrying capacity (which is linked proportionally to generative blocking force). Most commonly this is done with platinum or gold. As Pt is harder than Au, it makes for more stiffness in the final IPMC, thus could be viewed as less desirable.

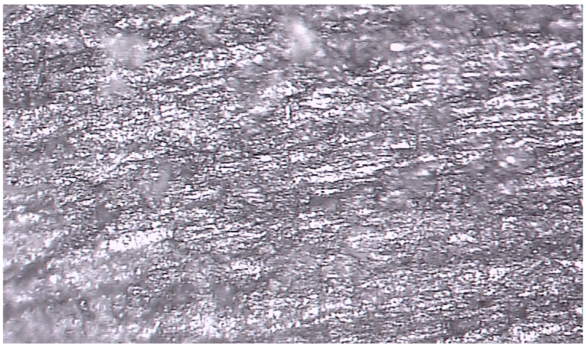

Figure 24: Sample Paladium IPMC after electroless plating (50x Magnification)

The plating process can be done in several ways. The most common method is to electroplate platinum, gold or palladium, though a combination of gold sputter coating and electroplating nickel [59] has been found to be quite effective, as it reduced the need to repeat the electroless plating stage multiple times. This quickens the fabrication process and reduces cost. They found an increase in elastic modulus and tensile strength and decrease in ductility of the bare Nafion film. High elastic modulus and tensile strength are preferable for the structural stability of IPMC actuators.

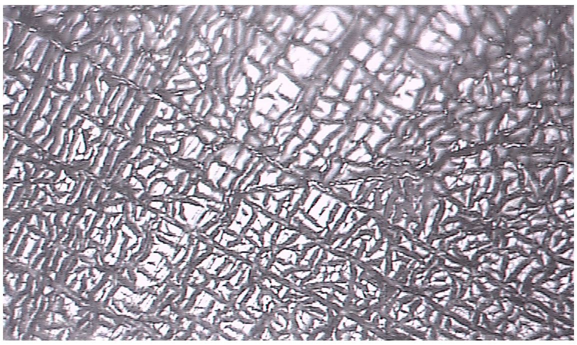

Figure 25: Gold electroplate cracking having been cycled a number of times (50x Magnification)

There has been research into substitutions for plating with expensive noble metals, including use of carbon nano-tubes, graphite and copper. While the use of non-noble metals within the electrodes does produce more cost effective results, (Bennet and Leo [60]), the material can become less stable and tends to have a shorter lifespan due to quicker oxidation. Their simple but effective solution to the cost vs longevity issue is to use noble/non-noble alloys such as a 50% platinum/copper mix – this gave satisfactory results as the surface resistance remains low (which is directly proportional to the actuators blocking force) while only loosing a fraction of the tip displacement.

While platinum and gold retain the accolade of best electrode in terms of output force, the cheaper metals do have some interesting associated properties, such as a reduction of 'back relaxation' when being held for a period by DC current.

IPMC Testing

A small number of varying IPMCs were tested against each other to measure blocking force. The standard publishable method to measure the force is using a 100-200mN Load Cell. This was not available, so measurements were taken from the amount of load recorded by a 4 decimal point balance. Displacement measurements were also attempted, but results were inconclusive. A laser deflection measurement device is required for verifiable readings.

The results found are not overly accurate – overcoming the surface tension of the wet actuator on the dry scales tended to skew the results, but nonetheless some basic forces and understanding of the actuators longevity in dry environment can be taken from the results.

	Surface Plating	Width (mm)	Length (mm)	Thickness (mm)	Dry Weight (g)
Sample 1	Palladium	9.1	33.2	0.11	0.0683
Sample 2	Silver	5.5	32.6	0.19	0.0815
Sample 3	Silver	5.7	24.2	0.18	0.0614
Sample 4	Palladium	5.5	23.6	0.19	0.0595
Sample 5	Gold	7.0	41.7	0.20	
Sample 6	Palladium	5.5	25.7	0.20	0.0635

Table 3: Details of IPMCs tested

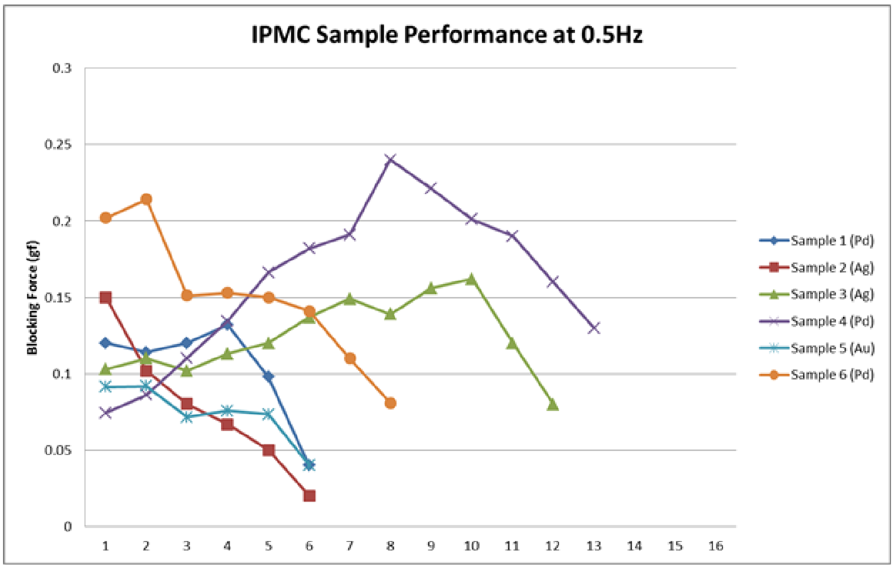

Figure 26: Measured blocking forces of IPMC samples varying in size and surface plating when subjected to 3V at 0.5Hz

As can be seen, the forces exerted by the samples are extremely low. Measurements were taken until displacement had reduced to the point that the sample no longer touched the balance. The samples with the best longevity in dry environment were also the freshest – ie had not be used often. The surface was relatively free of cracking which meant water was less able to escape. Figure 27 shows the typical actuation of a palladium IPMC taken fresh from deionised water.

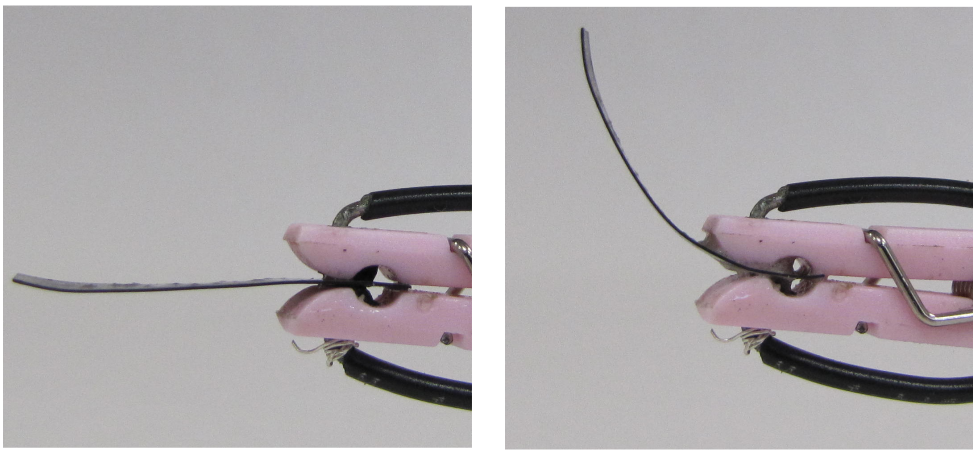

Figure 27: Sample Paladium IPMC

Inherently Conductive (Conjugated) Polymers (IPCs)

Conducting polymers like polypyrrole, polythiophene and polyaniline, can be electrochemically oxidized and reduced in a continuous and reversible way. [82]. When subjected to low voltages in the presence of an isotonic electrolytic salt solution they electrochemically switch, resulting in very large changes to their properties – Conductivity can change by ten orders of magnitude, colour will change, hydrophilic properties become hydrophobic, and mechanical deformation occurs due to a change in volume and Youngs Modulus [83].

ICPs exhibit high tensile strengths, and coupled with their low voltage requirements, they can be seen as quite an attractive option for artificial muscles. Unfortunately electromechanical coupling of these materials is usually found to be less than 1%, unless measured at small strains. This results in an efficiency that is very low unless powered along side substantial input energy recovery. Consequently very high currents can be required to operate at high power [45], which would limit the material in autonomous situations. The observed strain of the actuators is between 2-12% depending on the fabrication method and materials [84], though when immersed in an ionic working solution such as 1-butyl-3-methyl imidazolium tetrafluoroborate (BMIM-PF_6) [86]. Efficiency can be improved by deposition onto platinum wire [ding]. Doing so increases conductivity and enhances rigidity.

The only known attempts to create a full artificial facial musculature to date has been Tadesse et al . These muscles were firstly created using Polypyrrol, Gold and PVDF in sandwich form,arranged in a zig-zag format [85]. In comparison to actuation with single strip cantilevers their arrangement gave a 1.5 times amplification of exerted force, though this was still rather poor at 0.14 mN with a displacement of 0.7 mm. Following on, the same group [84] published their findings on the synthesis of helical PPy actuators for robotic facial muscles. This paper focuses mostly on the helical design and chemical / electrical characteristics, with little reference or attention to the face itself, its contortions or any special movements required for the artificial muscle to create a realistic expression. Nonetheless, they managed to exert 40mN of force with a potential of 0.5V from their 90mm long, low profile helix's. These strands in theory could be bunched together to create a force akin to natural muscle. Unfortunately, to achieve this force, the actuators had to be immersed in an electrolytic solution of tetrabuthylammonium perchlorate (TBAP) which even at the low concentration of 0.04M, is non bio-compatible. This electrolyte biocompatibility problem is perhaps the biggest problem facing ICPs with regard use in the human body.

Shape Memory Alloys

Shape memory alloys (SMA) have been investigated as far back as 1932, when researchers found the alloy of cadmium and gold (at roughly 50% each) exhibited pseudo-elastic properties, returning to their previous shape following heating. The Martensitic phase of the material gives way temporarily to an Austenite phase as temperature increased. The popularity and usefulness of SMAs increased dramatically in the early 1960s when a Nickel-Titanium (NiTi) alloy was shown to exhibit super-elastic properties, have far higher fatigue properties and great ductility than any SMA discovered before (or since). NiTi Nitinols characteristics depends markedly on the history of the sample. A freshly anmnealed wire is soft and pliable, but will become stiff and brittle after a few hundred cycles

NiTi wires and springs have a long history as artificial muscles [61,62,63] because of their non-toxicity and reasonable cost. The most common method for actuation comes as a result of a relatively high electrical resistivity which lends itself well to Joule heating.

The memory effect is normally only observed when an external stress is applied, but it has been shown that NiTi can exhibit a two-way shape memory effect (TWSM) [64] where the alloy will exhibit the shape memory effect without an external stress.

Unfortunately, the method of heating for actuation consumes a large quantity of current, even at low voltages, thus making it difficult to envisage it as the ideal candidate for autonomous in-vivo muscles. In terms of applied force and exhibited stress it is unsurpassed (see table), but hysteresis, non-linearity in position control and a relatively short lifespan due to brittleness after a few hundreds cycles may all prove to be blocking issues that cannot be overcome.

Some short tests were conducted to ascertain how fast a pair of helical SMA coils (8 and 15 turns, 0.5mm gauge) would react when subjected to 10 Volts. This was done by pre-stressing the coils with forces between 750mN to 1.5N with a spring balance, then videoing the resulting recovery.

Figure 28 and 29 show the results. While the gauge of the wire (0.51mm) and diameter of the coils (5mm) was far larger than would be used in an artificial muscle, the speed of recovery and contraction speed were quite slow – 15 to 30 seconds.

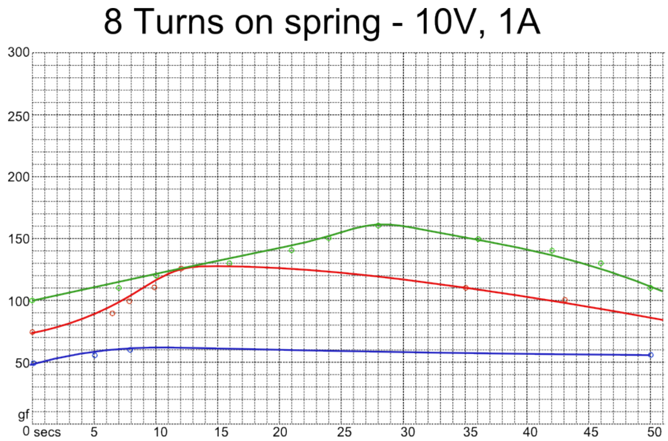

Figure 28: 8 turns in helix

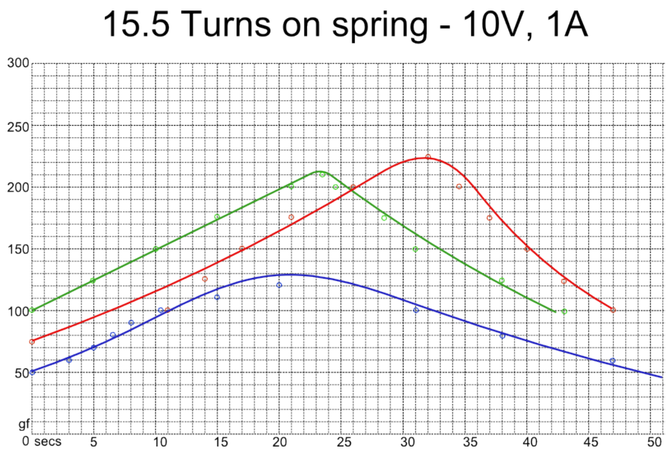

Figure 29: 15.5 turns in helix

	Natural Muscle		Dielectric EAP (Si) CF19-2186		Dielectric EAP VHB 4910		Conductive Polymer		Carbon Nanotube		IPMC Pt Coated Nafion		SMA	
	Typ	Max	Typ	Max	Typ	Max	Typ	Max	Typ	Max	Typ	Max	Typ	Max
Strain (%)	20	<40		120		380	2	12	0.2	1	0.5	3.3	5	8
Stress (MPa)	0.1 sustained	0.35 peak	0.3	3.2	1.6	7.7	5	34	1	27	3	15		200
Work Density (KJ/m^3)	1037			1100		960	100	1000	2	40		5.5	1000	10000
Strain Rate (% / s)		>50		34000		450	1	12	0.6	19		3.3	300	
Power (W/Kg)	50	284		5000		3600		150	10	270		2.56	1000	>50k
Lifespan (Cycles)				$>10^7$			$28x10^3$	$800x10^3$		$140x10^3$			300	10^7
Efficency (%)		40	25	80	30	90	<1	18	0.1	22	1.5	2.9		<5
Modulus (GPa)	$10x10^3$	$40x10^3$	$0.1x10^3$	$1x10^3$	$1x10^3$	$3x10^3$	0.2	0.8	1	10	0.05	0.1	20	83
Activation Potential (V)				$1x10^3$		$1x10^3$	1.2	10	1	30	1.23	7	4	
Tensile Strength (MPa)							30	120	5	>40	5.4	9.8		1000

Table 4: Comparison of Actuator Technologies [44] [45] [51] [66]

A table has been compiled of the various properties reported for the materials investigated in this report.

3.1 Product design specification

The product is to be an implantable 'artificial muscle' device with an actuation that closely mimics the speed, direction and strength of a natural facial muscle. The purpose of the device is as an active prosthetic for restoration of symmetry for the face of a sufferer of facial paralysis. A sensing element must be incorporated to know when actuation is to take place.

Performance

- The device must deliver actuation with a performance similar to that of human facial muscles (see Table 1).
- Actuation should be achievable along X and Y axis and 45° between
- Device must have a low power consumption, so can run continuously for 12 hours between battery recharges. A pacemaker battery is most the likely power source, and these can deliver 2Ah at 2.8V [65]*. This means the device must consume less than 0.47W, though multiple batteries could theoretically be used.
- Different areas of the artificial muscle should be addressable independently, giving various controllable actuation zones.

Maximum Strain	> 40%
Max Exerting Pressure	0.35 MPa
Elastic Energy Density	0.07 J / cm^3
Min speed of full contraction	< 1 sec

Table 1 : Facial Muscle actuation performance [66][67]

* These battery capacities were taken from a 2004 document. Since 2004, much improvement has been made in battery technologies, so this figure can be considered the bare minimum, and most likely modern battery charge density is considerably higher.

Environment

- Hermetic packaging is required to provide the implant's electronic circuitry with protection from the harsh environment of the human body.
- All components must be either autonomously embedded in vivo, or external and telemeteric. Transcutaneous system pose too high a risk of infection.

Competition

- There is currently no commercially available device designed for actuating the whole perioral area, sub-occular and nasolabial area.
- Development of an polypyrrol-metal composite artificial facial muscles for use in robotics is being developed by Virginia Tech University.[68]
- Development of an artificial eyelid closure device for sufferers of facial paralyisis using EPAM (Electroactive Polymer Artificial Muscle). has been developed by Artificial Muscle, Inc., Menlo Park, CA) [69]

Size

- Maxiofacial muscles size vary from person to person. An average size of 10 different cheeks were measured to be 91mm x 42mm, with standard deviation 9mm x 6mm (male) and 80mm x 43mm, with SD 8mm x 5.5mm (female). The 'cheek' in this case was taken to be lip corner to the *temporal styloid process* at the base of the ear, times the bottom of the *zygomatic* (cheek) bone to top of the *mandible* (jaw).
- The device should attempt to be as thin as possible, to minimise being aesthetically noticeable. Muscle atrophy on the paralysed side will increase as time goes on,so the device could have up to 8mm peak thickness

Materials

- The device must be fully encapsulated in a silicone or similar bio-compatible material.
- The actuators will most likely be Ionic Polymer Metal Composites – Either platinum or gold plated Nafion/Flemion, polypyrrol or sulfonated polystyrene.

- The actuators will be immersed in an ionic liquid. This must be non toxic in case of leakage. Water or Saline is the most likely candidate.

Lifespan

- The number of cycles an IPMC can perform varies from material to material. It has been claimed that they can have up to 10 million cycles without significant performance degradation
- (when using the non-biocompatible ethylene-glycol as ionic liquid), but this is less achievable in water based systems.
- The device should have at least a ten year lifetime, to minimise the need for repeat invasive surgery.

Standards

- The device must conform to :
  - ISO13485 – Risk Management and Design standards for implanted devices.
  - Active Implantable Medical Devices Directive Directive 90/385/EEC and 2007/47/EC
  - The American FDA would classify the device as Class III. This means it would be subject to general controls and require premarket approval. Guidelines are set out in CFR Title 21 – Chapter 1, Sub-chapter H. [71]
  - Further standards are IEC 60601-1, for electrical devices and IEC 62304 for medical software.

Ergonomics

- The device must be soft, flexible, lightweight and noiseless.
- There should be as few solid parts as possible.
- All circuitry should be printed directly onto the silicone casing, using silver or similar biocompatible conductive ink.

Quality and Reliability

- The device must be of highest reliability. As installation will require invasive surgery, there is no room for removal for servicing.
- To pass clinical trials, quality must be of the highest standard possible.
- The actuators will be platinum or gold plated, as that offers the best performance. This means the device will not be cheap to manufacture, so there should be no cost-cutting elsewhere in the production process.

Processes

- Fabrication of IPMC. This could be sub-contracted to one of the two suppliers of prefabricated IPMC in the world – Environmental Robots Inc USA, or EAMEX Japan. Cost would be reduced if the process was done 'in-house'
- Design and fabrication of application specific integrated circuit. (ASIC) for control of muscle matrix.
- Sensor network for healthy muscles – hardware, wireless communication and interpretation software required.
- Training software using computer vision based analysis, to re-adjust muscle matrix constantly, to strive for proper symmetrical movement across the users face.

Testing

- Rigorous testing must be carried out. Metrics include:
    - Load actuation ability,
    - Longevity of actuation under load
    - Resistance to corrosion from an in-vivo environment.
    - Impact resistance
    - Testing of electromagnetic output from sensors.

Patents

- There are a number of patents with regard the fabrication of IPMC.
- All software used should be based around open-source code to prevent software patent infringements.
- High quality EMG and EEG sensors are mostly covered by international patents.

Installation

- Installation will be carried out by a plastic, maxillofacial or neurosurgeon.

3.2 System Overview

The system developed comprises of three main sections.

1. An Arduino Mega micro-controller (μC) and power control circuitry designed to control the actuation of shape memory alloy muscles. These actuations are defined by a flex sensor and / or a computer vision system.
2. An animatronic head with silicone sheet representations of the full facial musculature. This musculature is connected to MigaMotor SMA motors at the "*Zygomatic Major*", "*Orbicularis Occuli*" and bottom of the "*Orbicularis Oris*". The timing and degree of these movements are as described in section 2.1.
3. The computer vision system is based on the open-source "Machine Perception Toolbox" (MPT) pSmile library [74], the jMyron WebCamXtra library [75], and pFaceDetect Processing library [76]. The system is designed to detect a face which may be looking at the animatronic head, then if the observing face smiles it will calculate the size of that smile (as an arbitrary percentage level) and actuate the artificial muscles to an equivalent level.

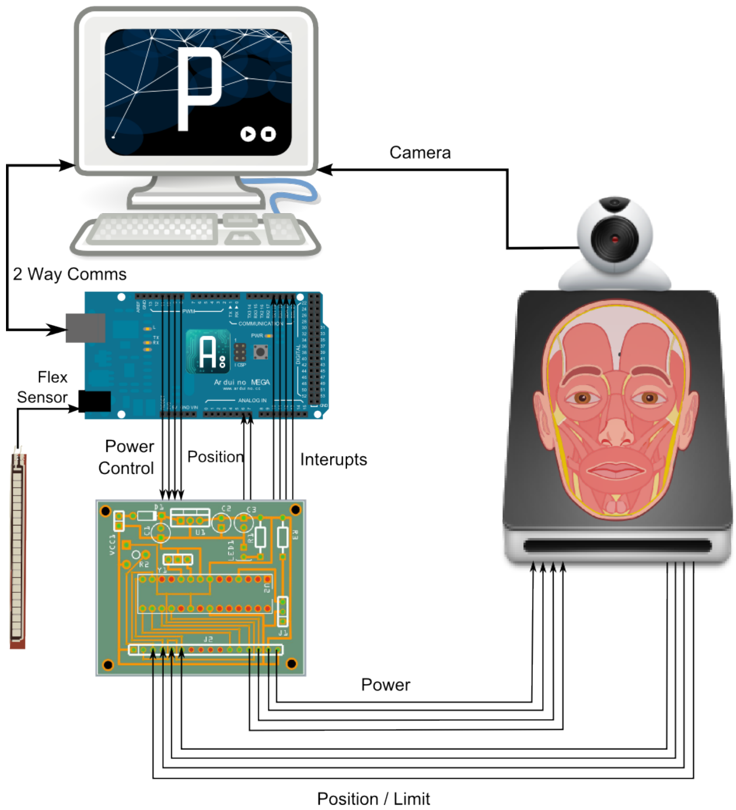

Figure 30: Block Diagram of overall system

3.3 Materials and Methods

The prototype was built around a vacuum formed plaster cast face with a full facial musculature representation cut from 1mm sheet silicone. To actuate the 'muscles' it was decided that Shape Memory Alloy based MigaMotors would be the most appropriate for use in the prototype. The reason for this was choice was their high output force to displacement. Also, like most other 'smart' actuators available they exhibit a non-linear response over time, which was seen as a good way to build a foundation for using other materials in a subsequent device. The solid form factor of MigaMotors mean they would not be suitable for use in an implantable device, but their cascade style design would lend itself to be the basis of a more compliant design based around dielectric EAPs. Also an excellent level of closed-loop control was available when the wiper arm was attached to a linear slide potentiometer.

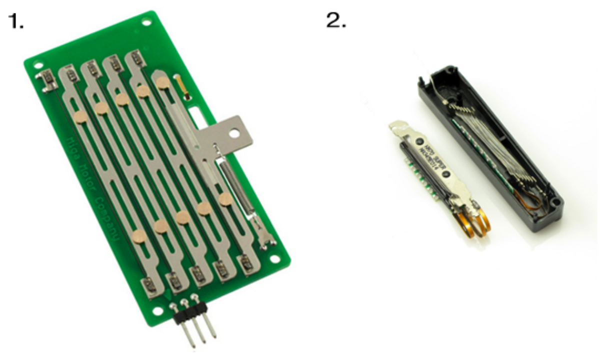

Figure 31: MigaOne Motor (1) and NM70 NanoMuscle (2)

There are two different types of MigaMotor used in the device – The main actuators used the 'MigaOne' (Fig 31) which was used to actuate the zygomatic major (AU12). The MigaOne has a maximum output force of 11N and a stroke of 9.5mm. For the eye and lower lip movement (AU6 and AU25 respectively), the much smaller Miga Nanomuscle (Fig 31) were used. These have a moderate 0.7N maximum force and 4mm stroke, which was sufficient for the purpose.

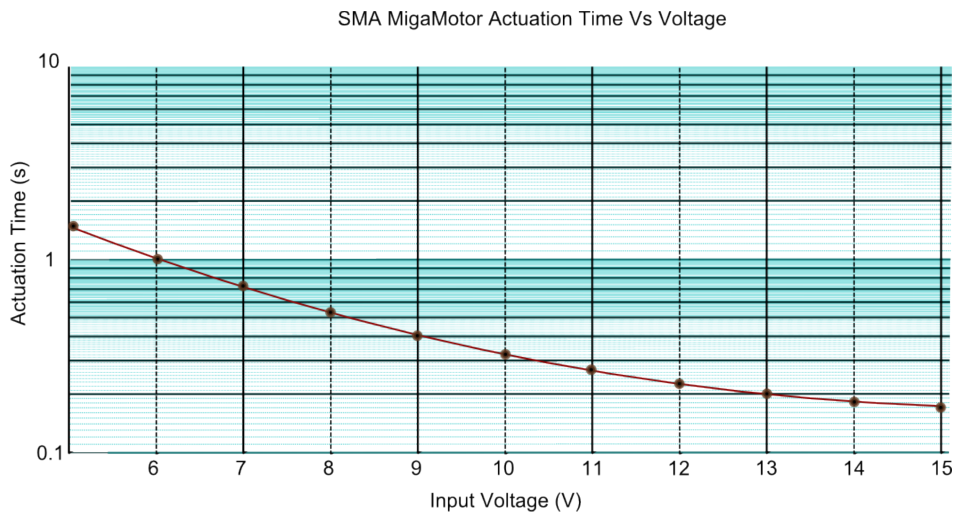

Figure 32: Quoted actuation time for MigaOne

Efforts were made to keep the profile of the actuators as low as possible, so a thin (2.5mm) Alpha 10kΩ linear potentiometers was chosen for position indication. An acrylic mounting was laser-cut to hold the motor and pot securely together (Fig 33 and appendix D)

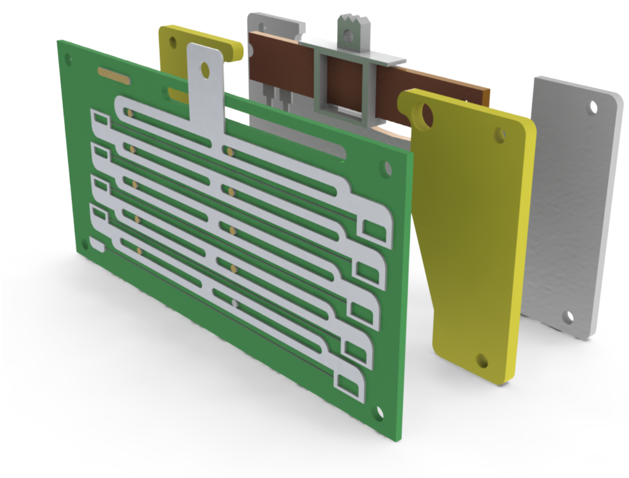

Figure 33: 3D representation of MigaOne, with position sensing potentiometer and acrylic support structure.

3.4 Circuit design

The circuit comprises of four parallel LM338 5A adjustable voltage regulator circuits arranged as current limiters. Two of the regulators were utilised to limit of each individual MigaOne motor, with a desired current limit of 0.85A each. The other two regulated each pair of NanoMuscles (NM70) that actuated the eyes and lower lip.

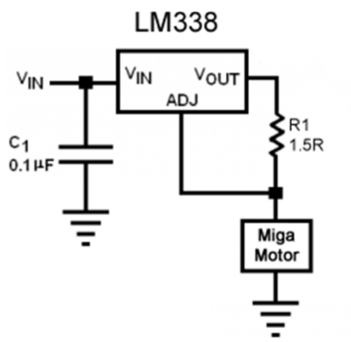

Illustration 34: LM338 Current Limiter

The desired maximum control current for each Nano-Muscles was 0.35A. It was decided to limit the current to 700mA and run two – one for either side of the 'face' in parallel, thereby splitting the current according to Kirchoff's current law. The current limit was calculated by the following formula :

$$I_{out}=\frac{V_{ref}}{R_1}$$

In this case R_1 for each MigaOne was 1.5Ω (with 1 Watt dissipation) and 1.8Ω for each pair of NM70s, where the internal reference voltage V_{ref} is 1.25V.

Two of the current regulators are preceded by a voltage limiter – These are for the Miga Nano-Muscles, which have a much lower voltage threshold. A simple LM7806 circuit was used to limit each pair of nano-muscles to 6V input.

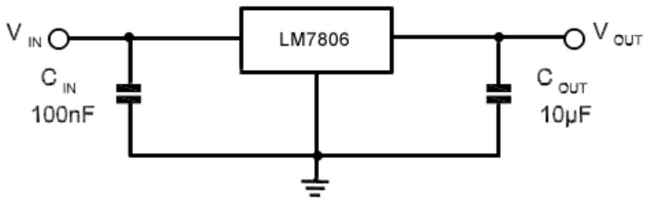

Figure 35: 7806 6V limiter

Following the power supply circuitry, there is a group of four Darlington NPN (TIP121) open collector circuits. These are controlled by the microprocessor digital output via pulse width modulation (PWM). The advantage of using an open drain circuit was one of protection from over-voltage for the fragile shape memory alloy wires, as voltage can be gradually increased via a processor loop until the 'contracted' signal becomes active. A 1kΩ pull up resistor is used across the four circuit blocks. The contracted signal was unaffected by the variable input voltage and could output at near TTL logic level. The ambient temperature susceptibility and hysteresis of the SMAs was also reduced through this method.

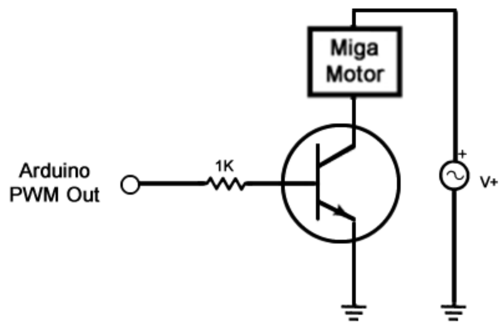

Figure 36: Open Drain Collector for Miga Motor Control

The Arduino is limited to six analog inputs, so to keep a watch on the state of the NM70 nano-muscles, the extended output pin of the nano-muscle is monitored for change via an LP339 comparator. The signal goes to TTL logic high when the pin voltage exceeds a reference 1.5V. This reference voltage was made by reducing the 3.3V Arduino power signal via an LM317 Voltage limiter circuit. As the NM70s are powered in pairs, corresponding to muscles on either side of the face, both extended pins are then fed through an 74LS08 AND gate. This was to economise on Arduino interupt pins, and to ensures both motors are symmetrical before being sent low. As the signal is converted to TTL and used to trigger an interrupt, the Arduino can watch each pair of motors independently of the running code – ie without constantly polling the muscles to check their situation. As soon as the logic gate goes high, signifying a pair of motors are fully contracted, then an interrupt function is triggered which has instruction to reduce the input voltage to 50% duty cycle PWM.

A 42Ω current drain is put on the non-inverting input pin of the LP339 (LM393 for the MigaOne limit pins). This was required as the current that flows from the extended limit pin of the SMA motors tended to damage the comparator chip after a small number of interrupts, driving the output to a constant V+ level, which meant a constant interrupt signal on the Arduino. It was calculated that a 12Ω 1 watt resistor would be required to drop the current down to the specified input current limit of the comparator – 50mA, but in doing this, the voltage dropped significantly as well. The result was the non-inverting input would never hit a voltage higher than Vref. Experimentally it was found that 42Ω was the lowest resistance that would work satisfactorily, and after numerous (100+) tests, the comparator has suffered no ill effects. The full schematic can be seen in **Appendix D.**

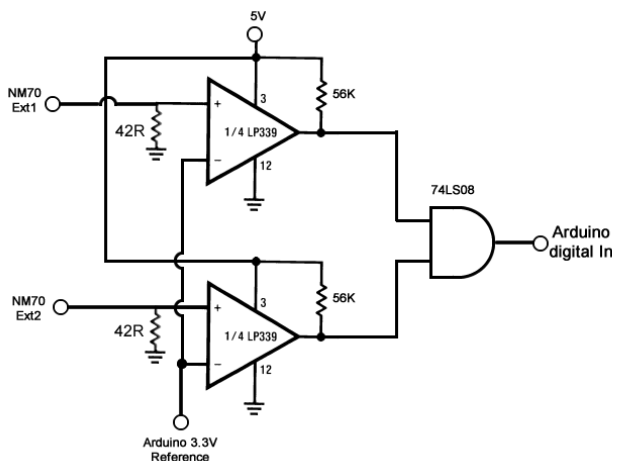

Figure 37: Comparator and logic circuit for Interrupt

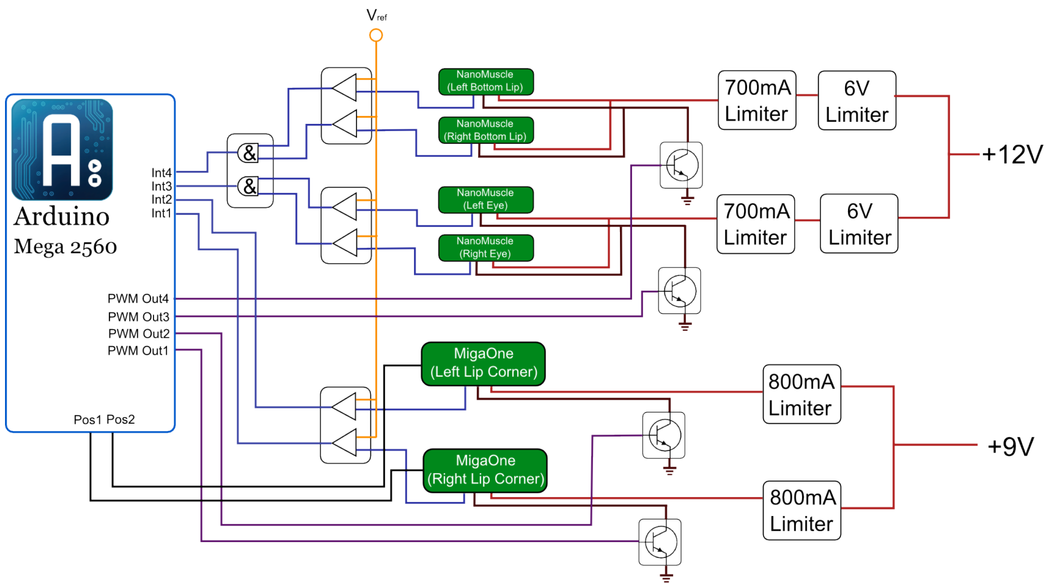

Figure 38: Power control circuit block diagram

3.5 Microprocessor development & control algorithms

The actual control of the circuitry was achieved using the variable pulse width modulation (PWM) outputs from an Arduino micro-controller (μC). Initially the Arduino Deumillnove was used, but as this board only had two interrupt pins, a larger Arduino Mega 2560 had to be utilised instead.

As the code begins, an initialisation procedure is carried out on the MigaOne motors. The position of the control pots are read ten times and averaged, then the motors are activated fully. When they reach their maximum stroke, the limit pin is short circuited and (as explained in the previous section), a comparator is triggered high which causes an interrupt on the μC. There is an individual interrupt function for each MigaOne which reads the position of the control pot at full extension, and takes note of the current time. The difference in lower and upper (less 5% safety margin) potentiometer positions are taken to be the full actuator sweep for each of the motors. Depending on the ambient temperature and previous stress exerted on the motors, it was noticed that their speed of actuation can vary – one often arriving at its limit before the other. By noting the difference in the time of interrupts, the faster motor can be slowed down proportionally, thus making the smiling motion of the silicone muscles symmetric in onset. The initialisation function flowchart and code is viewable in Appendix A.

The code itself is written to read from two different sensors. A variable resistive flex sensor was used as a representation of implantable flex sensors (discussed in chapter 1.4.3). The output of the sensor exhibits a near linear response from a bend of 0-180˚. This was mapped directly to the individual potentiometer control ranges. A threshold to ignore the first 10% of the flex sensor was set. This was deemed necessary as the sensor does not always go back to being absolutely flat having been bent for a period of time, and as it has precedence over the computer vision system control, this residue flex could lock the CV system out.

The other control method for the muscles is via a computer vision (CV) system for smile detection, written in Processing, with a Java Class that passes captured images from the video stream into the MPT pSmile API. This will be discussed in more depth in the next section, but in terms of Arduino, the percentage of smile read is sent from Processing via a serial port to the μC. As with the flex sensor, this value is mapped to the control potentiometer ranges. Within the system, the flex sensor takes precedence over the CV signal. The smile that is created is continuously variable according to the measured percentage of flex. If more than 10 seconds of continuous flex is recorded, the motors are switched off to protect and increase longevity of the SMA wires. Brittleness and reductions in speed became apparent during testing as the motors were continuously cycled.

In contrast to the flex sensor, the CV control performs an non-interruptible smile, whose duration and amplitude is proportional to the percentage size of smile recorded in by the Computer Vision / Processing. This ranges from 1.5 to 4 seconds as per measured values discussed in **section 1.2.4.**

Full program flow is available in Appendix A.

3.6 Computer Vision and interactive interface

As mentioned at the start of this chapter, the computer vision section of the prototype is built using a expression recognition library based around OpenCV called the “Machine Perception Toolbox” (MPT). This API has a whole suite of real-time perception primitives, including face detection, eye detection, blink detection and color tracking [74]. Currently, a move is being made to include a full suite for facial expression recognition. The pSmile library used is one of the early examples of this – one which has been now compiled for many platforms including iOS, Android, Processing etc. [75]. The major strength of this library is it was specifically designed for use in uncontrolled lighting situations, unlike most others which were built for facial detection in laboratory conditions [72]. The basic functional flow of the library is as described in section 1.3.4, where 63,000 smiling face photographs were used to build a Haar Classifier of varying smile intensities. When a oriented still image is passed to the API from a camera class, the algorithm uses a combination of Canny Edge detection (Edge Orientation Histogram) and Box Filters (Viola-Jones) to calculate a position and shape for the smile. Finally adaptive boosting (Gentleboost implementation) is used to classify and progressively add new components to the Haar Cascade [73].

The Processing program written for this project also uses the pFacedetect library in conjunction with a Haar Cascade taken from the OpenCV library (haarcascade_frontalface_default.xml). This was used to detect and track the movement of a face in front of the camera. When a face is detected, the Processing program begins to listen on the USB serial port for a signal from Arduino indicating that it is not busy (either with flex sensor actuation or completing a previous CV requested smile). The signal in this case is the transmission of an 'R' character - ASCII 82. Processing then implements a handshaking procedure (Fig 39) followed by transmission of an average of the previous two smile values recorded. The smile detector can be quite 'jumpy' in terms of its classification of smile intensity, though this improves in proportion to the computational power available. It was for this reason that the most recent two non-zero value smiles are averaged before TX. It would have been preferable to average more than two, but this affected the real time performance of the system. Any time a wait (while()) loop is instigated during handshake, a watchdog timer is set for five seconds to prevent the system from hanging, should data get lost or corrupted on the serial line. Should this timer ran out the Processing code is restarted (setup();) and all variables reset. This is also done in Arduino using the AVR watchdog function.

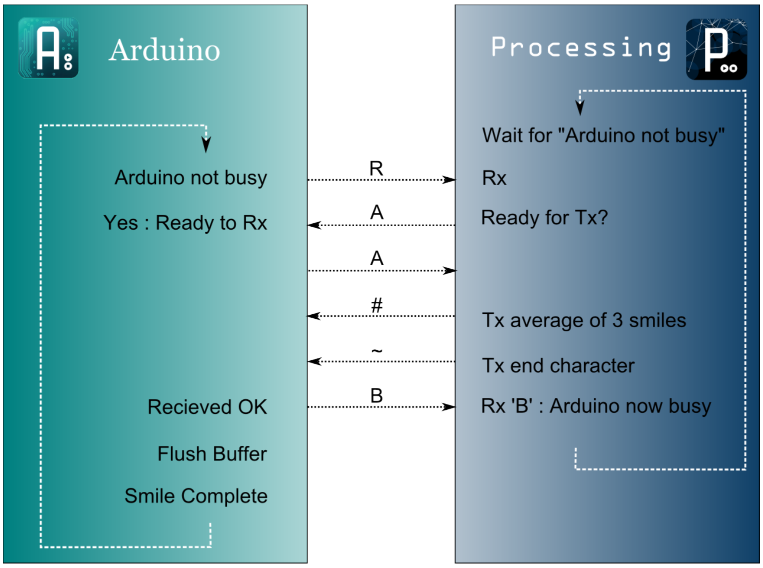

Figure 39: Arduino and Processing Serial Handshaking

It was noticed that measured smile intensities above ~60% were extremely difficult to achieve and maintain. For the purposes of the interactive model, a logarithmic 'delinearising' function was added, so small smiles would result in more visible actuation on the animatronic head. A graph of measured to transmitted values is presented in Fig 40.

For the Class to gather the prerequisite variables to be passed over to the pSmile API the jMyron WebCamXtra library was chosen. This Processing native library is quick and useful for video still capture, among other computer vision tasks.

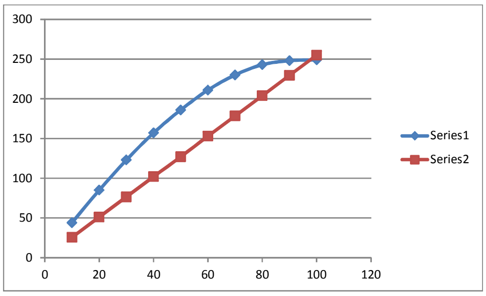

Figure 40: Delinearising Smile values for serial transmission

In terms of the front end interface, When a person comes into view of the camera, a faux LED will change on screen from red to green, and a circle is drawn around the face, moving as the face does. A 'smile-meter' needle class shows how much of a smile is detected. Figure **38** shows example of this. The full program flow SDL/UML and code is detailed in Appendix A and B respectively.

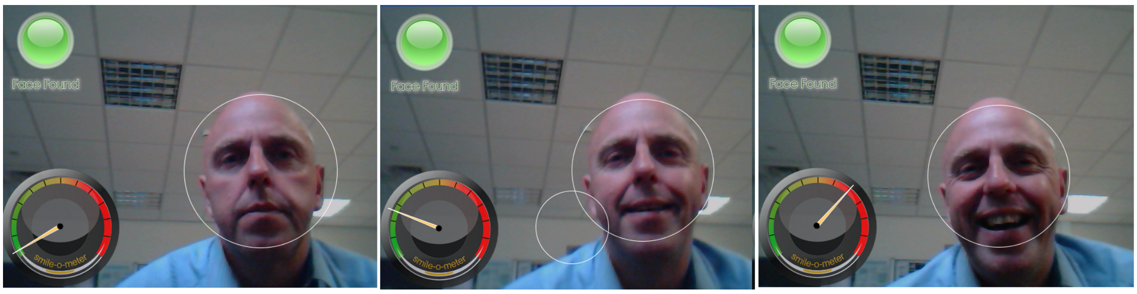

Figure 41: Screenshots from front-end interface

Note : False positive second face found in picture 2

3.7 Model design and conceptualisation

The model was build around a vacuum formed plaster cast face. Initially it was planned to put a silicone musculature beneath a thin latex 'skin' which could be actuated from behind silicone 'muscles'. Some tests were made to find the best method of creating a latex skin. Painting thickened latex gave too uneven a coat, and dipping the face created too thick a skin. A test was then made by sandwiching latex between two pieces of between high impact polystyrene (HIPS) to create a thin layer. When treated this way the latex, instead of drying while sandwiched, formed a vein like pattern.

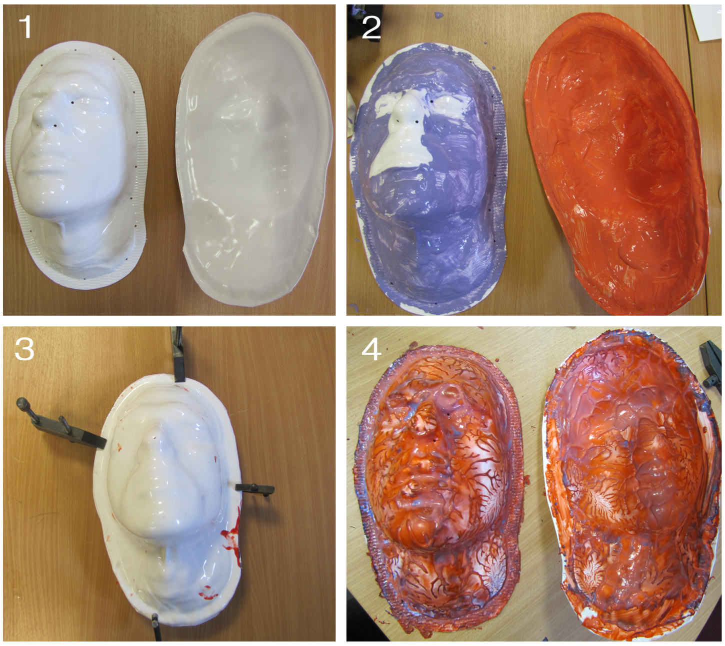

Figure 42: Creating the submusculature layer of the animatronic head.

It was subsequently decided to use this 'vein technique' to create a representation of the sub-muscluture layer, and forgo the skin. To achieve this, a sheet of 2mm HIPS was formed on the plaster cast face. The two were separated, and some small holes drilled into the nostrils and corner of the eyes. The plaster casting was replaced, then covered with a stretched elastic cloth followed by an nylon stocking which helped to keep the cloth tight. This was vacuum formed a second time (this time with 1mm HIPS). The nostril and eye holes helped the vacuum to form the second layer of plastic tightly around the features of the mask beneath. The resulting two HIPS masks constituted a male/female mould spaced approximately 0.5mm apart. This gap was left to create an even area for the 'veins' to form. When before putting the two moulds together Vaseline was applied to the outer mould to reduce the adherence of the latex to the HIPS. A thin layer of latex with added thickening agent (aprox 50:1 ratio) was painted to both moulds, and then clamped together and left over night to set. Separating the two moulds after 12 hours, as hoped the latex had not set due to a lack of aerification (the drilled holes being insufficient). The Vaseline made the latex coalesce into fractal vein-like patterns across both surfaces.

Subsequent experiments were made by layering different shades of blue and red latex with varying ratios of thickening agent, in an effort to create a realistic representation of the sub-musculature layer of the face. Step by step images of the process are shown in Figure 42, and development stages shown in Appendix F.

A musculature was then laser cut from 1mm silicone sheet. The outline, while not wholly realistic in term of anatomy (see section 2.1) was designed as a representation to show the position of the various facial muscles and their insertion and termination points. To improve ductility and deformation, the sheet was laser etched with numerous lines. These lines did not penetrate completely through the rubber, but their presence dropped the force required to move the eye area by half (1N to 0.5N). This was below the maximum output force of the NanoMuscles.

Illustration 43: Musculature laid out flat

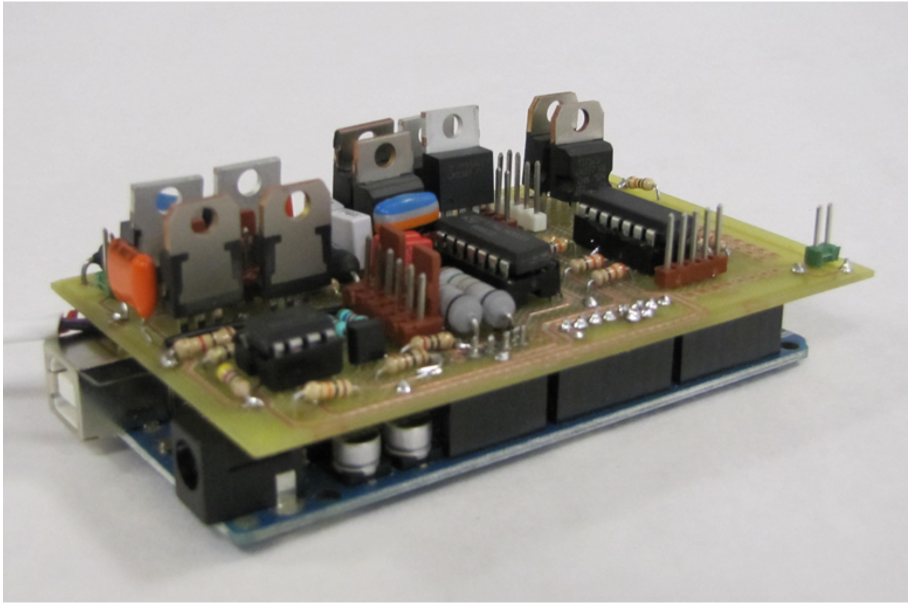

Figure 44: Final printed circuit board mounted on Arduino Mega

Figure 45: Sub-musculature layer (left) and Final device in aluminium stand with camera (right)

4. Future Development and Recommendations

There are many areas with great potential that could be explored in future. In terms of actual artificial muscle design, Dielectric EAPs and IPMC are well worth study, both in fabrication and integration. Of particular interest would be the use of silver (or similar) printed circuitry on a thin silicone substrate, to address a matrix of actuators. Printed circuits would afford better compliance, full encapsulation and reliability. That said, both technologies have issues that first must be overcome.

EAPs with their extreme voltage requirements (albeit whilst drawing minimal current) are unconfirmed in terms of biocompatibility. Any device designed would require years of clinical trials to be proven safe. Even though Artificial Muscle Inc (AMI) have been investigating how EPAMs react in live animals, they have released no findings after two years. It can only be speculative as to what this might mean.

On the other hand, EAPs have a huge number of advantages over all the other actuator technologies. They are relatively cheap and the various procedures required to fabricate are moderately simple. The reaction time is extremely fast – in the kHz range of frequency response. The blocking and actuation force exceed that of natural muscles, is easily shaped into whatever form is required, and it has an excellent level of compliance. In some respects, its control would be counter intuitive, as it would require power to maintain a neutral, relaxed expression. Contraction of the muscle would involve reduction of potential across its electrodes. The actual layout and shape of an EAP muscle would need to be experimentally refined. As the base polymer comes commercially in tape form (at least with NuSil and VHB) the actuator must be designed in layered two dimensional planes. This is contrary to something like the bending actuators standard linear form, Fig 46

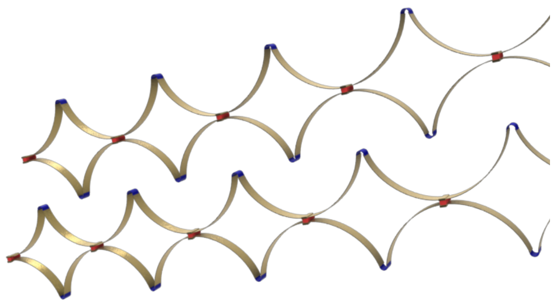

Figure 46: Bending actuators linear form

IPMCs on the other hand are almost inverse in terms of their strengths and shortcomings. Foremost in their favour is bio-compatibility, but also the ability to be liquid cast into any shape, thickness and configuration required. On the other hand, to be realistic in terms of facial muscles, their blocking force to speed ratio would need to be addressed. That said, proficiency in the fabrication of IPMCs would be interesting for research into applications outside of aesthetic facial muscles, where speed is less important. Valves, constrictive and expansive sphincters and micropumps in particular look like ideal candidates for these classes of artificial muscle.

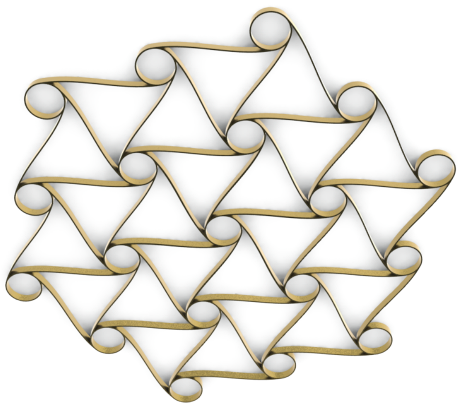

Figure 47: Auxetic layouts such as the 'Chiral Honeycomb' would lend themselves well to circular sphincter type muscles.

Research into resonant inductive coupling for the constant powering or charging of an implanted muscle could make for interesting findings, particularly as it would reduce dependency on small implanted batteries. Likewise wireless telemetry for control and sensing signals would mean the processing could be done ex-vivo – perhaps on a smart-phone or similar 'pocket computer'.

Improving the Computer Vision system could be a rich and fruitful area, both in terms of the machine learning and active recalibration of an artificial muscle, but also for use as a standalone program for use as occupational therapy aid, when a paralysis sufferers access to a clinical practitioner is limited. Work would have to be carried out to improve the accuracy, perception of a varying range of expressions and the real time performance of the program before this could become fully viable, but this would be very much an attainable goal. Accessing the MPT API in native C/C++

rather than via Processing libraries would be essential. An extremely interesting option would be to attempt 3 dimensional tracking via a stereoscopic camera such as the Xbox Kinect.

Sensing as a whole needs to be addressed. The prototype relied on computer vision or hand controlled flex sensors. This must be superseded by more accurate and realistic methods of control. Surface EMG along side actual size thin film piezoelectric flex sensors (which could be attached to the face) would be the recommended next avenue to peruse. The piezoelectric flexor could be very interesting - symmetrical sensors could be used on both sides of the face, with the artificial side to control and read its own position of actuation and the natural side to know when and where expressions are occurring.

Finally a more realistic model of the face must be built for testing purposes. A silicone musculature does not give a very realistic representation of the actual requirements to move a paralysed face. As any viable implantable solution is many years away, and much development work must be completed first, it is imperative to have an anatomically realistic test bed upon which to build the muscles.

5. Conclusion

Investigation of a wide range of materials and methods, along with a surface level investigation of facial anatomy and facial expressions has shown that an active prosthetic solution for facial paralysis requires more than a set of simple actuation devices. The speed, timing and power consumption are just a few of the many considerations.

It is clear from facial anatomy and expression research that an actuator with multiple degrees of freedom, with independently addressable 'actuation zones' is required to recreate even the most basic proto-expressions such as a smile. The maximum size/area of the artificial muscle is severely limited when correlated to the amount of strain that is required, especially in relation to the actuation stress that must be exerted. Stacking of thin film actuators should help to overcome this limitation.

The study of the Facial Action Coding System has helped demonstrate how many variables could potentially be involved if the muscle were to attempt to recreate multiple expressions. With this in mind, further development should still concentrate on the creation of a limited number of convincing movements such as smile and squint, rather than aim for universal expression. When the basic movements are being convincingly recreated then further expressions can be added to the muscles 'repertoire'.

The materials to be used are still debatable – every actuator type discussed has its own strengths and weaknesses. Much emphasis was placed on IPMCs within the research, as it seems they are the most likely to provide a stable long term solution. That stated, their relatively embryonic stage of development in terms of published fabrication methods and control mean they may not provide a mature enough technology to proceed directly with in the next stage. Their speed to force ratio must be addressed. Achieving a reduction of production cost must also be addressed. A combination of IPMC and Conductive Polymer actuators such as the sulphonated polystyrene (sPS) may achieve good results and provide a pathway towards addressing these concerns.

In the mean time, it seems most viable to concentrate on dielectric EAPs as a next prototype stage. Even if it subsequently transpires that their high voltage requirement creates bio-compatibility issues, they are currently the only compliant polymer actuator that matches almost all the performance metrics of natural muscle while retaining a low power consumption and price. Their robustness and longevity is perhaps the only major issue that must be addressed.

The technology for sensing healthy muscle is in a mature state of development. All the methods researched and discussed are viable (perhaps with the exception of EEG, which still needs more research), and are in a position to only require integration rather than amelioration. Further development may find that a combination of two or more of the methods discussed yield the most reliable results.

The ideas suggested and developed for a computer vision system show great potential. A refined expression recognition system for occupational therapy is perhaps one outcome from this project that could see market realisation far quicker than other aspects. Without the need for clinical trials or approval, such a program could be in the market place within a small number of years. If this were to be the case, a different approach to programming the system would need to be taken, much of which has been discussed in the Future Development section. Such a program would have usefulness far beyond helping those with permanent facial paralysis, including speech therapy and paresis, amongst others.

The physical prototype which was developed for the project has helped to confirm or disprove a number of assumptions that were taken early in the investigation. The use of non-flexible motors meant indirect actuation of the muscle was necessary. This lead difficulty in rigging the muscles, and an inability to push as well as pull. It is felt that every subsequent development should focus on an *in-situ* design which will change its own shape rather than expect the no-longer functional muscle to create expression on the face, having been pulled from a single or small number of point(s).

The use of shape memory alloys has confirmed two of their biggest downsides – namely power consumption and brittleness over time. Their 10W (average) power consumption would not be sustainable from an implanted pacemaker battery. Constant indirect resonant induction charging from an external power-pack would be an option, but it is the authors belief that the more efficient actuators who's movement is caused by either ionic transfer or Maxwell stresses would be a much better option.

The ideal situation for an eventual design would be to have all power and control signaling to the device inductively telemetered through the skin, preventing the need to embed digital signal processors or power sources. This is eminently possible with commercially available technologies.

In summary, the creation of robust artificial facial muscles with an ability for biomimetic actuation is certainly possible, but to do so successfully will require a multi-disiplinary team of clinicians and anatomists along side computer and material scientists and product designers. When that happens, there is little doubt that numerous other solutions to clinical problems will be discovered indirectly, as happened with the suggestion of the computer vision as an occupational therapy device in this project.

It is a very exciting time to investigate solid-state flexible polymer actuators, just as printed electronics and ultra low power computational and wireless communications systems are becoming increasingly available. This leads to potential for medical device and innovative healthcare development which could be considered near endless.

6. References

[1] Breedon P, Vloeberghs M. (2009) Application of shape memory alloys in facial nerve paralysis. *AMJ* 2009, 1, 11, 129-135. Doi 10.4066/AMJ.2009.86

[2] Ekman, P., & Friesen, W.V. (1978). Facial Action Coding System (FACS): A technique for the measurement of facial movement. Palo Alto, CA: *Consulting Psychologists Press.*

[3] Craig W. Senders C.W., Tollefson, T.T., Curtis S, Wong-Foy A, Prahlad H, (2010) Force Requirements for Artificial Muscle to Create an Eyelid Blink With Eyelid Sling. *Arch Facial Plast Surg*. 2010;12(1):30-36.doi:10.1001/archfacial.2009.111

[4] Facial Paralysis Institute webpage on facial nerve transfer :
http://www.facialparalysisinstitute.com/18/Hypoglossal_facial_nerve_transfer.html
Accessed June 2011.

[5] Brown, W.M. and Moore C. (2002) Smile asymmetries and reputation as reliable indicators of likelihood to cooperate: An evolutinary analysis. *Advances in psychology research* Vol 11 pp59-78

[6] Ekman P. (1982) Facial Expression and Facial Nerve Surgery. Disorders of the Facial Nerve. Graham M & House W (eds) *Raven Press* 1982

[7] Frank M.G. And Ekman P (1995) All smiles are not created equal : the differences between enjoyment and nonenjoyment smiles. *Humour* 6-1 (1993) pp9-26

[8] Rubin, L.R (1973) The anatomy of a smile : Its importance in the treatment of facial paralysis – *From Plastic and Maxillofacial Services of the Nassau County Medical Centre,* presented to AGM of the American assoc. of plastic surgeons, June 1973.

[9] Rubin, L.R. (1999) The anatomy of the Nasolabial Fold : The Keystone of the Smiling Mechanism. *Plastic and Reconstructive Surgery,* Vol 103(2) February 1999 pp 687-691

[10] Cohen J.F and Schmidt K.L. (2004) The timing of facial motion in posed and spontaneous smiles. *International Journal of Wavelets, Multiresolution and Information Processing* 2, pp1-12

[11] Schmidt K.L., Ambadar Z. Cohn J.F, and Reed I., (2006) Movement differences between deliberate and spontaneous facial expressions : Zygomaticus Major Action in Smiling. *Journal of Nonverbal Behaviour* 2006; 30(1) pp37-52. Doi:10.1007/s10919-005-0003-x

[12] Valstar, M.F., Gunes H, Pantic M, (2007) How to distinguish posed from spontaneous smiles using geometric Features. *Proceedings of The Ninth International Conference on Multimodal Interfaces (ICMI 2007). November 12-15 2007.* ACM 2007

[13] Bradski G and Kaehler A,(2008) Learning Open CV – Computer Vision with the OpenCV Library. *O'Reilly Books* 978-0-596-51613-0

[14] Viola, P. Jones M (2001) Robust Real-time Object Detection. *Second international workshop on statistical and computational theories of vision – modeling, learning, computing, and sampling.*

[15] Freeman W.T., and Adelson E.H.. (1991) The design and use of steerable filters. IEEE *Transactions on Pattern Analysis and Machine Intelligence*, 13(9):891–906, 1991

[16] Whitehill, J and Omlin C.W. (2006) Haar Features for FACS AU Recognition. FGR '06 *Proceedings of the 7th International Conference on Automatic Face and Gesture Recognition*

[17] Jang Y, Woo W, (2009) Adaptive Lip Feature Point Detection Algorithm for Real-Time Computer Vision-Based Smile Training System M. Chang et al. (Eds.): *Edutainment* 2009, LNCS 5670, pp. 379–389, 2009. Springer 2009

[18] Whitehill J, Littlewort G, Fasel I, Bartlett M, and Movellan J, (2008) Developing a Practical Smile Detector. IEEE Transactions on Pattern Analysis and Machine Intelligence (2009) Volume: 31, Issue: 11, pp: 2106-2111

[19] Harris C, Stephens M, (1988) A combined edge and corner detector. *White Paper* - Plessey Research Roke Manor, United Kingdom

[20] Lucas B.D. and Kanade T.(1981) An iterative image registration technique with an application to stereo vision. In *Proceedings of the 7th International Joint Conference on Artificial Intelligence,* pp 674–679, 1981

[21] Tomasi C and Kanade T. (1991) Detection and Tracking of Point Features - *Carnegie Mellon University Technical Report* CMU-CS-91-132 : Shape and Motion from Image Streams: a Factorization Method– Part 3

[22] T. Kanade, J. Cohn, and Y.-L. Tian, "Comprehensive database for facial expression analysis," in *Proceedings of the 4th IEEE International Conference on Automatic Face and Gesture*

Recognition (FG'00), March 2000, pp. 46 – 53.
[23] T. Sim, S. Baker, and M. Bsat, "The CMU pose, illumination, and expression database," *IEEE Transactions on Pattern Analysis and Machine Intelligence*, vol. 25, no. 12, pp. 1615–1618, 2003.

[24] M. Pantic, M. Valstar, R. Rademaker, and L. Maat, "Web-based database for facial expression analysis," in Proc. IEEE Int'l Conf. Multmedia and Expo (ICME'05), Amsterdam, Netherlands, 2005.

[25] A. OToole, J. Harms, S. Snow, D. Hurst, M. Pappas, and H. Abdi, "A video database of moving faces and people," *IEEE Transactions on Pattern Analysis and Machine Intelligence*, vol. 27, no. 5, pp. 812–816, 2005.

[26] Nigg B.M., & Herzog W., 1999. *Biomechanics of the Musculo-Skeletal system.* Wiley. pp 349

[27] Kamen G & Gabriel D.A. (2010) Essentials of Electromyography. Published by Human Kinetics. ISBN 10:--7360-6912-4

[28] Abbs J.H., Gracco V.L. and Blair C, (1984) Functional muscle portioning during voluntary movment : facial muscle activity for speech, *Experimental Neurology* 85 pp 469-479

[29] Roy, S.H., De Luca G, Cheng, M.S., Johansson A, Gilmore L.D., 2007 Electromechanical stability of surface EMG sensors. *Medical and Biological Engineerin and Computing* 45, pp447-457

[30] Merrill D.R., Lockhart J., Troyk P.R., Weir R.F., and Hankin D.L. (2011) Development of an Implantable Myoelectric Sensor for Advanced Prosthesis Control. *Artificial Organs* 35(3):249–252, Wiley Periodicals, Inc.

[31] Weir R.F., Troyk P.R. and DeMichele G.A., (2009) Implantable myoelectric sensors (IMESs) for intramuscular electromyogram recording. *IEEE Trans Biomed Eng 2009*;56:159–71.

[31] Niedermeyer E, Lopes da Silva, F.H., (2005) *Electroencephalography: basic principles, clinical applications, and related fields*, Lippincott Williams & Wilkins, 2005 p18

[33] Boot, L (2009) Facial expressions in EEG/EMG recordings. University of Twente *MSc Thesis.* http://essay.utwente.nl/58633/1/scriptie_L_Boot.pdf

[34] Korb S. Grandjean D Scherer K, (2008), Motor Commands of Facial Expressions: The Bereitschaftspotential of Posed Smiles. *Brain Topography* DOI 10.1007/s10548-008-0049-2

[35] Rinn W.E., (1984) The neuropsychology of facial expression: A review of the neurological and psychological mechanisms for producing facial expressions, *Psychological Bulletin*, Volume 95, Issue 1, January 1984, Pages 52-77, ISSN 0033-2909, DOI: 10.1037/0033-2909.95.1.52.

[36] Korb S. Grandjean D Scherer K, (2008), Investigating the production of emotional facial expressions : a combined electroencephalographic (EEG) and electromyographic (EMG) approach. *8th IEEE International Conference on Automatic Face & Gesture Recognition*, 2008. FG '08.

[37] Laukhina E, Pfattner R, Ferreras L.R., Galli S., Mas-Torrent M, Masciocchi N, Laukhin V., Rovira C, and Veciana J. (2010) Ultrasensitive Piezoresistive All-Organic Flexible Thin Films. *Advance. Materials*. 2010, 22, 977–981.

[38] University of Southampton – *Automation and Robotics* – Sensors webpage
http://www.soton.ac.uk/~rmc1/robotics/artactile.htm (accessed June 2011)

[39] Measurement Specialties, Inc. Piezo Film Sensors Technical Manual. P/N 1005663-1 REV B 02 APR 99

[40] Bar-Cohen Y. (2002) Electroactive polymers as artificial muscles. *Reality, Potential and Challenges. SPIE Course on EAPAD 2002*

[41] Wu, Y.. Electroactive Polymer Actuators and Sensors – *Experimental Characterization and Modeling of Ionic Polymer metal Composites for Biomedical Applications*. Lambert Academic Publishing 2010

[42] NASA Jet Propulsion Laboratory - Comparison of EAPs with Other Actuator Technologies http://ndeaa.jpl.nasa.gov/nasa-nde/lommas/eap/actuators-comp.pdf (accessed May 2011)

[43] Pelrine R, Kornbluh R, Pei Q, Stanford S, Oh S, Eckerle J. (2002) Dielectric Elastomer Artificial Muscle Actuators: Toward Biomimetic Motion. *Smart Structures and Materials 2002: Electroactive Polymer Actuators and Devices (EAPAD)*, Proceedings of SPIE Vol. 4695 (2002)

[44] Bar-Cohen Y. Artificial Muscles using Electroactive Polymers (EAP): Capabilities, Challenges and Potential – *NASA Jet Propulsion Laboratory Whitepaper* 2007

[45] University of British Columbia – Actuator Selection Tool
http://www.actuatorweb.org/index.php?page=actuatorDE (accessed May 2011)

[46] Tollefson T.T., Senders C.W. (2007) .Restoration of eyelid closure in facial paralysis using artificial muscle: preliminary cadaveric analysis. *Laryngoscope*. 2007 Nov;117(11):1907-11.

[47] Oguro, K., Kawami, Y and Takenaka H (1992) Bending of an Ion-Conducting polymer film electrode composite by electric stimulus at low voltage. *Journal of Micromachine society*, Vol 5, p 27-30

[48] Nemat-Nasser, S and Thomas, C (2001) in *Electroactive Polymer Actuators as Artificial Muscles – Reality, Potential and Challenges*, ed Y Bar-Cohen,SPIE, Chapter 6 p139-191

[49] Shahinpoor M., Soft Plastic Robots and Artificial Muscles . *Bionics pp161 – 174* http://www.intechopen.com/download/pdf/pdfs_id/4131 (accessed June 2011)

[50] Shahinpoor M. and Kim K. J. (2004) Ionic polymer–metal composites: II. Manufacturing techniques. *Smart Material Structures* v13 p 1362-88.

[51] Luqman M, Lee J.W, Moon KK, Yoo YT (2011) ,Sulfonated polystyrene-based ionic polymer–metal composite (IPMC) actuator. *Journal of Industrial and Engineering Chemistry* 17 (2011) 49–55

[52] Lee S., Park H.C., Pandita S. D., and Yo Y. (2006) Performance Improvement of IPMC (Ionic Polymer Metal Composites) for a Flapping Actuator
International Journal of Control, Automation, and Systems, vol. 4, no. 6, pp. 748-755.

[53] He, Q., Yu M., Song L., Ding H., Zhang X., Dai, Z. (2011) - Experimental Study and Model Analysis of the Performance of IPMC Membranes with Various Thickness. *Journal of Bionic Engineering 8* (2011) pp 77-85.

[54] Lee S J, Han M J, Kim S J, Jho J Y, Lee H Y and Kim Y H (2006b) A new fabrication method for IPMC actuators and application to artificial fingers *Smart Materials and Structures* 15 1217-2

[55] Fang, B.K., Ju, B.S., Lin, C.C.K (2007) A new approach to develop ionic polymer–metal composites (IPMC) actuator: Fabrication and control for active catheter systems.
Sensors and Actuators A: Physical Volume 137, Issue 2, 4 July 2007, Pages 321-329

[56] Kim, S.J., Lee I.T., Kim Y.H, (2007) - Performance enhancement of IPMC actuator by plasma surface treatment *Smart Materials and Structures* Vol16 (2007) N6-N11

[57] Nguyen V.K., Lee J.W., Yoo Y. (2007) Characteristics and performance of ionic polymer–metal composite actuators based on Nafion/layered silicate and Nafion/silica nanocomposites
Sensors and Actuators B 120 (2007) 529–537

[58] Lee J.W., Kim, J-H, Chun Y.S., Yoo Y.T. The Performance of Nafion-Based IPMC Actuators Containing Polypyrrole/Alumina Composite Fillers. (2009)
Macromolecular Research, Vol. 17, No. 12, pp 1032-1038 (2009)

[59] Siripong, M, Fredholm S,. Nguyen Q.A, Shih B., J. Itescu J, and Stolk J. (2006) A Cost-Effective Fabrication Method for Ionic Polymer-Metal Composites . *Mater. Res. Soc. Symp. Proc.* Vol. 889

[60] Bennett, M., and Leo, D.J., "Manufacture and characterization of ionic polymer transducers with non-precious metal electrodes," *Smart Materials and Structures*, vol. 12, no. 3, 2003, pp. 424-436.

[61] Bergamasco, M. Salsedo, F. and Dario, P.(1989) Shape memory alloy micro-motors for direct-drive activation of dexterous artificial hands. *Sensors and Actuators*, 1989, 17, 115-119.

[62] Hunter, I.W., Lafontaine, S., Hollerbach, J.M. and Hunter, P.J. (1991) Fast reversible NiTi fibers for use in microrobotics. *Proceedings IEEE Micro Electro Mechanical Systems*, 1991, 2, 166-170.

[63] Ikuta, K. Micro/miniature shape memory alloy actuator.(1990) *Proceedings IEEE Micro Electro Mechanical Systems*, 1990, 3, 2156-2161.

[64] Perkins J and Sponholz R. O. (1984) Stress-Induced Martensitic Transformation Cycling and Two-Way Shape Memory Training in Cu-Zn-Al Alloys. *Metallurgical and Materials Transactions A,* 1984, Volume 15, Number 2, Pages 313-321

[65] Mallela V.S., Ilankumaran V, and Rao N.S. (2004) Trends in Cardiac Pacemaker Batteries, *Indian Pacing Electrophysiology* J. 2004 Oct-Dec; 4(4) pp201–212.

[66] Comparison of EAPs with Other Actuator Technologies
http://ndeaa.jpl.nasa.gov/nasa-nde/lommas/eap/actuators-comp.pdf

[67] Hunter, I.W., and S. Lafontaine. 1992. "A Comparison of Muscle with Artificial Actuators," *Technical Digest of the IEEE Solid-State Sensor and Actuator Workshop, Hilton Head, South Carolina*, pp. 178–185

[68] Tadesse Y, Grange W, and Priya S. (2009) Synthesis and cyclic force characterization of helical polypyrrole actuators for artificial facial muscles. *Smart Materials and Structures 18* (2009) 085008 (17pp)

[69] Tollefson T.T, . Senders C.W. (2009) Restoration of Eyelid Closure in Facial Paralysis Using Artificial Muscle: Preliminary Cadaveric Analysis. *The Laryngoscope* Volume 117, Issue 11, pages 1907–1911, November 2007

[70] Shahinpoor M., Kim K.J., Solid-state soft actuator exhibiting large electromechanical effect. *Appl. Phys. Lett*. 80 (2002) 3445.

[71] Food and Drug Administration - Code of Federal Regulations Title 21
http://www.accessdata.fda.gov/scripts/cdrh/cfdocs/cfcfr/CFRSearch.cfm?CFRPart=814&showFR=1

[72] Whitehill J , Littlewort G , Fasel I, Bartlett M, and Movellan J (2009) Towards practical smile detection. *IEEE transactions on pattern analysis and machine intelligence* November 2009 (vol. 31 no. 11)

[73] Whitehill J , Littlewort G , Fasel I, Bartlett M, and Movellan J (2009) Developing a practical smile detector. http://mplab.ucsd.edu/~jake/pami_paper.pdf

[74] Fasel I, Fortenberry B and Movellan J.R. (2004) Machine Perception Toolbox Manual - Machine Perception Laboratory
http://mplab.ucsd.edu/grants/project1/free-software/mptwebsite/Manual/MPTManual.pdf

[75] pFaceDetect Library
http://code.google.com/p/face-detection-processing/downloads/detail?name=pFaceDetect.zip&can=2&q=

[76] Open frameworks Smile detection
http://wiki.openframeworks.cc/index.php?title=OF%C2%A0Goldsmiths (# day 3)

[77] Kornbluh, R., Pelrine, R., Pei, Q., Rosaenthal, M., Shastri S.V., EAP Actuators, Devices and Mechanisms – *Application of Dielectric Elastomers. In Electroactive polymer (EAP) actuators as artificial muscle*, 2nd edition, Bar-Cohen, Y., (ed.), SPIE Press, Bellingham, WA, (2004)

[78] Carpi, F., and Rossi, D.D., Improvement of electromechanical actuating performances of a silicone dielectric elastomer by dispersion of titanium dioxide powder. *IEEE Trans. Dielec. Elec. Insul.* (2005) 12, 835

[79]. Zhang, M., Fan S., Zaljodpv AA. Lee S.B, Aliev A.E. Williams C.D.Baughman R.H, Strong Transparent Multifunctional Carbon Nanotube Sheets.., *Science* (2005) 309, 1215

[80] Voodoo Cameral Tracker : http://www.digilab.uni-hannover.de/docs/manual.html

[81] EyesWeb http://www.infomus.org/EywMain.html

[82] Sansiñena J. M., Olaz´ abal V., Otero T. F., Polo da Fonsecab C. N., and De Paolib M-A (1997) A solid state artificial muscle based on polypyrrole and a solid polymeric electrolyte working in air. Chem. Commun., 1997 p2217-8

[83] Spinks G.M, Alici G. McGovern S, Xi B and Wallace G.G (2009) *Conjugated Polymer Actuators : Fundamentals. Biomedical Applications of Electroactive Polymer Actuators*, Edited by Fredrico Carpi and Elisabeth Smela (2009) pub Wiley & Sons Ltd.

[84] Tadesse Y.,Grange R.W. and Priya S (2009) Synthesis and cyclic force characterization of helical polypyrrole actuators for artificial facial muscles .
Smart Mater. Struct. 18 (2009) 085008 (17pp)

[85] Tadesse Y., Priya S, Chenthamarakshan C.R., De Tacconi, N.R. Rajeshwar K. (2008) Polypyrrole–polyvinylidene difluoride composite stripe and zigzag actuators for use in facial robotics *Smart Mater. Struct.* 17 (2008) 025001 (8pp) doi:10.1088/0964-1726/17/2/025001

[86] Anquetil P (2004) Large contraction conducting polymer molecular actuators *PhD Thesis* MIT

[87] Ding J, Liu L, Spinks G M, Zhou D, Wallace G G and Gillespie J (2003) High performance conducting polymer actuators utilising a tubular geometry and helical wire . *Interconnects Synth. Met*. 138 pp 391 - 398

Appendix A – Arduino and Processing SDL and UML Flowcharts

1. Main Arduino Program Flow.

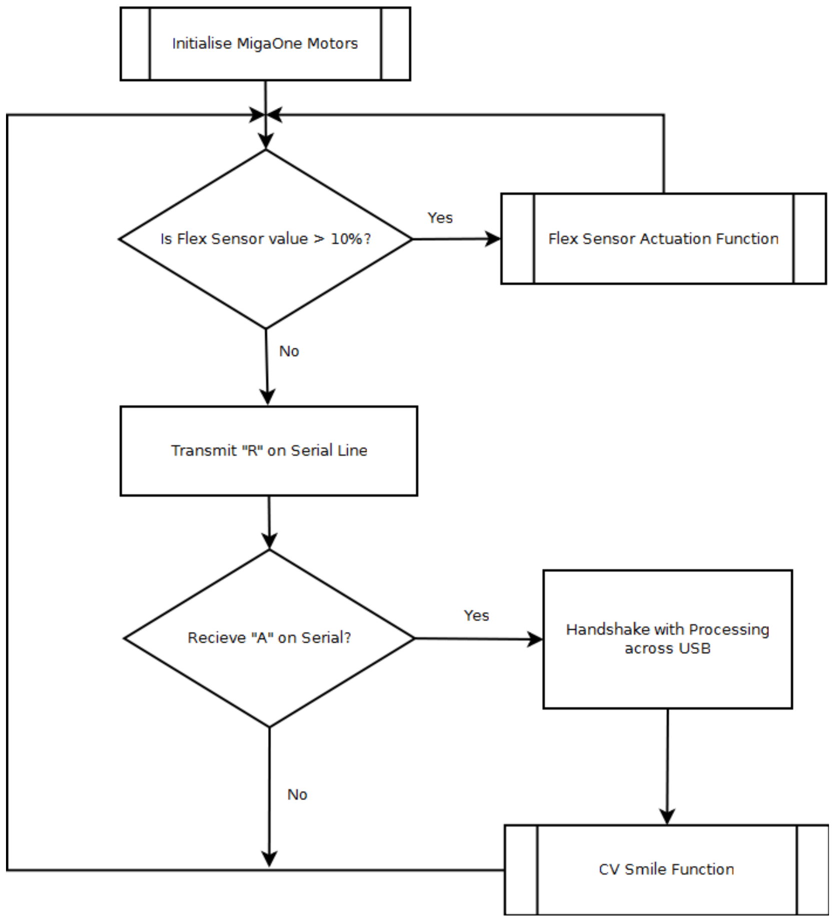

2. Arduino Initialisation function, and MigaOne interupts.

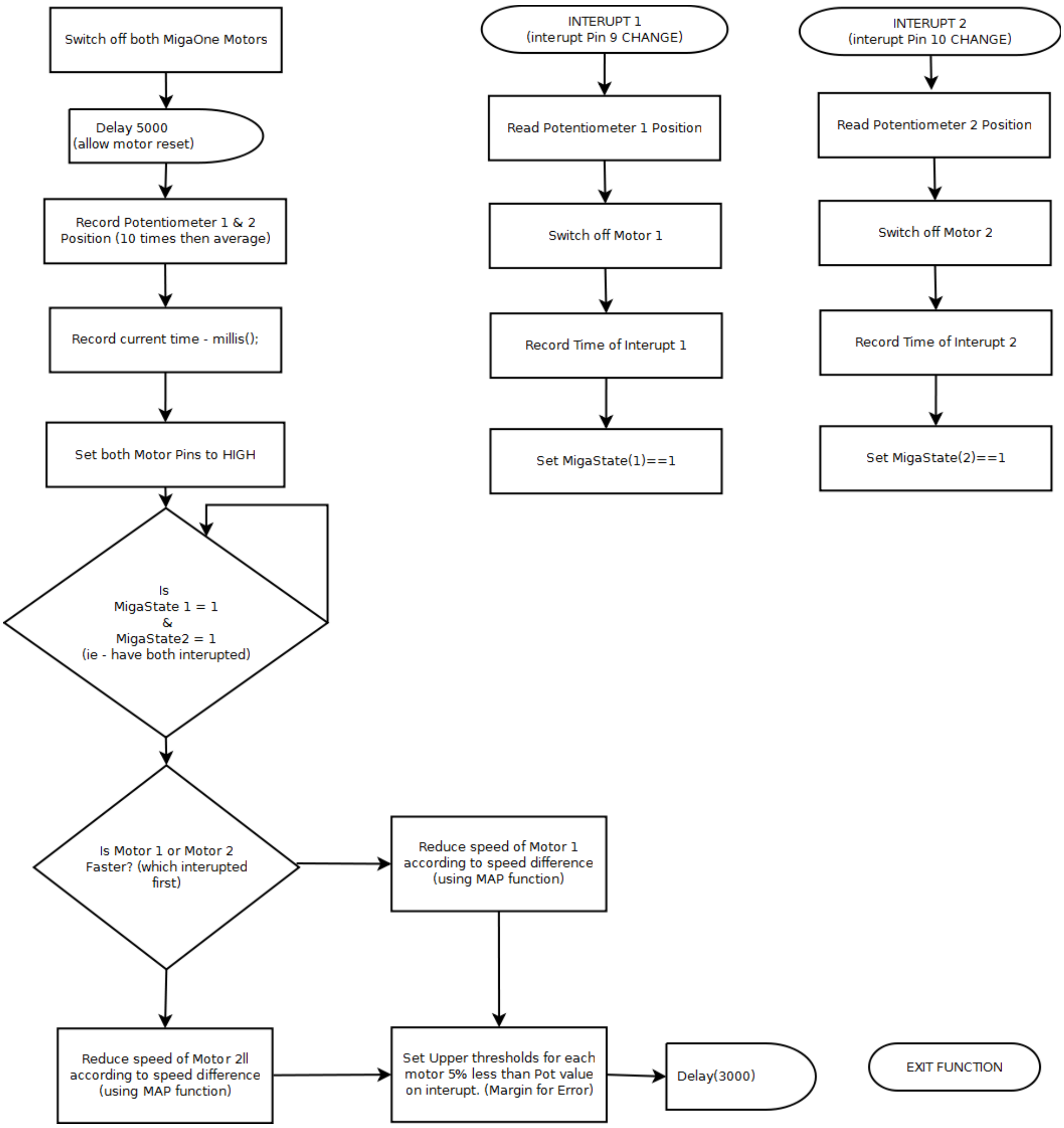

3. Arduino main function.

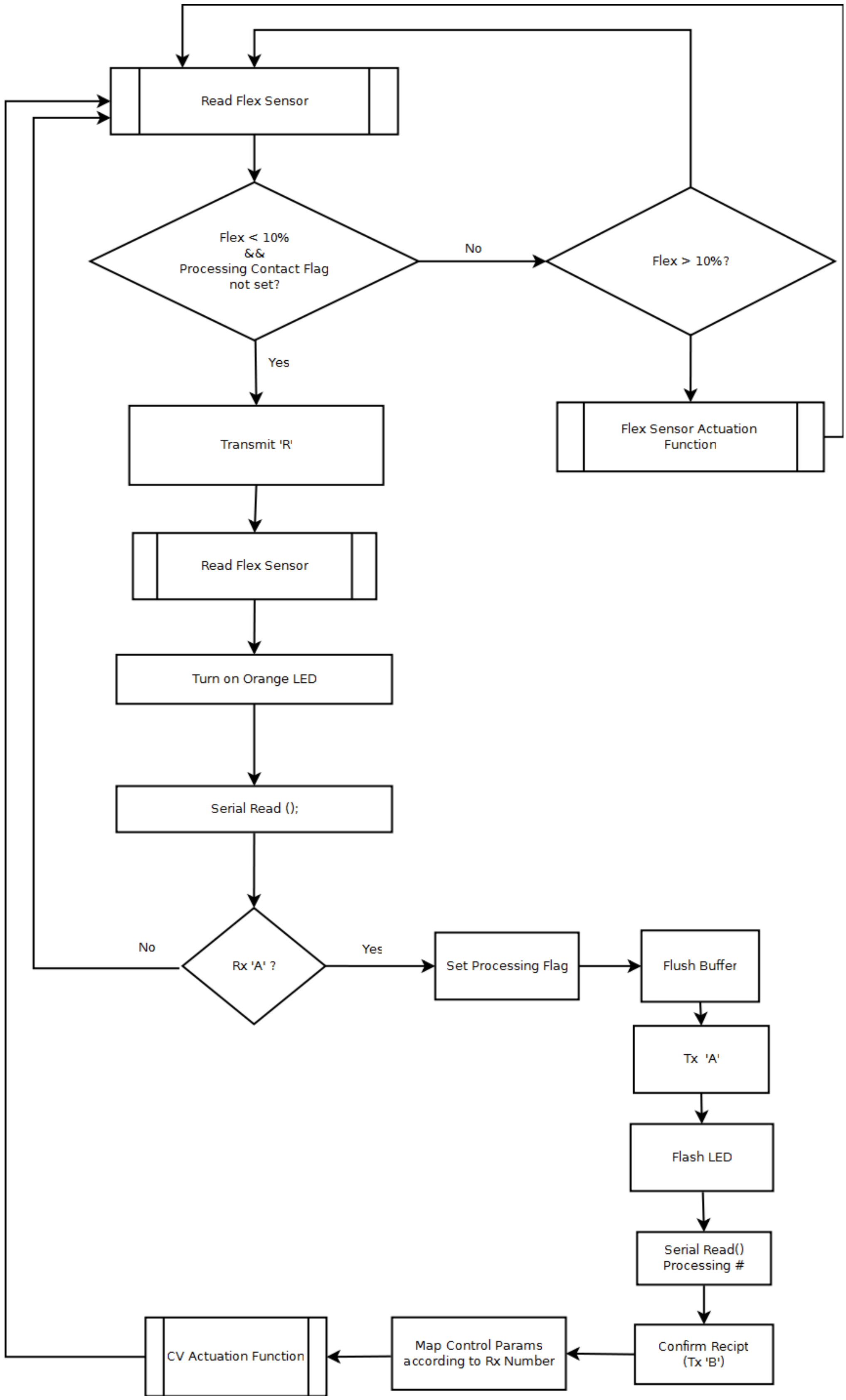

4. Arduino CV Actuation Function

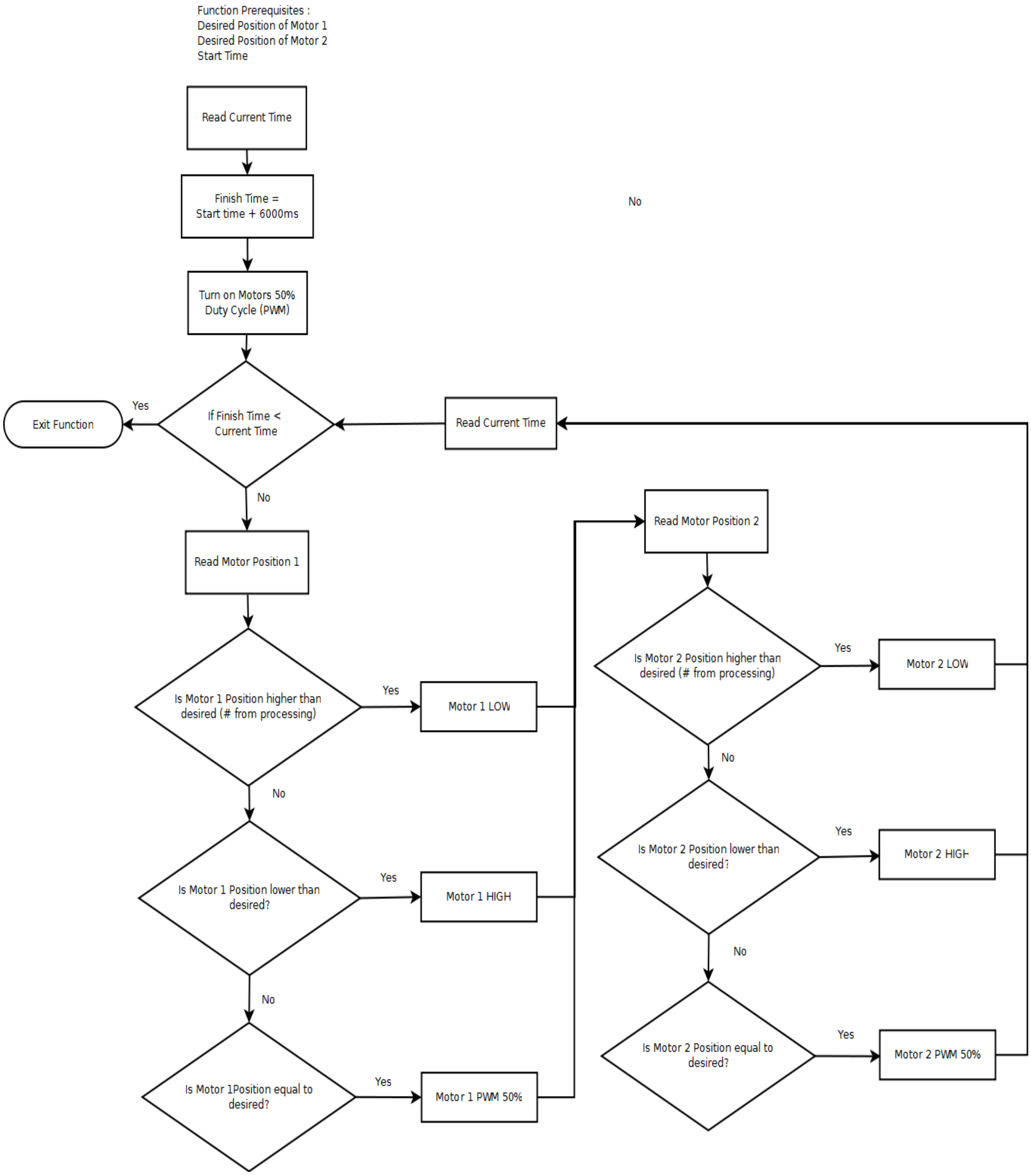

5. Flex Sensor Actuation

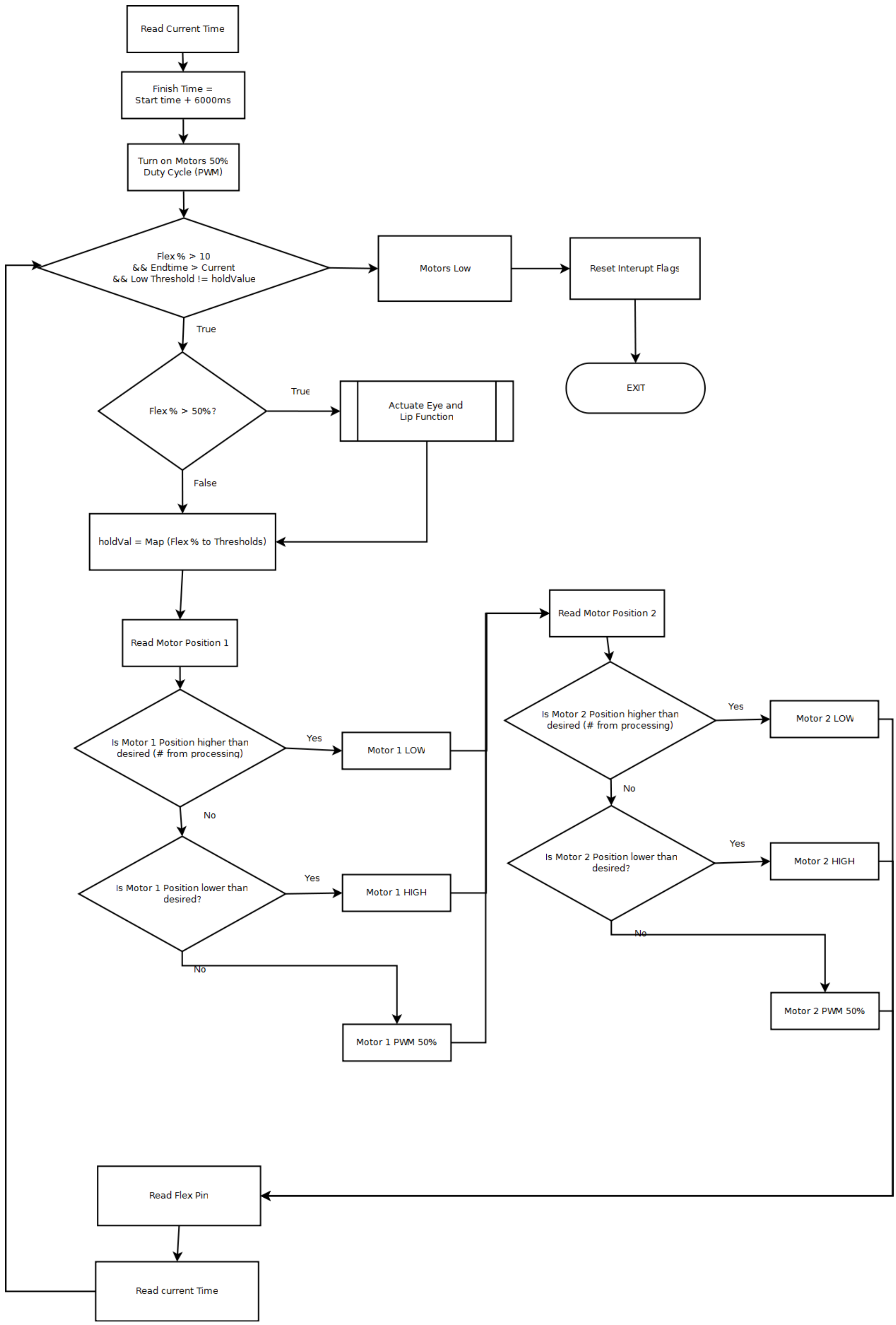

6. Smile Detection - Class UML

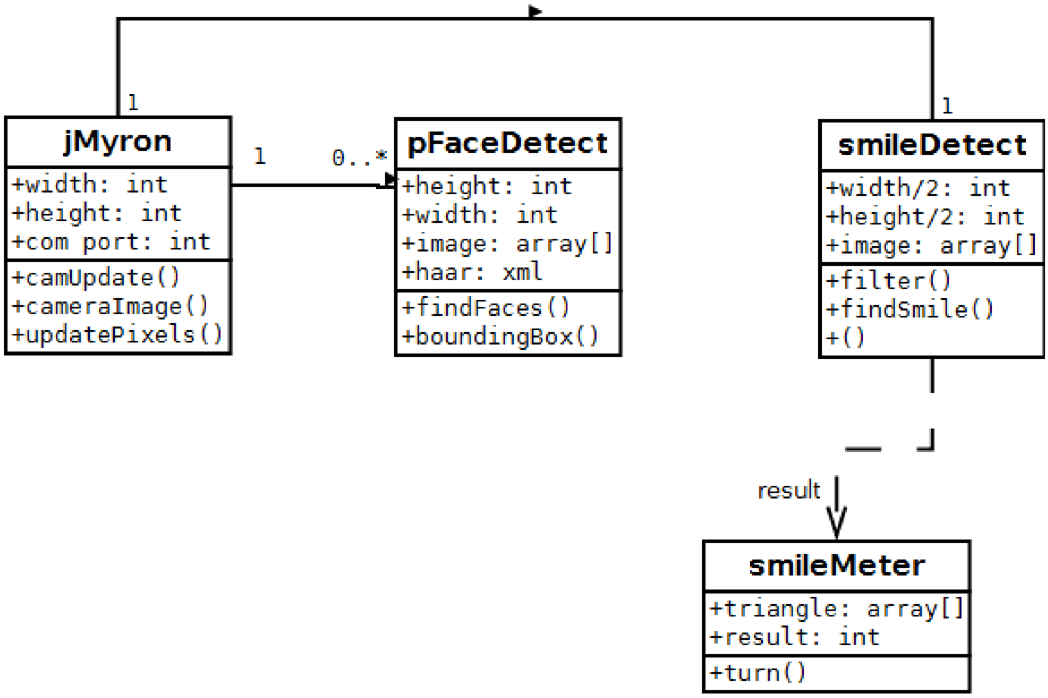

7. Processing Setup( );

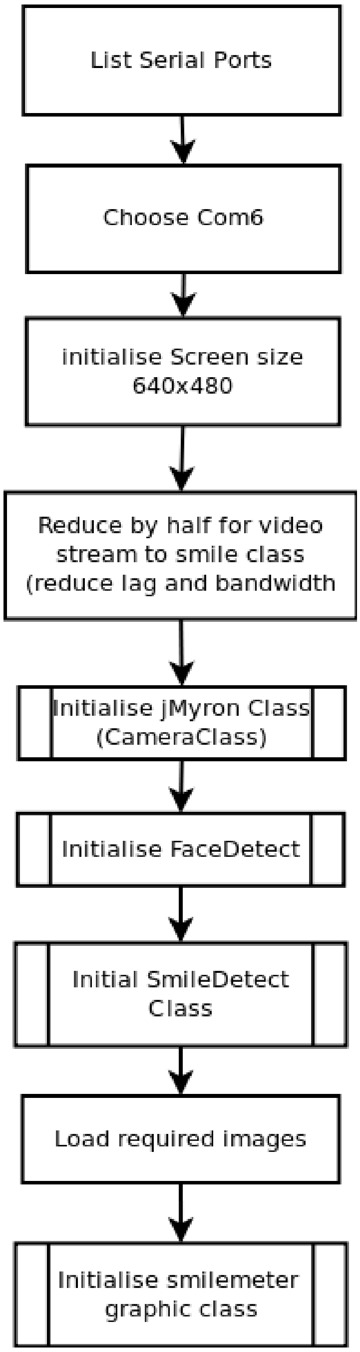

9 Processing Draw ( );

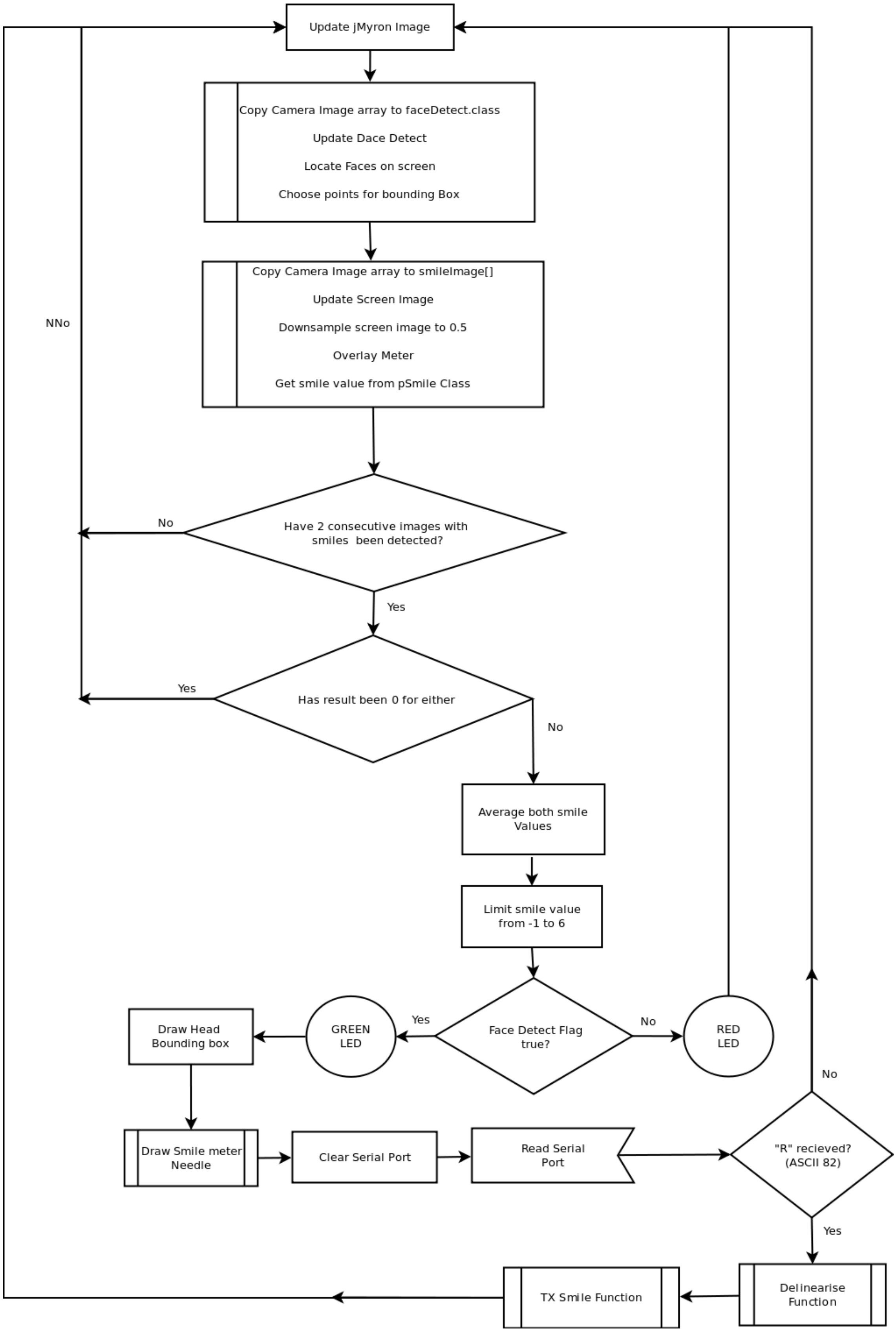

10. Processing TX function

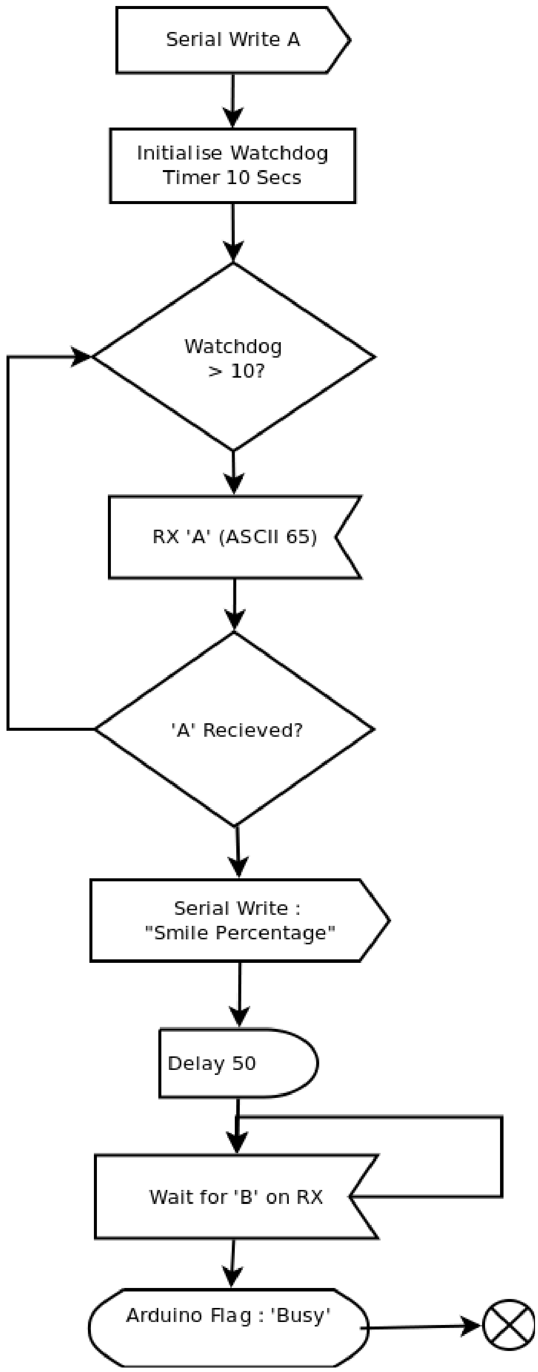

Processing Code :

```
import JMyron.*;
import pSmile.PSmile;
import pFaceDetect.*;
import processing.serial.*;
Serial port;


PFaceDetect face;
JMyron jMyfacialObject;
PSmile smile;
PImage faceDetecter, screenImage, smileDetectImage, meter, needle, ledR, ledG;
float res, t_h, quarterRes, newRes, cumulativeRes,amount,delin;
boolean faceDetected=false;, arduinoReady=false;
int wdt, hght, sendControl=0,detectCount, noOfZeros=0;
Triangle t1;

void setup() {

 println("Available serial ports:");
 println(Serial.list());
 port = new Serial(this, Serial.list()[2], 9600);

  size(640,480);
  wdt = 320;  hght = 240; //to reduce framerate lag
  background(0);
  jMyfacialObject = new JMyron(); //begin library
  jMyfacialObject.start(width,height);
  jMyfacialObject.findGlobs(0); //disable globs for multiple objects

  face = new PFaceDetect(this,width,height,
       "haarcascade_frontalface_default.xml"); //evoke haar Cascade
  faceDetecter = createImage(width,height,ARGB);

  screenImage = createImage(width,height,ARGB);
  smileDetectImage = createImage(wdt,hght,ARGB);

  smile = new PSmile(this,wdt,hght); //initialise PSmile class
  res = 0.0;

  rectMode(CORNER);
  stroke(255,255,255);
  fill(255,200,0);

 meter = loadImage("smile-meter.png");
 needle = loadImage("point.png");
 ledR = loadImage("led_circle_red.png");
 ledG = loadImage("led_circle_green.png");
 t1 = new Triangle(); //class : needle on smileometer
}
```

```
void draw() {
 jMyfacialObject.update();

/////////////////////////////
//facedetection
/////////////////////////////

 arraycopy(jMyfacialObject.cameraImage(),faceDetecter.pixels);
 faceDetecter.updatePixels();
 face.findFaces(faceDetecter);
 image(faceDetecter,0,0);
 drawFace();

///////////////////////////////
// Smile Detection
///////////////////////////////

  int j=0;
  for(int i=1;i<3;i++){

        arraycopy(jMyfacialObject.cameraImage(),screenImage.pixels);
        screenImage.updatePixels();
        smileDetectImage.copy(screenImage,0,0,width,height,0,0,wdt,hght);
        smileDetectImage.updatePixels();
        image(screenImage,0,0);
        image(meter, 3, 277);

         cumulativeRes=-1;
         res = smile.getSmile(smileDetectImage);
         quarterRes=res*0.1;


       newRes=smile.getSmile(smileDetectImage);

      if((newRes>(res-quarterRes)) && (newRes<(res+quarterRes))) {
           cumulativeRes = cumulativeRes+newRes;
           j++;
        delay(5); //time to move to next frame
    }
  }
  res=cumulativeRes/j; //smooth out result

  if (res>6){
    res=6;     //set maximum smile limit
  }
  if (res<-1) {
    res=-1;   //set minimum smile limit
  }


   if(faceDetected == false){ // pseudo LED on screen
      image(ledR, 3, 3); //Red LED
   }
   else {
      image(ledG, 3, 3); //Green LED

       int [][] faceRect = face.getFaces();
        for (j=0;j<faceRect.length;j++) {
         int x_r = faceRect[j][0];
         int y_r = faceRect[j][1];
```

```
          int w_r = faceRect[j][2];
          int h_r = faceRect[j][3];


        ellipseMode(CORNER); //bounding box for head tracking
       noFill();
        ellipse(x_r,y_r,w_r,h_r);
          smooth();
          fill(255,200,100);
       }
    }


    t1.turn();
    t1.drawTriangle();
   smooth();
   image(needle,97, 370);
   amount=((res+1)/7)*100; //turn amount into %

    port.clear();
    delay(70);
    int ready = port.read(); //poll for arduino 'ready' signal
    println("state :" + ready + " " + arduinoReady);

    if(ready=='R' && arduinoReady==false){
      println("Arduino Ready Signal");
       arduinoReady=true;
       detectCount=0;
       ready=0;
       port.clear();
       }


  if(faceDetected==true && arduinoReady==true){
     if(amount>0 && detectCount<=2){
        detectCount++;
        sendControl+=amount;
     }
     if(amount==0 && detectCount<=2) {
       noOfZeros++;
     }
     if(noOfZeros >5) { //5 zeros in a row
       detectCount=0;
       noOfZeros=0;
     }

   }

   if(detectCount==1 && arduinoReady==true)  {
       sendControl/=detectCount;
       println("Send = " + sendControl);
       delin=float(sendControl);
       sendControl = delinearise(delin);  //delinearise function
       arduinoReady=TXSmile(sendControl);  //start transmit
       println("arduino actuating, ready? : " + arduinoReady);
       }

} //end main draw() loop

////////////////////////////////////////////////////
boolean drawFace() {
```

```
 int [][] faceArray = face.getFaces();
  if (faceArray.length>0) {
     faceDetected=true;
     }
  else {
     faceDetected=false;
     }
  return faceDetected;
 }
/////////////////////////////////////////////////////

void stop() {  // kill jMyron Class Instance.
  jMyfacialObject.stop();
  super.stop();
}
```

Arduino Code

```
//--------------MigaOne Percentages--------------------------
// Controls 2 migaOnes according to the bend of flex sensor
// Or Processing smile detection
// PSU A : 12V, 2.0A (MIN)
// PSU B : 12 V 1.45
//
//-------------------------------------------------------------

// ISR interrupt service routine
#include <avr/interrupt.h >
#include <stdlib.h>
///////////////////////////////////////
// Control Declarations
//////////////////////////////////////
int initPot1 = 0, initPot2 = 0;
int thresh1 = 0, thresh2 = 0;
int val, flex, flexLow, i = 0, flexPercent = 0, faceDetect=0;
char facebuffer[4];
unsigned long startTime, endTime, currentTime;
int controlParam1 = 0, controlParam2 = 0 ;


///////////////////////////////////////
// Motor Declarations
//////////////////////////////////////

int motorPin1=5, motorPin2=6, eyeMotorPin=7, mouthMotorPin=8, ledPin=9 ;
int potPin1 = 4, potPin2=5, flexPin=0 ;

// IRQ Flags
volatile int zygoState1 = 0, zygoState2 = 0;
volatile int eyeIntState = 0;
volatile int mouthIntState = 0;

float actuationTime1, actuationTime2, speedDiff;

int control1=0, control2=0;
int migaSpeed1 = 255, migaSpeed2 = 255;

///////////////////////////////////////
// Function Declarations
///////////////////////////////////////

int heldValue = 0; // MegaHold function return

//initial pot value
int inital=0;
int highThresh1 = 0, highThresh2 = 0;
int lowThresh1 = 0, lowThresh2 = 0;

int count = 0, aveVal = 0, control=0, PWMCount=0, MFE;
byte serialValue;

int confirmA=0,confirmB=0,confirmC=0;
//pot value threshold

void setup() {
```

```
/////////////////////////////
////////////////////Pin setup

  pinMode(motorPin1,OUTPUT);
  pinMode(motorPin2,OUTPUT);
  pinMode(potPin1,INPUT);
  pinMode(potPin2,INPUT);

  pinMode(flexPin,INPUT);
  pinMode(ledPin, OUTPUT);

  pinMode(eyeMotorPin,OUTPUT);
  pinMode(mouthMotorPin,OUTPUT);


  attachInterrupt(0, zygoIRQ1, CHANGE); //Attach ISR 0
  attachInterrupt(1, zygoIRQ2, CHANGE); //Attach ISR 1
  attachInterrupt(2, mouthIRQ, CHANGE); //Attach ISR 2
  attachInterrupt(3, eyesIRQ, CHANGE); //Attach ISR 3

  Serial.begin(9600); //Begin serial communication
}


void loop() {

//Initialization - Do Once
while (inital==0){
    initialisation();
}

flexPercent = flexFunct();

while(confirmA==0 && flexPercent < 10) { //include flex pin later
    Serial.println('R'); //I'm Ready!
    flexPercent = flexFunct();
    Delay(100);
    analogWrite(ledPin,10);

  int temp =  Serial.read();
  if (temp =='A'){
        confirmA = 'A';
        Serial.flush();
        }
  }

  while (confirmA=='A') {

        Serial.println('A');  //Good to RX
        analogWrite(ledPin,160);    //
        delay(50);                  //  LED for debugging purposes
        digitalWrite(ledPin,LOW);   //
        delay(50);                  //


     if (Serial.available() > 0) {
       serialValue = Serial.read();

         if (serialValue > 20) {
            analogWrite(ledPin, serialValue);
```

```
            serialValue=255;
         }
         if (serialValue < 20) {
            analogWrite(ledPin, serialValue);
            serialValue=160;
         }
            constrain(serialValue, 0, 255);
            controlParam1 = map(serialValue,0,255,lowThresh1,highThresh1);
            controlParam2 = map(serialValue,0,255,lowThresh2,highThresh2);
            Serial.flush();
            faceControlFunct(controlParam1, controlParam2, serialValue);


          confirmA=0;
       }
      delay(50);
  }




if(flexPercent > 10) { //as flexor is not always 0
  //    Serial.print("flex at 1 : "); Serial.print(controlParam1);
  //    Serial.print(" and 2 : ");Serial.println(controlParam2);
      heldValue = percentControlFunct(controlParam1, controlParam2, flex);
      delay(500); //relax smile after timeout
      }

} ///// end loop()


int flexFunct(){
 int percentage;

  flex = analogRead(flexPin);
  flex = constrain(flex,flexLow,680);
  percentage = (flex-flexLow)/2;

  controlParam1 = map(flex,flexLow,680,lowThresh1,highThresh1);
  controlParam2 = map(flex,flexLow,680,lowThresh2,highThresh2);

return percentage;
}
```

```
///////////////////////////////////
// Initialise thresholds
///////////////////////////////////


void initialisation() {

  delay(50);
  initPot1 = analogRead(potPin1);
  initPot2 = analogRead(potPin2);

  //lowThresh1=initPot;
  digitalWrite(motorPin1,LOW);
  digitalWrite(motorPin2,LOW);
  Serial.println("Initialising");
  delay(5000); // allow any resetting of wiper arm
  Serial.print("Initialise Pot : ");
  Serial.println(initPot1);
  Serial.println(initPot2);

  for (count=0; count < 10; count++ ) {
      initPot1 = analogRead(potPin1);
      initPot2 = analogRead(potPin2);

      lowThresh1 = lowThresh1+initPot1;
      lowThresh2 = lowThresh2+initPot2;
      delay(100);
    }

  lowThresh1 = lowThresh1/10;
  Serial.print("Low Thresh 1 : ");
  Serial.println(lowThresh1);

  lowThresh2 = lowThresh2/10;
  Serial.print("Low Thresh 2 : ");
  Serial.println(lowThresh2);

  for (count=0; count < 1 ; count++ ) { //run 3 cycles to check upper limit
      int motorsStart = millis();
      analogWrite(motorPin1,migaSpeed1); //
        Serial.println("migaSpeed1");
//      int motorStart2 = millis();
      analogWrite(motorPin2,migaSpeed2); //
              Serial.println("migaSpeed2");

      while((zygoState1==0) || (zygoState2==0)) { // first time - bring to
interupt
          delay(20);
         }

      if (actuationTime1<actuationTime2){
             //speedDiff=actuationTime1-actuationTime2;
             //slowTo=actuationTime1-speedDiff;
             migaSpeed1=map(actuationTime1,motorsStart,actuationTime2,200,255);
             Serial.print("Motor 1 slowed to :"); Serial.println(migaSpeed1);
      }
      if (actuationTime1>actuationTime2){
          //speedDiff=actuationTime2-actuationTime1;
          migaSpeed2=map(actuationTime2,motorsStart,actuationTime1,200,255);
          Serial.print("Motor 2 slowed to :"); Serial.println(migaSpeed2);
      }
```

```
    analogWrite(motorPin1,0);
    analogWrite(motorPin2,0);
    Serial.print("zygoState1=");
    Serial.println(zygoState1);
    Serial.print("zygoState2=");
    Serial.println(zygoState2);
        delay(3000);
    Serial.println("No More Delay");



    Serial.print("HighThresh 1 : ");
    Serial.println(highThresh1);
    Serial.print("HighThresh 2 : ");
    Serial.println(highThresh2);

    digitalWrite(motorPin1,LOW);
    digitalWrite(motorPin2,LOW);
    delay(6000);
  }


  thresh1 = highThresh1-lowThresh1;
  MFE=int(thresh1*0.05); //5% from the top
  highThresh1=highThresh1-MFE;
  thresh2 = highThresh2-lowThresh2;
  MFE=int(thresh2*0.05); //5% from the top
  highThresh2=highThresh2-MFE;

  Serial.print("Ave High Thresh 1: ");
  Serial.println(highThresh1);

  Serial.print("Ave High Thresh 2: ");
  Serial.println(highThresh2);

  Serial.print("Thresh 1: ");
  Serial.println(thresh1);

  Serial.print("Thresh 2: ");
  Serial.println(thresh2);
  inital=1;
  flexLow =  analogRead(flexPin);
  Serial.print("Flex : ");Serial.println(flexLow);
  Serial.println("Initialisation Complete!");

}
```

```
//////////////////////////////////////
// mini Motors held
//////////////////////////////////////
void miniSmile(float ctrl, long eTime, long eTime2) {
int logical = 0;
long cTime;
 Serial.println("Increasing Mini Motors");


cTime=millis();

    analogWrite(eyeMotorPin,255);
    analogWrite(mouthMotorPin,255);

if(eTime2 < cTime) {
    analogWrite(eyeMotorPin,128);
    analogWrite(mouthMotorPin,128);
     Serial.println("Times Up");
    }

}

 ////////////////////////////////////
//Interupts Service Routines (ISRs)
//////////////////////////////////


void zygoIRQ1() { //this should only be used at initialisation
  highThresh1 = analogRead(potPin1);
  analogWrite(motorPin1,0);
  actuationTime1=millis();
  Serial.println("Intrpt Zygo 1");
  zygoState1 = 1;
}


void zygoIRQ2() { //this should only be used at initialisation
  highThresh2 = analogRead(potPin2);
  analogWrite(motorPin2,0);
  actuationTime2=millis();
  Serial.println("Intrpt Zygo 2");
  zygoState2 = 1;
}

void eyesIRQ() {
  analogWrite(eyeMotorPin,128);
    Serial.println(" ");
  Serial.println("Intrpt Eye Motor ");
      Serial.println(" ");
  eyeIntState = 1;
//  count=256;
}

void mouthIRQ() {
  analogWrite(mouthMotorPin,128);
      Serial.println(" ");
  Serial.println("Intrpt Mouth Motor ");
      Serial.println(" ");
  mouthIntState = 1;
//  count=256;
}
```

```
////////////////////////////////////////
////Non interuptable Smile from Processing Command
//////////////////////////////////////

int faceControlFunct(int ctrlLeft, int ctrlRight, int processingAmount){

int holdVal1, holdVal2, positionVal1, positionVal2;
int PWMCount1=0, PWMCount2=0;
boolean processingReset=false;


  startTime=millis();
  currentTime=millis();
  endTime=startTime+3000;

   analogWrite(motorPin1,255);
   analogWrite(motorPin2,255);

while(endTime>currentTime){

    positionVal1 = analogRead(potPin1);
    positionVal2 = analogRead(potPin2);

    if(ctrlLeft > positionVal1){
      analogWrite(motorPin1,migaSpeed1);
    }

    if(ctrlRight > positionVal2){
       analogWrite(motorPin2,migaSpeed2);
    }

    if( ctrlLeft < positionVal1){
        digitalWrite(motorPin1,LOW);
       }

    if(ctrlRight < positionVal2){
        digitalWrite(motorPin2,LOW);
       }


    if(positionVal1==ctrlLeft){ // alternate between high and low (auto variable
duty cycle PWM)
        analogWrite(motorPin1,100);
    }

     if(positionVal2==ctrlRight){ // alternate between high and low (auto
variable duty cycle PWM)
        analogWrite(motorPin2,100);
    }


currentTime=millis();

} //close while
digitalWrite(motorPin1,LOW);
digitalWrite(motorPin2,LOW);

//while(processingReset==false){

    digitalWrite(ledPin,LOW);
  delay(500);
```

```
    digitalWrite(ledPin,HIGH);
  delay(500);
    digitalWrite(ledPin,LOW);
  delay(500);
    digitalWrite(ledPin,HIGH);
  delay(500);


if (endTime<currentTime) {

digitalWrite(mouthMotorPin,LOW);
digitalWrite(eyeMotorPin,LOW);
eyeIntState = 0;
mouthIntState = 0;



}
confirmA = 0;
confirmB = 0;
confirmC = 0;
return endTime;

}


////////////////////////////////////////
////Mega hold function /
//////////////////////////////////////

int percentControlFunct(int ctrlLeft, int ctrlRight, int flx){

int holdVal1, holdVal2, positionVal1, positionVal2;
int PWMCount1=0, PWMCount2=0;

  startTime=millis();
  endTime=startTime+10000;
  long miniTime=startTime+2000;
  long miniTime2=startTime+4000;


while ((flexPercent > 10) /* && (endTime>currentTime)*/ && (lowThresh1!
=holdVal1)) {
   if(flexPercent>50){
     miniSmile(flexPercent, miniTime, miniTime2);
   }
   else {
    analogWrite(mouthMotorPin,0);
    analogWrite(eyeMotorPin,0);
    eyeIntState = 0;
    mouthIntState = 0;
   }

////////////////////////////////////
//values for left and right sensor
       positionVal1 = analogRead(potPin1);
       positionVal2 = analogRead(potPin2);

       holdVal1 = map(flex,480,680,lowThresh1,highThresh1);
       holdVal2 = map(flex,480,680,lowThresh2,highThresh2);
   analogWrite(motorPin1,128);
```

```
   analogWrite(motorPin2,128);

    if(holdVal1 > positionVal1){
       analogWrite(motorPin1,migaSpeed1);
      //Serial.print("Left high | ");
      }

    if(holdVal1 > positionVal2){
      analogWrite(motorPin2,migaSpeed2);
      //Serial.println("Right high | ");
      }

    if(holdVal1 < positionVal1){
      digitalWrite(motorPin1,LOW);
      //Serial.print("Left Low | ");
       }

    if(holdVal2 < positionVal2){
       digitalWrite(motorPin2,LOW);
      //Serial.println("Right Low | ");
      }


    if(positionVal1==holdVal1){ // alternate high and low (variable duty cycle
PWM)
        analogWrite(motorPin1,100);
      //Serial.print("Left PWM | ");
      }

     if(positionVal2==holdVal2){ // alternate high and low
        analogWrite(motorPin2,100);
      //Serial.println("Right PWM | ");
      }

  flexPercent = flexFunct();
  currentTime=millis();

} //close while
digitalWrite(motorPin1,LOW);
digitalWrite(motorPin2,LOW);


if (endTime<currentTime) {

Serial.print("startTime ");Serial.println(startTime);
Serial.print("endTime ");Serial.println(endTime);
Serial.println("can't hold a smile that long");

digitalWrite(mouthMotorPin,LOW);
digitalWrite(eyeMotorPin,LOW);
digitalWrite(motorPin1,LOW);
digitalWrite(motorPin2,LOW);
eyeIntState = 0;
mouthIntState = 0;


}
return endTime;
}
```

Processing - pSmile Class

```
package pSmile;

import processing.core.PApplet;
import processing.core.PConstants;
import processing.core.PImage;

public class PSmile
  implements PConstants
{
  private int wdt;
  private int hght;
  private PApplet parent;
  public long ptr;

  static
  {
    System.loadLibrary("PSmile");
  }

  public PSmile(PApplet _p, int _wdt, int _hght)
  {
    this.parent = _p;
    this.wdt = _wdt;
    this.hght = _hght;
    init(this.wdt, this.hght);
  }

  private native void init(int paramInt1, int paramInt2);

  public native float findSmile(float[] paramArrayOfFloat, int paramInt1, int
paramInt2);

  public float getSmile(PImage _i) {
    PImage img = this.parent.createImage(this.wdt, this.hght, 2);
    img.copy(_i, 0, 0, _i.width, _i.height, 0, 0, this.wdt, this.hght);
    img.updatePixels();
    img.filter(12);
    int total = this.wdt * this.hght;
    float[] buffer = new float[total];
    for (int i = 0; i < total; i++) {
      buffer[i] = (img.pixels[i] >> 16 & 0xFF); // int to byte array

    }
    float res = findSmile(buffer, this.wdt, this.hght);
    return res;
  }
}
```

Appendix C – Serial Communication between Arduino and Processing

A problematic area of the program was getting the Arduino and Processing code to communicate reliably. There were two aspects to this : synchronisation and decoding. Sending data on the USB serial line required handshaking between the two programs, which was relatively simple, and detailed in Chapter 2.

The difficulty occurred in the decoding of received/transmitted (RX/TX) data. Initial testing of transmitted smile data (0-255) was conducted with a simple PWM LED circuit. The smile value from Processing was sent, and Arduino would correspondingly light the LED, according to the code snippet below.

```
if (Serial.available() > 0 ) {

  // read the most recent byte (which will be from 0 to 255):
  brightness = Serial.read();
  // set the brightness of the LED:
  analogWrite(ledPin, brightness);
}
```

Code Snippet : 1

It later transpired that the smile value was actually being translated to an ASCII value before TX, and so the PWM value would never get above 126, and also would involve a large degree of randomness. The issue was difficult to debug, as the COM port that would normally be used to extract data from the Arduino was being held by Processing to send camera and smile data. In effect this made the system a black-box with only an LED output as a readable value

```
if (Serial.available() > 0) {

  int buffsize = 3; //maximum number of bits expected on serial

     while ((Serial.available()) && (buffsize>=0)) {
        *pbuffer++ = Serial.read();
         buffsize--; //decrease for buffer pointer
         delay(20); //give time for next bit to arrive
        }

        *pbuffer++ = '/0'; //make LSB of array end character (/0)
        serialValue = atoi(buffer); //merge ASCII buffer to single variable
        serialValue = int(serialValue);    //convert from ASCII to INT
      Serial.print('A'); //confirm receipt to processing
      }
  }
```

Code Snippet : 2

An attempt was made to rectify the problem using the C function atoi[ ] which converts the RX ASCII function into an integer. This involved creating an array, setting a pointer to that array which would read in the serial buffer, then converting the original array to an integer. (see code snippet 2). During serial hyperterminal testing this worked well, but did not work when Processing sent values.

Next, the sscanf[ ] C function was attempted. This reads the whole string on the input buffer, stores it as a whole variable while converting it to whatever the variable was initialised as. Again this worked in Hyperterminal – being able to convert HEX values to integers, but failed when Processing sent its smile data.

```
if ( Serial.available() > 0 )
{

int serialInputVal;
    while ( Serial.available()) {
      serialInputVal = Serial.read();
      sscanf(buffer, "%x", &serialInputVal);
         //Reads data from str and stores them according
         //to the initialisation of serialInputVal
       }
       Serial.print('A'); //confirm recipt to Processing
  }
  smileFunctionCall(positionMotor1, positionMotor2, serialInputVal);
```

Code Snippet : 3

Next a solution was found by using a 'shift register' style soft buffer set to 10 bits long. This would keep previous values as well as new ones. On every TX from Processing, an end character (in this case the '~') is sent. The value to be used is then the most recent (least significant bits) data situated between two end characters.

```
  char buff[]= "0000000000"; //10 characters for multiple ASCII Strings

  while (Serial.available()>0) {
    for (int i=0; i<10; i++) {
      buff[i]=buff[i+1];          // create a 'soft' buffer including
    }                             //previous values

      buff[10]=Serial.read();     //read in whole string to array
    if (buff[10]=='~') {          //Arbitary end character from Processing
      serialVal=int(buff[9]);     //previous 9 characters
    }
  }
  AnalogWrite(LED,serialVal);
  delay(10);
}
```

Code Snippet : 4

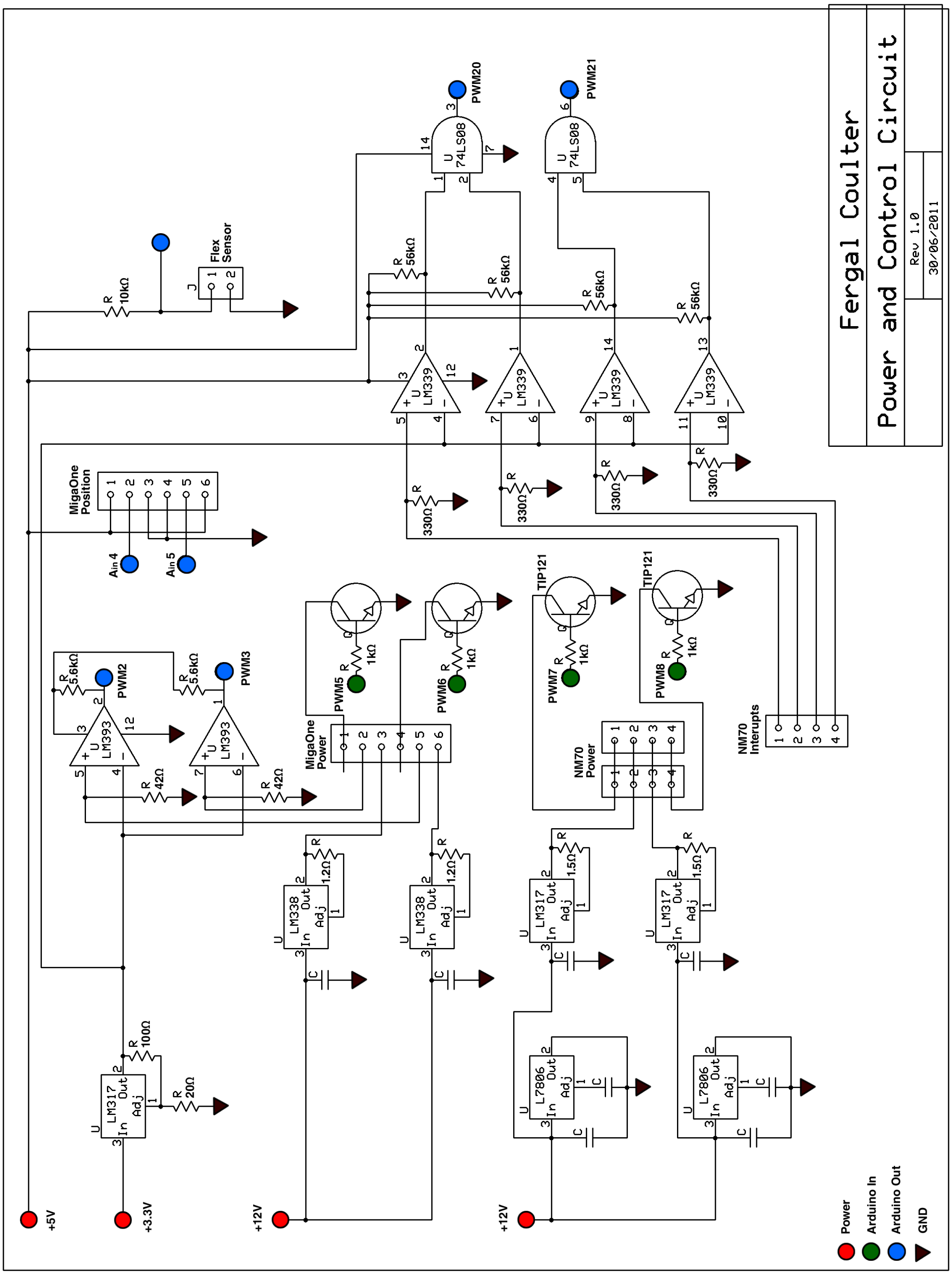
Fergal Coulter
Power and Control Circuit
Rev 1.0
30/06/2011
Power
Arduino In
Arduino Out
GND
MigaOne Position
MigaOne Power
NM70 Power
NM70 Interupts
Flex Sensor
TIP121
LM339
LM393
74LS08
LM338
LM317
L7806
PWM20
PWM21
PWM2
PWM3
PWM5
PWM6
PWM7
PWM8
+5V
+3.3V
+12V

PCB Layout

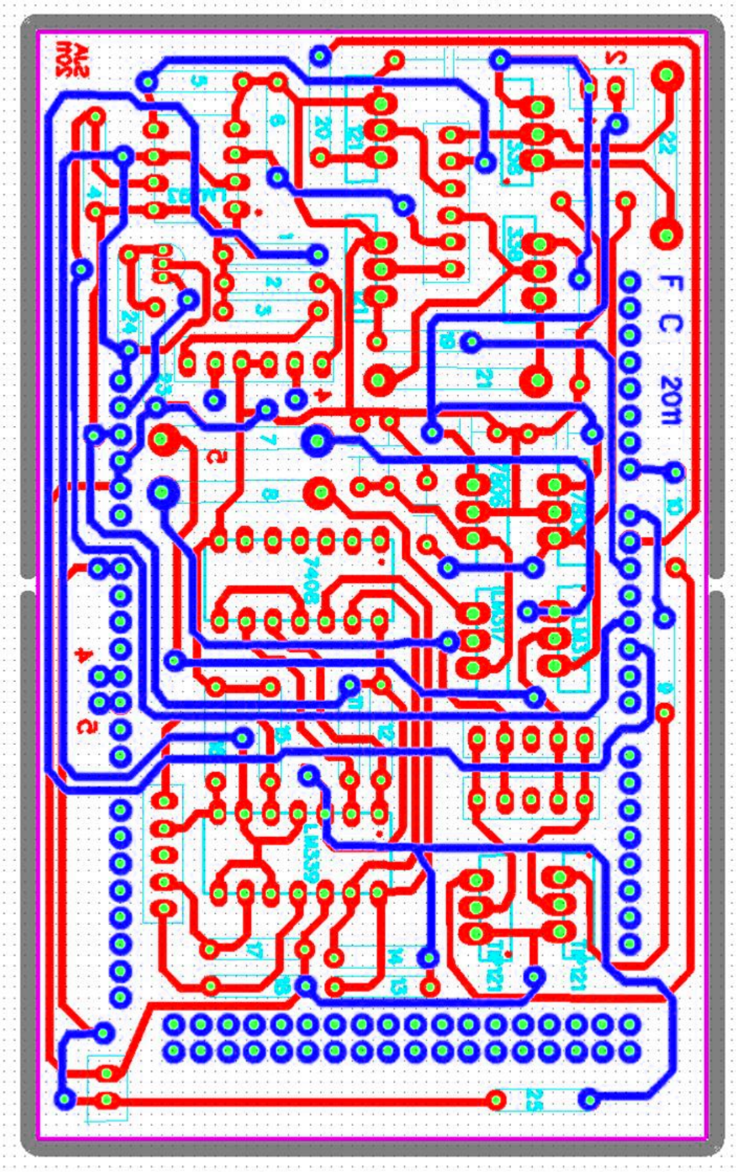

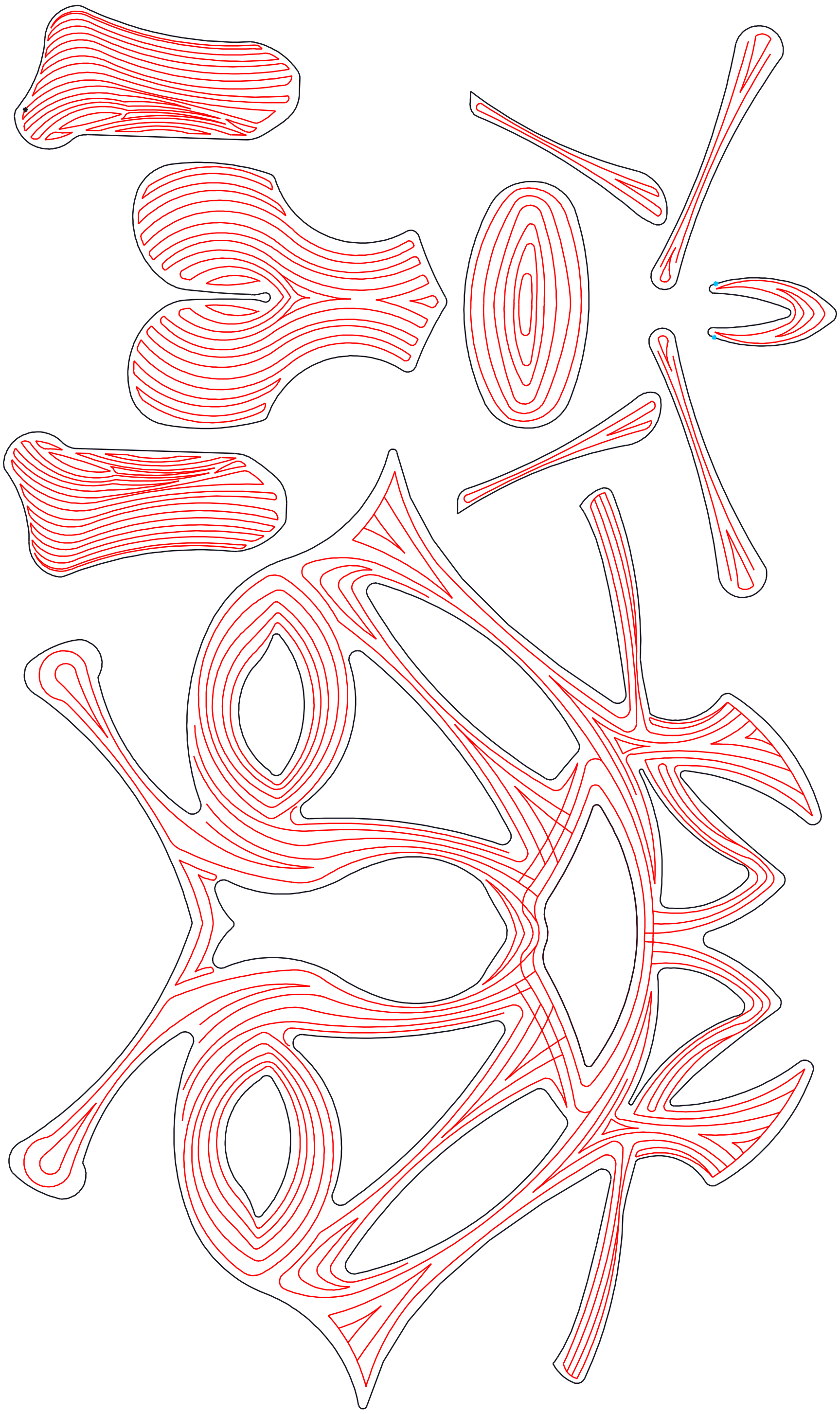

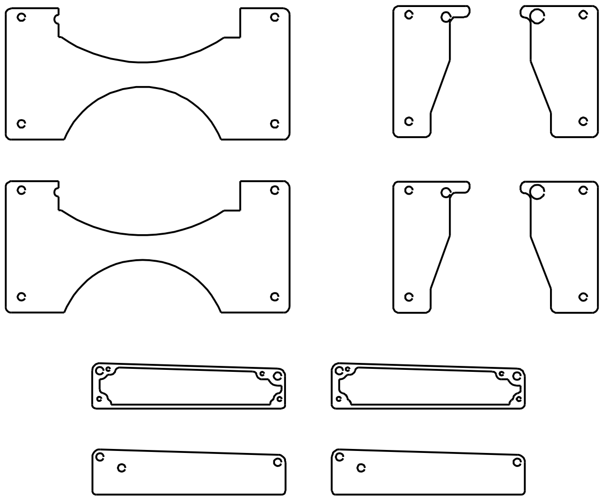

Appendix F : Example recorded smiling sequence

Eight individuals were video taped while watching comic sketches on a screen in front of them. Head motion has been normalised around the centre forehead spot. Each frame in this sequence is 66ms

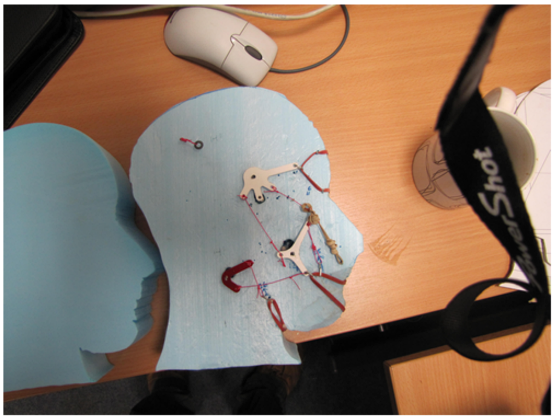

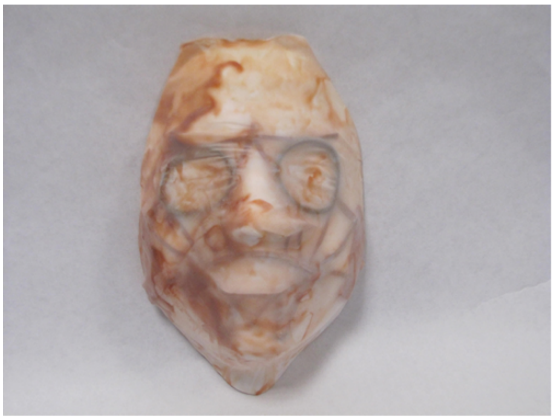

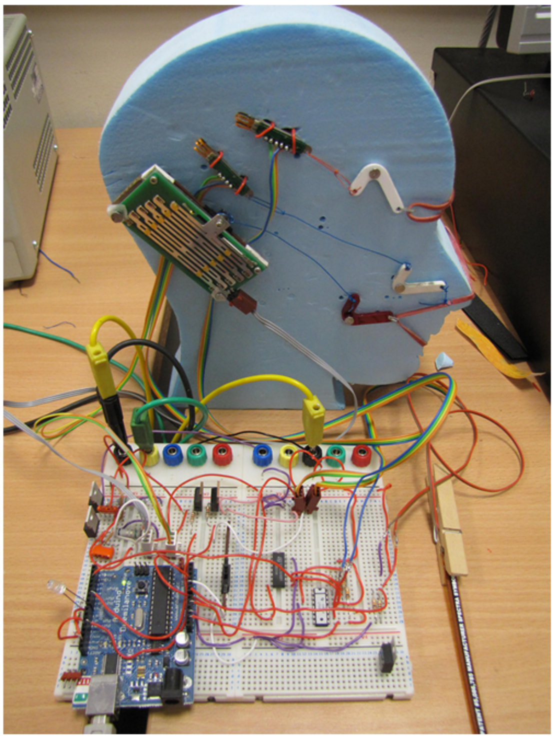


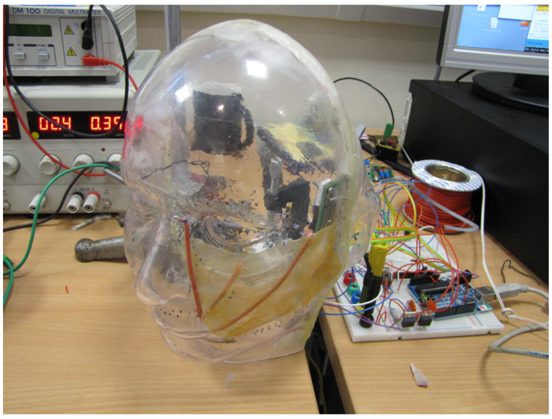
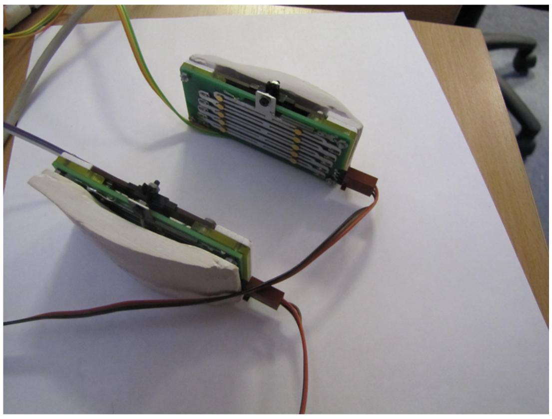
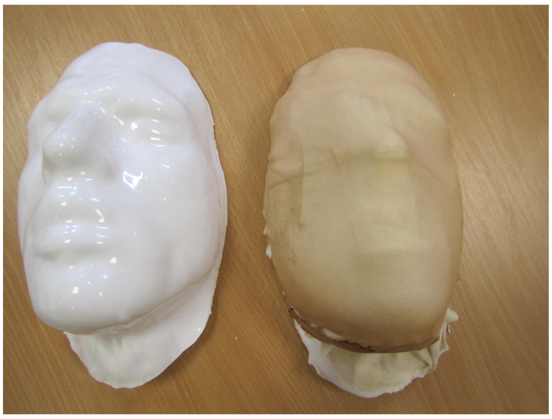

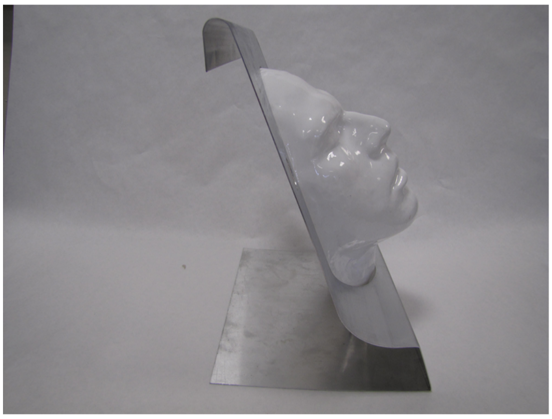
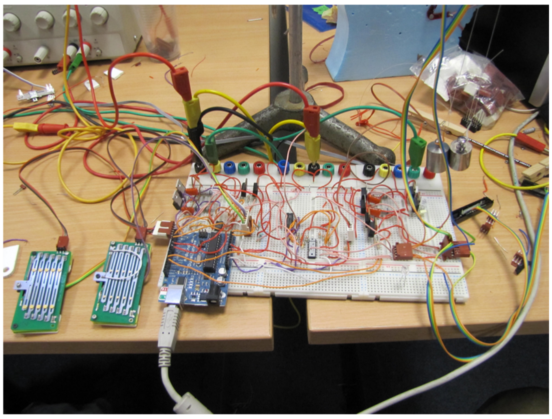
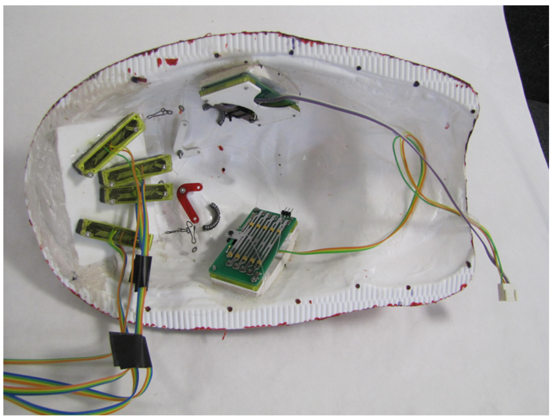
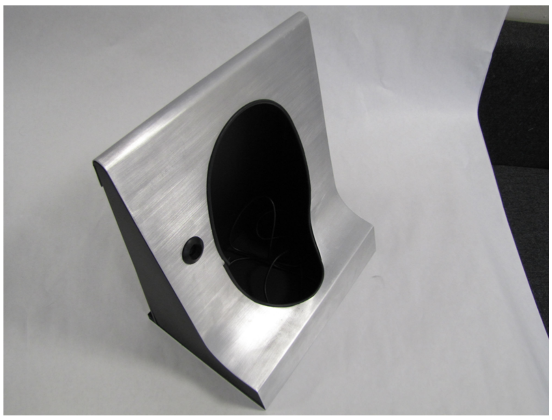

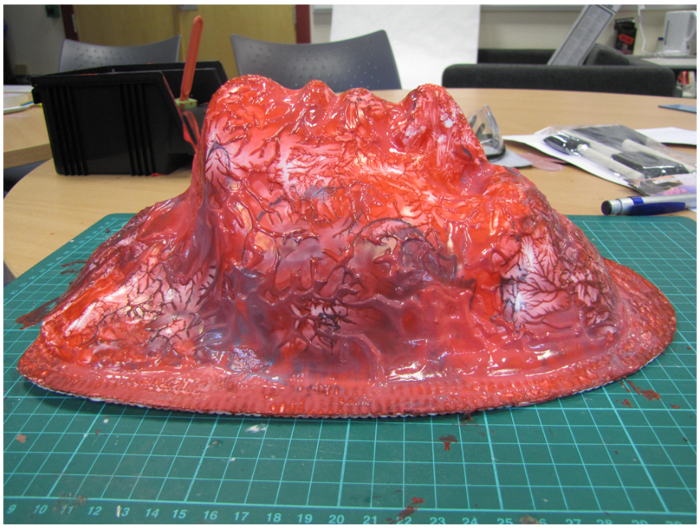

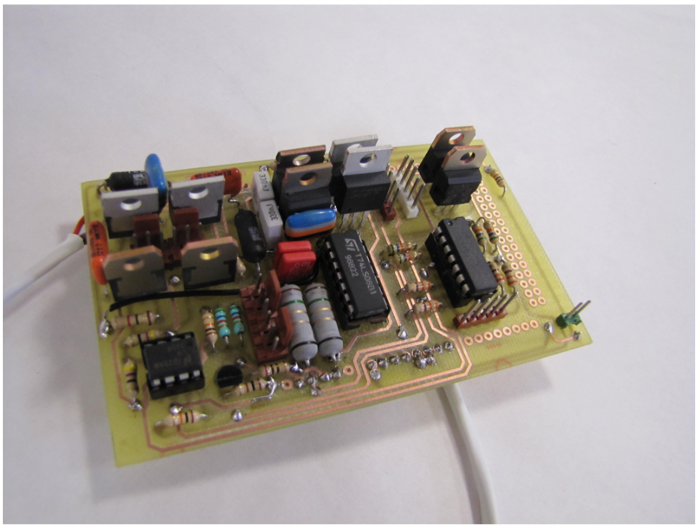

Acknowledgments

Sincerest thanks to the many who helped throughout the duration of this project.

Special thanks to Dr. Philip Breedon for his ever encouraging suggestions, advice and supervision, alongside all the academic team in the ADBE department of Nottingham Trent University. Also thanks to Prof. Michael Vloeberghs for his advice and suggestions both early and later in the project.

All the technical staff who came to the rescue with advice and solutions to any problems that arose along the way. Special thanks to Sue for her help with the electronics and PCB work, along side Dave and Jez. Judith for materials and testing advice. Mark and Alan for all their help and advice in metals and methods, Kerry, Carl and Adriana for help with the model making, Chris and John for laser and RP, and Graham for supplying all the necessary bits. pieces and gentle reminders of how late it was getting to be still down in the workshops!

Tony and Stewart in Maudslay security, who gave me an extra hour every evening to press on with work, and a chat when things got too hectic.

All the guys in 'The Box', who put up with me constantly going on about cheeks, smiles, muscles and expressions, then supplying their ever beautiful faces for me to pull, poke and measure!

Lastly, of course my Parents and Family who have helped, advised and been there every step along the way, before hand and without doubt wil be for anything yet to come.